

INFORMATION TO USERS

This manuscript has been reproduced from the microfilm master. UMI films the text directly from the original or copy submitted. Thus, some thesis and dissertation copies are in typewriter face, while others may be from any type of computer printer.

The quality of this reproduction is dependent upon the quality of the copy submitted. Broken or indistinct print, colored or poor quality illustrations and photographs, print bleedthrough, substandard margins, and improper alignment can adversely affect reproduction.

In the unlikely event that the author did not send UMI a complete manuscript and there are missing pages, these will be noted. Also, if unauthorized copyright material had to be removed, a note will indicate the deletion.

Oversize materials (e.g., maps, drawings, charts) are reproduced by sectioning the original, beginning at the upper left-hand corner and continuing from left to right in equal sections with small overlaps.

Photographs included in the original manuscript have been reproduced xerographically in this copy. Higher quality 6" x 9" black and white photographic prints are available for any photographs or illustrations appearing in this copy for an additional charge. Contact UMI directly to order.

**Bell & Howell Information and Learning
300 North Zeeb Road, Ann Arbor, MI 48106-1346 USA
800-521-0600**

UMI[®]

**Methane and Ventilation Studies in Coal Mining
in the Sydney Coalfield, Nova Scotia**

by

David A. Young, B.Sc.

**Department of Mining and Metallurgical
Engineering**

McGill University, Montreal

March, 1997

**A Thesis Submitted to the Faculty of
Graduate Studies and Research**

as

**Partial Fulfillment of the Requirements
for the degree of
Master of Engineering**



National Library
of Canada

Acquisitions and
Bibliographic Services

395 Wellington Street
Ottawa ON K1A 0N4
Canada

Bibliothèque nationale
du Canada

Acquisitions et
services bibliographiques

395, rue Wellington
Ottawa ON K1A 0N4
Canada

Your file Votre référence

Our file Notre référence

The author has granted a non-exclusive licence allowing the National Library of Canada to reproduce, loan, distribute or sell copies of this thesis in microform, paper or electronic formats.

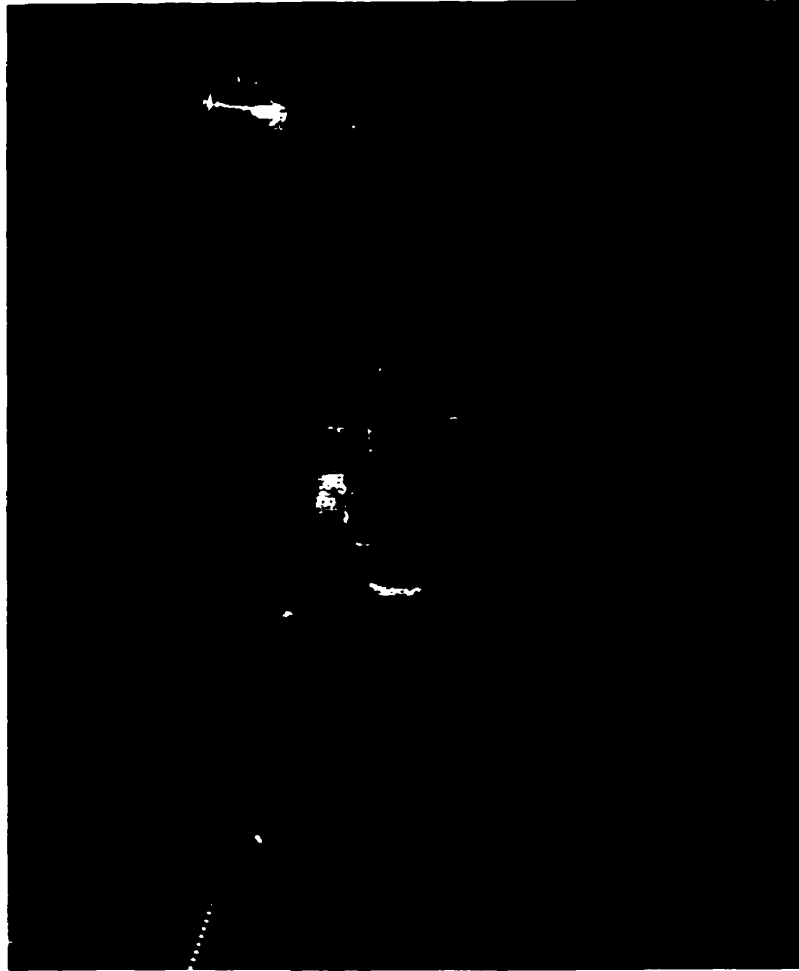
The author retains ownership of the copyright in this thesis. Neither the thesis nor substantial extracts from it may be printed or otherwise reproduced without the author's permission.

L'auteur a accordé une licence non exclusive permettant à la Bibliothèque nationale du Canada de reproduire, prêter, distribuer ou vendre des copies de cette thèse sous la forme de microfiche/film, de reproduction sur papier ou sur format électronique.

L'auteur conserve la propriété du droit d'auteur qui protège cette thèse. Ni la thèse ni des extraits substantiels de celle-ci ne doivent être imprimés ou autrement reproduits sans son autorisation.

0-612-50679-7

Canada



*In the memory of Fabian Young
a Cape Breton Coal Miner*

ABSTRACT

Methane and Ventilation Studies in Coal Mining in the Sydney Coalfield, Nova Scotia

For centuries human society has relied on coal as a principal source of fuel for heat and power. Extraction of this valuable fuel has always been influenced by control over hazards such as water inflows and potentially explosive dust and methane gas. A major focus of the research has been on methane including: methane properties of seams; insitu and laboratory testing; methane emissions; investigation of operational issues (e.g. Phalen 7 East); and refinement of prediction models.

Below 600 m depth, the Phalen and Harbour Seams in the Sydney Coalfield are classified as gassy, having specific emissions in the 10-15 m³/tonne range. Research efforts have focussed on methane emissions increase with depth and its effect on these deeper workings.

This thesis gives an overview of methane and ventilation research covering the following aspects:

Defining coal seam characteristics: specific emissions - the relationship between methane content, coal 'rank' and depth; the geothermal gradient; insitu gas pressure; and associated hydrocarbon content of mine air samples analyzed.

Defining the performance of Sewergate ventilation, particularly on Phalen 7 East. Sewergate ventilation is a marriage between a typical 'U' and a bleeder ventilation system. Underground measurements including a novel use of 'tubebundles', have provided a clearer understanding of factors affecting Sewergate performance.

This research has helped mine operators to control methane-related production delays to tolerable levels. In particular two principal factors have influenced methane emissions on 7 East longwall at Phalen Colliery: the predominant thickness (>20 m) and proximity of the Lower Sandstone Unit (<4 m) and the Sewergate ventilation system employed. In future, triple entry ventilation (UK style) and methane drainage will have to be considered if Phalen Colliery is to mine longwalls below 850 m in depth.

RÉSUMÉ

Études sur le méthane et la ventilation dans les mines de charbon du bassin houiller de Sydney, en Nouvelle-Écosse

Pendant des siècles, le charbon a constitué pour les humains la principale source de chaleur et d'énergie. L'extraction de ce précieux combustible dépendait toujours de la mesure dans laquelle on pouvait contrôler des dangers comme les venues d'eau et la présence de poussières explosives et de méthane. Une part importante de la recherche a porté sur le méthane et, entre autres, sur les propriétés méthanogènes des couches, sur les essais sur place et en laboratoire, sur les émissions de méthane, sur l'étude des questions opérationnelles (par exemple, Phalen 7 East) et sur l'affinage des modèles prévisionnels.

Au-dessous de 600 m, les couches Phalen et Harbour du bassin houiller de Sydney sont classées comme grisouteuses, leurs émissions spécifiques étant de l'ordre de 10 à 15 m³/tonne. Les recherches ont surtout porté sur l'augmentation des émissions de méthane avec la profondeur et sur l'effet de cette augmentation sur les chantiers plus profonds.

Dans cette thèse, on donne un aperçu des recherches sur le méthane et la ventilation et plus particulièrement sur les aspects suivants:

Définition des caractéristiques des couches de charbon: émissions spécifiques - relation entre la teneur en méthane, le «rang» du charbon et la profondeur, le gradient géothermique, la pression du gaz dans les couches, et la teneur en hydrocarbures apparentés des échantillons d'air de mine analysés.

Définition de la performance de la ventilation de type «égout» (Sewergate ventilation), en particulier dans la galerie Phalen 7 East. Ce type de ventilation allie les caractéristiques d'un système de ventilation typique en U et d'un système de ventilation de purge. Des mesures effectuées sous terre, y compris une nouvelle utilisation de «faisceaux tubulaires», ont permis de mieux comprendre les facteurs influant sur la performance de la ventilation de type «égout».

Cette recherche a aidé les exploitants à diminuer à des niveaux tolérables les retards de production causés par la présence de méthane. Plus particulièrement, deux facteurs principaux ont influé sur les émissions de méthane lors de l'exploitation par longues tailles dans la galerie 7 East de la mine Phalen: l'épaisseur prédominante (≥ 20 m) et la proximité de l'unité inférieure de grès (< 4 m), et le système de ventilation de type «égout» qui y était utilisé. À l'avenir, il faudra envisager la ventilation à triple entrée (du type utilisé au R.-U.) et le drainage du méthane, si l'on décide de procéder à l'exploitation par longues tailles à des profondeurs de plus de 850 m dans la mine Phalen.

ACKNOWLEDGEMENTS

The author would like to acknowledge the following people and organizations for their support during the preparation of this Thesis:

A special thank you to CANMET management and staff, especially those at the Sydney Laboratory. To David Forrester, program manager of the Coal Mine Health and Safety Program, for his encouragement in conducting my research work. To Danny Chipman, Mine Environment Technologist, for his major contribution to this research as presented herein and for his strong support and understanding through out the past years.

To Dave Genter, Ventilation Engineer, Cape Breton Development Corporation Phalen mine, thank you for your support of this research over the years.

To Ferri Hasani, Director of Mining and Metallurgical Engineering, McGill University, thank you for this opportunity to obtain my Masters Degree at McGill and for your support through the last two years.

To Malcolm J. McPherson, Dean of Engineering, Virginia Polytechnic Institute and State University, thank you for the opportunity to study under your direction. Your hospitality and professional demur will not be forgotten.

Finally, to my son Jarrett and daughter Christen, I thank god for you. Your good behavior and loving support while I was studying has made me very proud of you as always.

Last, but not least, to my wife Jacqueline and soul partner. This Thesis is yours as well as mine. Thank you for your love, trust and understanding during this Thesis study and preparation.

TABLE OF CONTENTS

TABLE OF CONTENTS

LIST OF FIGURES

LIST OF TABLES

1.0	INTRODUCTION	18
2.1.0	Sydney Coalfield	22
2.1.1	Formation of coal	23
2.1.2	Geological setting of the Sydney Coalfield	24
2.1.3	Facies changes in the Sydney Coalfield	25
2.1.4	Coal rank	27
2.1.5	Coal rank determination	28
2.1.6	Phalen mine	29
2.2.0	Coalbed gases	30
2.2.1	Origin of coalbed gases	30
2.2.2	Variation of coal gas content with coal rank	32
2.2.3	Gas content of coal seams in the Sydney Coalfield	33
2.2.4	Coal gas content of coal face lump samples	34
2.2.5	Coal gas content determination	35
2.2.6	Methane isotherm of coal	37
2.2.7	New methane isotherm method	38
2.2.8	Modeling adsorption on coal, Langmuir analysis	42
2.2.9	Methane isotherm of Geological Survey of Canada coal samples A and B	44
3.0	Estimate of in-situ gas content of a coal seam	46
3.1	Creedy's method for estimating in-situ gas content of coal	46
3.2	Creedy's estimates of Harbour and Phalen coal seams	46
3.3	Previous measurements of the in-situ gas pressure of the Phalen coal seam	52
3.4	H ₂ borehole methane isotherm temperature and pressure corrections	53

3.5	Estimate of in-situ gas pressure for the Phalen coal seam by isotherm analysis	58
3.6	In-situ gas content versus depth of coal seams in the Phalen mine	60
3.7	An in-situ gas content curve for the Phalen coal seam	61
4.0	Methane prediction methods	63
4.1	European	63
4.2	North American methods	65
4.3	Airey's Prediction model	66
4.4	Simplified Airey's method	73
4.5	Model limitations	74
4.6	Methane prediction for Phalen mine 4 and 5 East districts	78
5.0	Coal mine ventilation	
5.1.0	Phalen mine ventilation	84
5.1.1	Z and Bleeder Deep U ventilation	85
5.1.2	Sewergate ventilation system	87
5.1.3	BM Methane sensor locations	88
5.2.0	Methane patterns databases	90
5.2.1	BM methanometer sensitivity	90
5.2.2	Ventilation measurements	93
5.2.3	Anemometry versus tracer gas	93
5.2.4	Methane flow and specific emissions calculations	95
5.3.0	A comparison of the methane emissions and ventilation system	96
5.3.1	Methane emissions from the face, Bleeder Deep U and Sewergate ventilation	102
6.0	Comparing measured and predicted methane emissions	105
6.1	Phalen 4 and 5 East emissions from the adjacent strata of the worked seam	108

7.0	Sewergate ventilation	
7.1	Principal of operation	111
7.2	Phalen 7 East longwall - Case study	112
7.3	7 East Seweragate performance	114
7.4	Lower Sandstone Unit as a gas source	115
7.5	Water and gas emissions from the undermined Lower Sandstone Unit	117
7.6.0	Tubebundle experiment - 7 East Top Level	119
7.6.1	Differential air pressure measurements	120
7.6.2	Tracer gas determination of neutral point of 7 East Top Level gob	123
7.6.3	Channel flow in 7 East Top Level	129
7.7.0	45 m Tubebundle experiment - 7 East Wall Face	130
7.7.1	45 m Tubebundle layout	131
7.7.2	Final results	134
7.8	Observations of the Fabricated Back Return System	135
7.9	Composition of gas/air mixtures in the of 7 East gob	135
8.0	Methane flow and caving processes of the longwall gob	141
8.1	Longwall Mining	142
8.2.0	Caved material volumetric relationships	142
8.2.1	Composition of caved gob rock	143
8.3	Porosity of caved material	145
8.4	Bulking factor as a function of compressive stress and caved rock shape	145
8.5	Phalen gob compaction	146
8.6.0	Methane flow into the gob	147
8.6.1	Models for airflow in porous mediums	148
8.6.2	Fluid flow through porous mediums	149
8.6.3	Laminar and turbulent resistances in porous mediums	151
9.0	V-Net Model - Phalen Sewergate	154

10.0	Conclusions and Recommendations	163
10.1	Conclusions - Measured and predicted methane emissions from Phalen mine	163
10.2	Conclusions- Sewergate Performance – phalen 7 East	164
10.3	Summary Conclusions	166
10.4	Recommendations for Phalen 8 East	167

REFERENCES

LIST OF FIGURES

2.1	Regional geology of Sydney Coalfield	22
2.2	Structural development of the western part of the Sydney Coalfield	24
2.3	Relative position of coal seams of Lingan and Phalen mine	26
2.3a	Phalen mine layout	29
2.4	Water displacement apparatus used to measure desorbed gas	35
2.5	Gas content of coal – mills and roller apparatus	36
2.6	Methane isotherm apparatus	39
2.7	Void measurement apparatus	40
2.8	Methane isotherm of Phalen 8 East Bottom coal sample	44
3.1	Geothermal gradient of the Phalen coal seam	55
3.2	Extrapolation of Patching's and Mickhail's temperature and pressure correction factors for bituminous coal	56
3.3	Methane isotherm for H2 borehole sample before and after application of temperature and pressure correction corrections	57
3.4	Langmuir pressure/volume versus pressure plot for H2 borehole sample	58
3.5	Gas content estimates Phalen mine's 4, 5, 6 East and Lingan 12 and 13 East districts, borehole 140 and H2 methane isotherm estimate from Figure 3.4 versus depth	58
3.6	Langmuir type analyses plot of $0.84 \times \text{hydrostatic head}$ /in-situ gas content versus $0.84 \times \text{hydrostatic head}$	60
3.7	In-situ gas content versus depth model for coal seams adjacent to the Phalen district derived from the equation in Figure 3.6	61
4.1	Airey model of gas desorption measurements from Donkin Harbour seam coal core sample	67
4.2	Distribution of gas, strain and t_0 in coal seam	69
4.3	Degree of gas emission function for MRDE prediction method with correction for depth of working	71

5.1	Phalen mine layout	84
5.2	Phalen mine Z type ventilation layout and methane monitoring locations	85
5.3	Phalen mine Bleeder Deep U ventilation layout and methane monitoring locations	86
5.4	A Sewergate ventilation layout	87
5.5	Phalen 7 East Sewergate ventilation layout and methane monitoring locations	89
5.6	Specific emissions and and run of the mine tonnes per shift at Phalen 4 East Face, Bleeder Deep U ventilation	97
5.7	Specific emissions and run of the mine tonnes per shift at Phalen 5 East Face, Bleeder Deep U ventilation	97
5.8	Specific emissions and run of the mine tonnes per shift at Phalen 7 East Face, Sewergate ventilation	98
5.9	Specific emissions and run of the mine tonnes per shift at Phalen 4 East Top (outside end), Bleeder Deep U ventilation	99
5.10	Specific emissions and run of the mine tonnes per shift at Phalen 5 East Top (outside end), Bleeder Deep U ventilation	99
5.11	Specific emissions and run of the mine tonnes per shift at Phalen 6 East Top (outside end), Sewergate ventilation	100
5.12	Specific emissions and run of the mine tonnes per shift at Phalen 7 East Top (outside end), Sewergate ventilation	100
5.13	A comparison of methane flow for Phalen 4, 5 and 7 East Face emissions	101
5.14	A comparison of methane flow for Phalen 4, 5, 6 and 7 East Top (outside end)	101
6.1	Measured versus Predicted methane flow from coal seams in the adjacent strata of Phalen 4 East district	108
6.2	Measured versus Predicted methane flow from coal seams in the adjacent strata of Phalen 5 East district	109
7.1	7 East fabricated back return system (not to scale)	113

7.2	7 East Sewergate performance	115
7.3	Specific gob emissions versus wall face location and Lower Sandstone Unit iso-pache	116
7.4	Methane emissions and water flow from roof strata of Phalen 7 East district prior to first major roof fall	118
7.5	Tubebundle experiment Phalen 7 East Top Level	119
7.6	Differential air pressure measurements between stations no. (1 and 2), (2 and 3), (3 and 4), and (4 and 5)	120
7.7	Differential air pressure measurements between stations no. (6 and 7), (7 and 8), (8 and 9), and (9 and 10)	121
7.8	Neutral point in gob versus sandstone height above coal seam	122
7.9	Neutral point in gob versus sandstone thickness above coal seam	122
7.10	Projected air pressure drop across the gob from station no. 10 to the face start line	123
7.11	7 East top neutral point study - 28 m inby the T-junction (August 28, 1996)	124
7.12	7 East top neutral point study - 32 m inby the T-junction (August 30, 1996)	125
7.13	7 East top neutral point study - 26 m inby the T-junction (November 5, 1996)	126
7.14	7 East top neutral point study - 28 m inby the T-junction (November 7, 1996)	127
7.15	7 East top neutral point study - 12 m inby the T-junction (March 3, 1997)	128
7.16	7 East top neutral point study - 15 m inby the T-junction (March 23, 1997)	128
7.17	Tracer gas study of Phalen 7 East Top Level gob - Channel flow and air velocity	129
7.18	45 m tubebundle location and tracer gas release system on face support	131
7.19	Differential pressure drops along the face and 45 m tubebundles	133

7.20	% Methane + % Ethane of samples collected behind the T- junction from tubebundle stations in the gob	136
7.21	Methane / Ethane ratio of samples collected behind the T- junction from tubebundle stations in the gob	138
8.1	Zingg's diagram showing classification of different shapes associated parameters (after Krumbain and Sloss, 1963)	144
8.2	Spacially periodic structures and particle for modelling porous medium	148
8.3	Airflow pathways in two orthogonal directions for constructing a grid pattern for mine airflow analysis	149
8.4	Grid pattern for airflow in two orthogonal directions representing the gob	149
9.1	V-net - Model of Phalen mine ventilation system	154
9.2	V-net - Gob model of Phalen 7 east	155
9.3	V-net - Model of Phalen 7 East - High resistant gob	157
9.4	V-net model of Phalen 7 East - 1st stage of reduced upper gob resistance	158
9.5	V-net model of Phalen 7 East - 2nd stage of reduced upper gob resistance	159
9.6	V- net model of Phalen 7 East - 3rd stage of reduced upper gob resistance	160

LIST OF TABLES

Table 3.1	Creedy's estimate of in-situ gas content for Phalen mine 4 East coal seam	47
Table 3.2	Creedy's estimate of in-situ gas content for Phalen 5 East coal seam	48
Table 3.3	Creedy's estimate of in-situ gas content for Phalen mine 6 East coal seam	49
Table 3.4	Creedy's estimate of in-situ gas content for Lingan mine 12 East coal seam	50
Table 3.5	Creedy's estimate of in-situ gas content for Lingan mine 13 East coal seam	51
Table 3.6	In-situ gas content estimates for the Harbour and Phalen coal seams	52
Table 3.7	In-situ gas pressure measurements and composition of the Phalen coal seam and Lower Sandstone Unit	52
Table 3.8	Proximate and vitrinite reflectance test results for H2 coal sample for 1978 and present	54
Table 3.9	Calculation of the percentage reduction in adsorption capacity for methane isotherm on H2 borehole coal based on Patching's and Michail's extrapolated temperature and pressure correction curve of Figure 3.2	56
Table 3.10	Final results of methane isotherm correction for H2 borehole isotherm	57
Table 4.1	Borehole log data for the Harbour, Boutillier, Backpit, Phalen and Emery coal seams	75
Table 4.2	Depth correction values for the coal seams of table 4.1	76
Table 4.3	Airey's emission factors for coal seams adjacent to the working seam of Phalen 4, 5 and 7 East districts	76,77
Table 4.4	Airey predicted specific emissions factors for coal seams adjacent to the 4 East district	79

Table 4.5	Airey predicted specific emissions factors for coal seams adjacent to Phalen 5 East district	80
Table 4.6	Airey predicted specific emissions factors for coal seams adjacent to Phalen 7 East district	81,82
Table 5.1	BM methane sensor calibration checks and sensitivity	91,92
Table 5.2	Anemometry versus Tracer gas determined air quantities	94
Table 6.1	Predicted and measured methane flow from coal seams in the adjacent strata to Phalen 4 East district	106
Table 6.2	Predicted and measured methane flow from coal seams in the adjacent strata to Phalen 5 East district	107

Introduction

Introduction

In order to plan the future ventilation requirements of a coal mine it is essential to have knowledge of the in-situ gas parameters in order to predict methane emissions. Despite the long history of gassy mines in the Sydney Coalfield, very little data is available on the in-situ parameters that lead to these emissions. An extensive review of the mine ventilation records at CBDC's now closed Lingan mine, located in the Harbour seam, reported specific methane emissions from all gas sources of 20 to 40 m³/tonne (Kochhar and Konda., 1985), while others gave reported much lower values of 4.1 to 12.8 m³/tonne for Phalen and Lingan mines respectively (Cecala, Konda, and Klinowski., 1988).

In late 1989, the CANMET Cape Breton Coal Research Laboratory (CBCRL) and the Cape Breton Development Corporation (CBDC) initiated the methane release patterns program. Its purpose was to collect methane emissions data from the ventilation network of CBDC's longwall panels to be stored in a long-term computer database. This data base of methane emissions, ventilation and production records may be used by CBDC engineers and CBCRL researchers to determine future mine ventilation requirements.

Methane emissions data was collected on a continuous, real time basis from CBDC methane underground sites within selected longwall panels. The data were collected from CBDC's methane monitoring system by analog voltage data recorders, which acted as storage devices for methane emission measurements. This data was retrieved, and processed and put into permanent computer databases or storage.

The second part of the methane studies has been to determine the in-situ gas content of the Harbour and Phalen coal seams in CBDC mines by several methods. Gas content is a critical parameter required to simulate or predict methane emissions from coal during mining. The majority of the effort has been in the collection of wall face "Lump samples" for the determination of gas content according a slightly modified direct method which has led to the development of a large data base of gas contents and associated proximate

analysis results. Through various statistical approaches estimates of in-situ gas content of the coal seam can be made.

To a much lesser extent because of the inability to retrieve quality coal core from in-seam drill holes, the direct method has been employed where a few coal core samples have been collected, desorbed, and tested for residual gas content to provide an estimate of in-situ gas content.

Finally, the indirect method has been used which utilizes the determination of the in-situ gas pressure of the coal seam with the relevant adsorption isotherm of the coal (Curl, 1978). CBCRL has developed a procedure to determine the methane isotherm of a pulverized coal sample and have conducted one measurement of the in-situ gas pressure of the Phalen coal seam. The packing of the borehole was only partially successful and suffered a high-pressure leak at 1.55 MPa (225 psia). The report will present a description of both the calculations of methane flows from databases and will comment on the accuracy of airflow and methane measurements made by anemometry and BM type continuous methanometers.

It will also describe the testing methods for the determination of methane isotherms of coal and the in-situ gas content of the Phalen and Harbour coal seams. This gas content relationship was used to obtain the following:

- (1) Description and comparison of Airey's predicted methane flow from coal seams in the adjacent strata of Phalen's 4 and 5 East coal districts versus measured flows.
- (2) Comparison of methane flow for Bleeder Deep U and Sewergate ventilation as measured at Phalen mine 4, 5, 6 and 7 East return airways. Bleeder Deep U Ventilation in other conventions is known as a variant of "Y" Ventilation (McPherson, 1993).

Finally, a case study of 7 East Sewergate Ventilation was conducted to determine its performance (methane capture) and includes the following:

- (1) Methane Monitoring
- (2) Tubebundle and tracer gas experiments
- (3) Sewergate performance based on methane prediction model.
- (4) Theoretical discussion on gas and air flow in a gob
- (5) Mechanisms of airflow from the gob to the return airway using V-Net

Sydney Coalfield

2.1 Sydney Coalfield

The Sydney Coalfield sits on the Northeast end of the province of Nova Scotia, Canada (Figure 2.1).

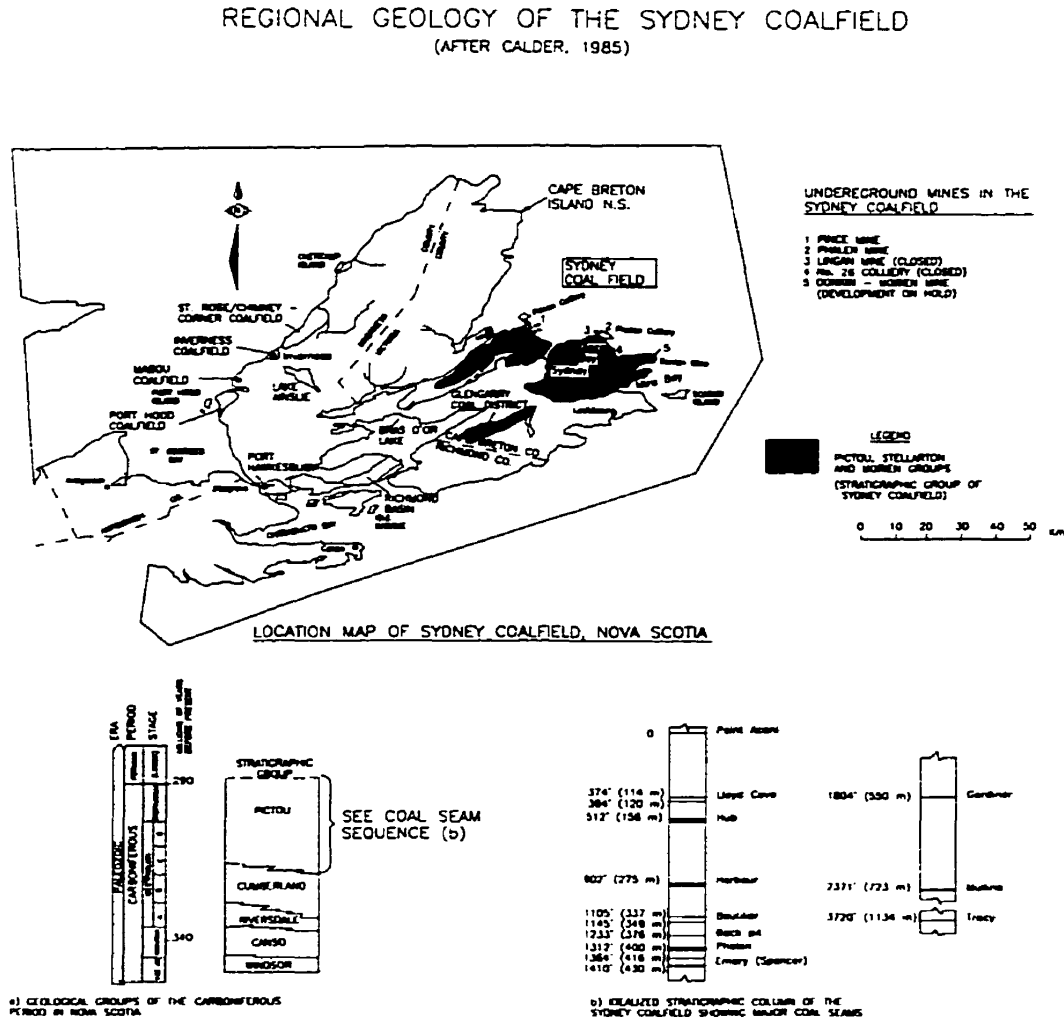


Figure 2.1 Regional geology of Sydney Coalfield (Coal in Nova Scotia, 1985)

The coalfield has been extensively mined under a small land area, but the majority of the mined area has been submarine. The coal mines are considered gassy and ventilation planning is inhibited by the submarine nature of the workings where ventilation shafts fall further away as mining proceeds under the sea. As much as

half of the known coal reserves available remain un-mined because it is neither economically, nor technically possible to proceed to further depths.

2.1.1 Formation of coal

Coal is a combustible sedimentary rock composed of microscopic organic constituents derived from the compaction and induration of plant remains and inorganic mineral matter. The formation of coal deposits depended on specific characteristics of tectonic setting, geographical location, climate and flora, permitting the development of swamps. Coalification therefore refers to the progressive transformation of peat through lignite, brown coal, sub-bituminous, bituminous and anthracite coals.

Most coalbed gases are generated during the progressive burial and maturation of the coal (Coalification). The major gas components generated from coalbeds include methane, carbon dioxide, nitrogen, and wet-gas components (ethane, propane, etc.) (Walker, 1993).

2.1.2 Geological setting of the Sydney Coalfield

The Sydney Coalfield is located in north Eastern Nova Scotia on the Island of Cape Breton. It consists of two parts: a small land area of about 520 km² and a region where mining is carried out below the sea (Figure 2.2). Both form part of a large Carboniferous basin that extends almost as far as Newfoundland, occupying some 36,300 km² and is referred to as the Sydney basin.

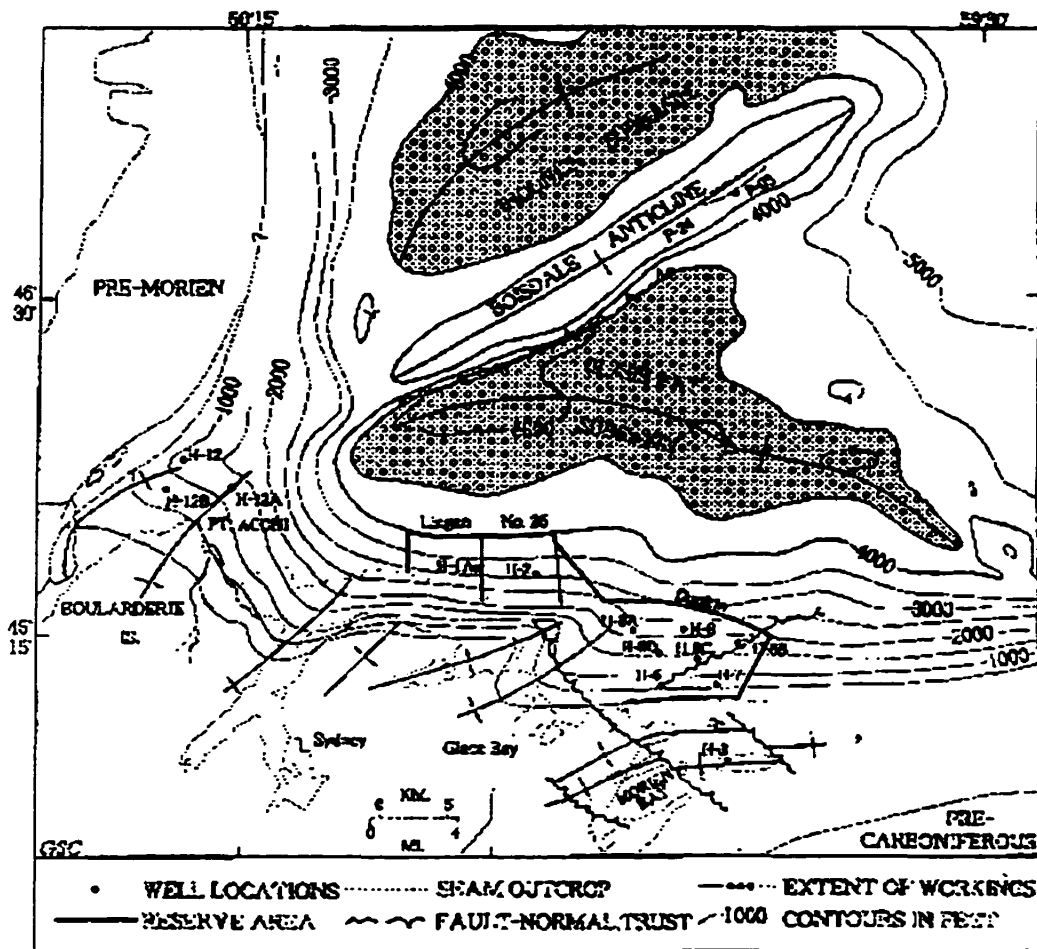


Figure 2.2 Structural development of the western part of the Sydney Coalfield (Hacquebard, P.A., 1976)

Coal measures reach a maximum thickness of 2200 m and contain thirteen seams that are 0.9 to 4.3 m thick. The coal bearing rocks are Pennsylvanian in age. All but the youngest three coals, two of which do not outcrop in the land area, have been mined. The two most productive seams have been the Harbour and Phalen seams, which have been worked extensively since the early 1900's in the submarine area adjacent to the coast (Hacquebard, P.A., 1964).

Tectonic development of the Sydney Coalfield has been comparatively gentle, and serious structural dislocations have not been encountered in mine workings. Structurally the field is relatively simple and, except for local folding, is essentially saucer shaped with the beds dipping toward the deeper and central parts of the basin. The folding was initiated by warping during deposition. Deposition of the coal seams and accompanying fluvial and fluvial lacustrine sediments took place in a valley flat or floodplain environment. The distribution of clastic sediments was controlled entirely by river courses and their transporting powers (Hacquebard, P.A., 1964).

Coal seams in the Sydney Coalfield are uniform and show relatively minor fluctuations in ash content. They are, however, relatively high in sulphur content.

2.1.3 Facies changes in the Sydney Coalfield

Coal seams (Figure 2.1) in the Sydney Coalfield are uniform and show relatively minor fluctuations in ash content within and between seams. Peat formation appears to be centred in the Glace Bay sub-basin and spread westward because of the greater influx of clastic sediments in the western area (Figure 2.2).

The following describes in general the coal seams of interest for this report and will be further described from borehole logs of seams thickness and depths relative to Phalen mine (Figure 2.3).

Backpit Seam The Backpit has a mineable thickness of between 0.9 and 1.5 m. The ash content is ~ 11 %, 8% sulphur. This seam represents the most continuous and wide spread peat formation in the coalfield.

Phalen seam Next to the Harbour seam, the Phalen seam is the most extensively worked coal seam. Because of splitting it has a variable mining thickness of between 1.5 to 2.1 m. The mined areas indicate an ash content of between 3 and 8 %. Sulphur content ranges from 2 to 4%.

Emery Seam The Emery seam is the thinnest mined seam in the coal field. The mined portion is between 0.9 and 1.2 m, and is actually the middle bench of a much thicker seam farther east in the Port Morien district. The ash content is in the 8 % range. In a westward direction the middle bench thins and disappears (Hacquebard, P.A., 1976a).

The uniform nature of coal seams and the absence of structural disconformities make the coalfield a good candidate for methane emissions modeling.

2.1.4 Coal rank

The rank of a coal is the degree or stage the coal has reach during its Coalification; that is, the degree of metamorphism or geochemical maturity. Coalification represents the natural chemical and physical transformation of peat into coal, firstly, by biochemical processes and subsequently by geochemical processes, which are predominantly controlled by increases in temperature, pressure and time that accompany the progressive burial of coal by sediments within a subsiding basin. The Coalification process can be accelerated by subsequent exposure of the coal seams to extremes of heat, such as localised igneous intrusions. Pressure, a less important factor in the Coalification process than temperature usually results from orogenic movements, which also cause folding and faulting. Rank and coal are not, therefore, purely a result of age, original plant material and subsequent tectonics (Walker, S., 1993).

2.1.5 Coal rank determination

Reflectance: Reflectance is defined as the percentage of vertically incident light reflected from a highly polished surface. This can be used to determine the rank of coal and degree of Coalification. It is important to note that at all ranks there is considerable natural variation in vitrinite reflectance that is due to factors other than thermal history. The types of plants, depositional environment, and the type of gelification or humification that took place. (Jones Jones, J.M., Davis, A., Cook, A.C., Murchison, D.G., and Scott, E., 1984).

For the purpose of coal rank determination, reflectances are normally measured at 546 nm, on a band-type vitrinite in oil immersion medium ($R_{o,vit}$). The reflectance of huminite /vitrinite maceral increases more or less steadily through Coalification and is therefore commonly used as a coal rank parameter. Macerals are the microscopically recognizable constituents of coal that originate from the organs or tissues of plants (e.g. spores, algae, bark). All macerals contain the suffix $R_{o,vit}$ designation (ICCP, 1971).

Pyrolysis (Proximate Analysis). The most widely used Pyrolysis techniques used to classify coal rank are proximate analysis. According to proximate analysis, coal can be divided into four products, moisture, volatile matter, fixed carbon and ash. These four products form the basis for ASTM's rank parameter for the classification of medium to high rank coals. Proximate analysis is analogous to coalification, in that both processes liberate volatile products rich in hydrogen and oxygen, leaving behind a residue rich in fixed carbon (Law, B.E., and Rice D.D., AAPG, 1993).

In the Sydney Coalfield coalification is predominantly post-deformational. (Hacquebard and Donaldson, 1976b) showed that the rank of coal increases with the present depth below the surface, but does not alter in surface exposures in relation to stratigraphic occurrence.

From studies in a series of surface coals exposed in cliff sections of the Sydney Coalfield the rank (as measured by vitrinite reflectance) does not increase with the

stratigraphic depth. Also, from boreholes and underground mine studies, the rank of individual seams increases with the depth of mining (Hacquebard and Donaldson, 1976b). To conclude, the coal obtained its present rank from the maximum overburden that existed after deformation.

2.1.6 Phalen mine

Phalen mine is one of two underground collieries operated by the Cape Breton Development Corporation in Nova Scotia. The mine produced approximately 1.4 million tonnes of coal in 1997 from the 2.6 m thick Phalen seam by retreating longwall method. The workings are submarine.

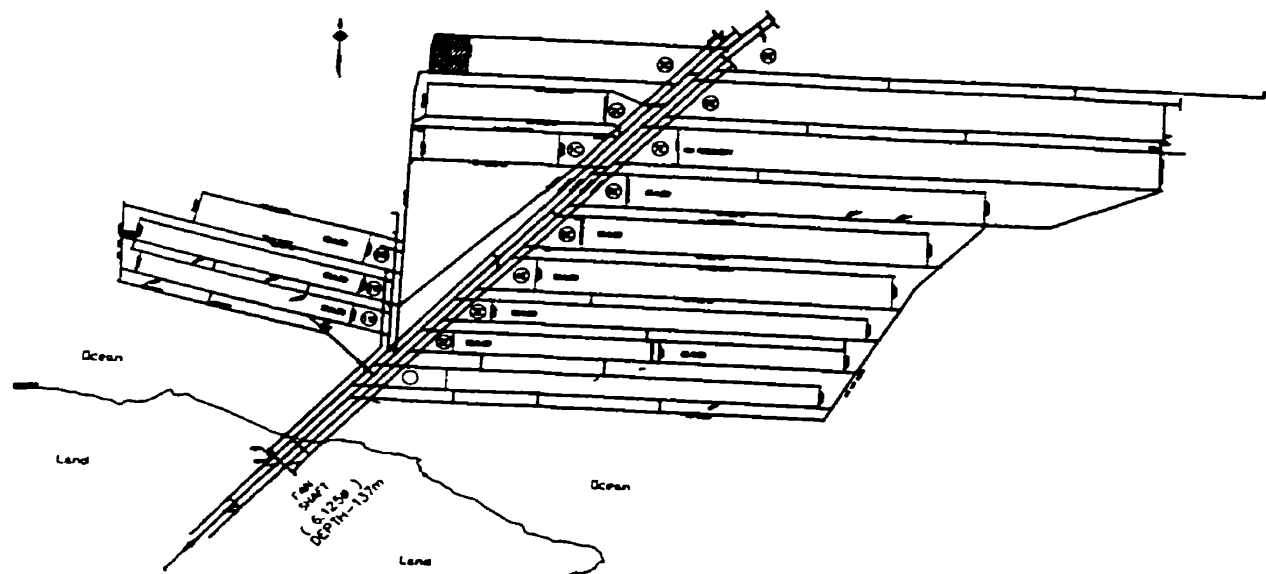


Figure 2.3a Phalen mine layout

Phalen mine is a 'slope' mine, which are driven beneath the seabed. The main slope system, driven down-dip, divides the mine reserves into three blocks termed Westside, Centre, and Eastside.

A Howden centrifugal fan provides ventilation at Phalen with variable inlet vanes exhausting at 200 m³/s and 5-kPa water gauge. Phalen currently operate a system of retreat longwall mining with single entry development of intake and return

airways. Each wall is supplied with 25 to 30 m³/s of air. The faces are connected to a Sewergate (collapsed tailgate) road where gob produced methane migrates through a collector roadway to an abandon bleeder roadways where it is discharged and diluted below 2% in the system's main return airways. This ventilation arrangement is known as Sewergate ventilation and will be discussed extensively in section 7.

2.2.0 Coalbed gases

Gases normally associated with coal have common names such as firedamp, and in the majority of cases this is synonymous with methane which usually makes up 90 % of most coal gas composition. However, coal related gases vary in composition which are further described in the following section.

2.2.1 Origin of coalbed gases

Previous studies on the origin of coalbed gases have generally assumed that coalbed gases are predominantly thermogenic and that biogenic gases, when recognised, in coalbeds were generated during the early stages of Coalification (peatification).

The generation of thermogenic coalbed gases can be separated into early thermogenic and main-stage thermogenic stages. Early thermogenic gases are generated from coal beds during high-volatile bituminous coal rank (R_m between 0.50 and 0.80) before the threshold of thermogenic methane generation is reached. Laboratory pyrolysis of lignite indicates that an economic threshold for methane generation is not reached until vitrinite reflectance values of approximately 1.0% are attained.

Using data from a variety of United States and German coals, the economic quantities of methane (9 cc/g) occurs during the formation high-volatile A bituminous rank between vitrinite reflectance values of 0.8 and 1.0% (Scott, A.R., 1993). This value of gas content is similar to those reported for Sydney Coal field with R_o of 1.0%.

Carbon dioxide is released from the coal structure during coalification, (128 cc/g) for peat-through anthracite range. Over 50% of the total carbon dioxide generated from the coal is released before the high volatile A bituminous rank. There is very low CO₂ content in the coal seams in the Sydney Coal field (Scott, A.R., 1993).

A possible source of CO₂ in the Lower Sandstone Unit of Phalen mine may originate from bicarbonate-rich formation waters which liberated carbon dioxide when the pressure had been relieved from the system (Walker, S., 1993). CO₂ content in Phalen mine air has been found to increase significantly when undermining thick sandstone beds, which periodically release large quantities of formation water when distressed.

Ethane, propane, butane, pentane, and heavier n-alkanes hydrocarbon gases are generated from hydrogen-rich coals during coalification. In the Sydney Coalfield, higher hydrocarbons have been associated with coal and sandstone. The source of the gas in the sandstone can be from a combination of coaly material in the sandstone or from adjacent coal seams. Gas outbursts have occurred when the sandstone bed has intersected the coal seam. It's possible that at this point, the sandstone acts as a carrier bed for hydrocarbons excluded from the coal seam. Research in Germany has indicated that for type III keritans, from which most carboniferous coals are composed, a characteristic oil/gas window exists for coal in the volatile matter content range between 30 and 32% (Littke, R., and Leythaeuser, D., 1993). Since the Phalen coal seam is at this characteristic rank and volatile matter content, it's possible that the source of oil and gas in the sandstone has been a result of its expulsion from the coal seam at these contact points, if the porosity and permeability of the sandstone accommodate the petroleum migrating from the seam. The implications are that where a carrier bed of sufficient porosity is close enough to a coal seam that has passed through the oil gas window, then it can become a significant source of gas and hydrocarbons. The report did caution that the quantity of the oil and gas expelled depends on the coals micro-pore structure and whether it is possible for the oils and gases to

escape from the coal matrix. The sandstone bed as a significant source of hydrocarbons and gas must be considered in light of the emissions from the drilling programs (Forgeron S., 1996).

On the basis of over 985 gas analyses for 1,386 coalbed methane wells in the United States, an average coalbed gas will contain 93.2% methane, 3.1% carbon dioxide, 2.6% wet gases (ethane, propane, etc.), and 1.1% nitrogen with a heating value of 1,005 Btu/lb. However, the composition of coalbed gases can vary significantly among basins, between individual wells within basins, and vertically among different coalbeds within the same well (Scott, A.R., 1993). In comparison with the above, there is a much lower percentage of CO₂. In general, the gas composition is similar to coal gases from mining in the Sydney Coalfield i.e. Phalen 3 slope coal rib borehole gas sample contained 93.5% methane, 0.2% carbon dioxide, 3.2% wet gases (ethane, propane, etc.), and 3.3% nitrogen.

2.2.2 Variation of gas content with coal rank

The variation of gas content with coal rank has two trends. One states that methane sorption has a 'U' shaped with a minimum sorption occurring for high volatile "A" coals at ~ 62 % fixed carbon content and the other is of increasing gas content with rank (Patching, T., 981). Although common among many investigators, the U shape relationship as reported contains a large degree of data scatter, making most of the interpretations qualitative at best (Clayton, J.L., 1993). One common theme among previous test samples is the degree of moisture lost between samples and according to (Clayton after Levine, J.R.) could place the trend of increasing gas content with rank in terms of moisture alone; since, the lower rank coals contain a higher degree of moisture. Despite this, it has been generally accepted that sorption capacity increases with coal rank (Clayton, J.L., 1993). Nevertheless, the effects of coal petrology was found to have a secondary effect on the sorption capacity and depends more on the U shaped trend above and the porosity of the coal

(Levine, 1991a) has found that despite depth and ash content, the inertite and maceral content and elemental carbon to hydrogen ratio, were the most significant factors affecting gas content. (Ulery, 1988), using data from 18 boreholes studies, found no correlation between maceral content and desorption tests. Overall, there appears to be no consistent trend reported between sorption capacity and petrology. In any case the only way to relate gas content and coal rank in any coalfield is to core and retrieve a sample and perform the necessary tests.

2.2.3 Gas content of coal seams in the Sydney Coalfield

As mentioned the gas content, in general, increases with burial depth and rank. There is scant information regarding this relationship for the Sydney Coalfield. Off shore drilling exploration in the coalfield did not include any provision for gas content testing of coal samples. Most analyses were concerned with rank determining tests; therefore, a great opportunity had been lost in terms of characterizing the gas potential of the coalfield not only from a mine planning point of view but also from a commercial basis.

In terms of the Phalen resource block, some limited coring and gas content testing of samples had been conducted in 1982 (Feng and Cheng, 1982). Drilling was carried out from CBDC's No. 26 mine and had intersected the strata sequence between the Harbour seam down to and including the Phalen seam at a depth of 806 m, in the present Phalen 10 East area. From this testing, the gas content of the Back pit and Phalen seam, as well as a shale and sandstone core, was determined for the sequence.

2.2.4 Coal gas content of coal face lump samples

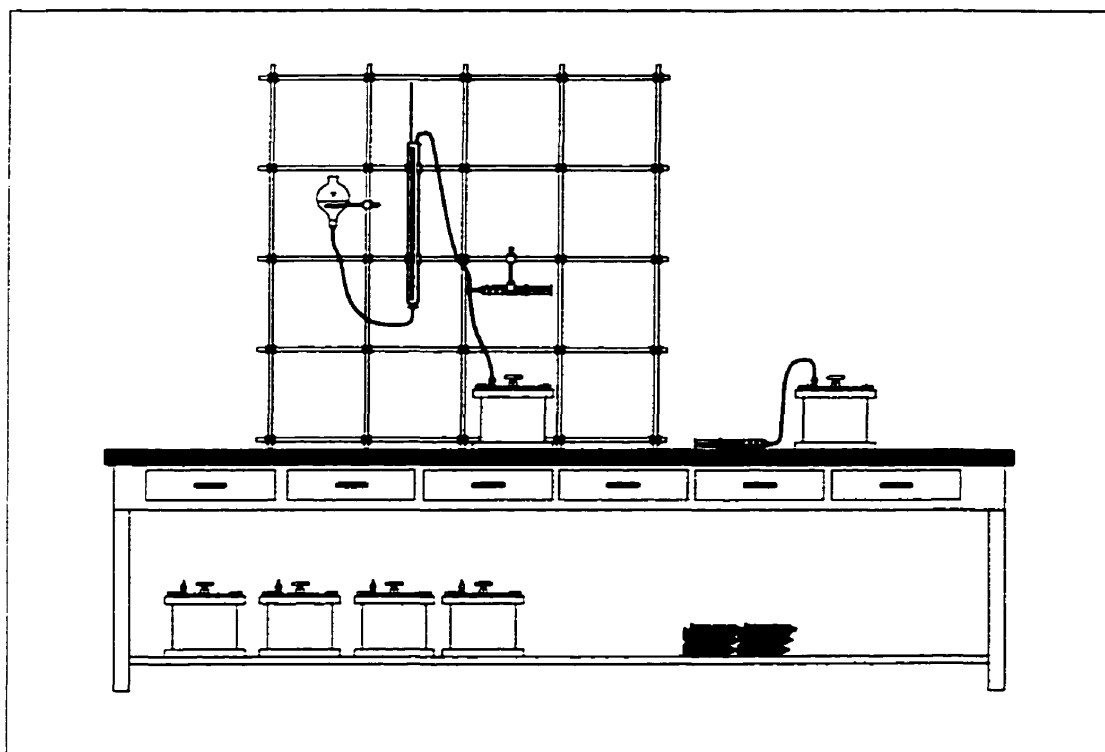
Because of the difficulty that has been associated with retrieving suitable core samples from horizontal drilling practices, CANMET have conducted sampling of coal lumps from the active wall faces of CBDC's mines.

Wall face samples have been collected from the working of Phalen 4, 5 and 6 East walls and Ligan 12 and 13 East panels. The majority of the effort has been in the collection of large coalface lumps (~25 cm cubes) during a period of active mining, over the life of each panel. Typically 5-cm cubical samples were reduced from the center portions of larger face lumps that which were removed by hand from the wall. The samples selected from the coalface were bright and blocky in appearance, normally associated with vitrane rich and tightly bonded coal lithotypes (no noticeable stress fractures from mining). Since desorption occurs through the outer surface of the samples, it's assumed that the inner most part of the sample has suffered the least amount of degassing.

Upon its retrieval, the broken sample (100-300 g) was placed in a small container and was sealed airtight with a properly applied rubber sealed screw type cover lid. The coverlid was fitted with an appropriate gas tight on/off valve for later use. Site temperature and pressure were recorded for each group of samples collected (usually 6). Because the sample was removed from the center of a larger portion, no estimate of lost gas was made since the selection of time zero would have been somewhat arbitrary. Previous testing on sample by the author and others indicate that the early desorption of Phalen and Harbour seam face coal lump was very low, typically < 0.20 cc/g for the first 60 min from time of sampling (Feng, K.K., Cheng K.C, and Augsten R., 1981). In theory, if enough of these sample types were collected, then the probability of retrieving a few samples close to the original seam gas content was possible; therefore, an estimate of in-situ gas content would be made according to certain statistical methods.

2.2.5 Coal gas content determination

The samples as collected above were then taken back to the laboratory and tested using a slightly modified direct method (Feng, K.K., Cheng, K.C, and Augsten, R., 1981). In general, the gas desorbed from the coal sample and contained in the jar was released through the on/off valve on the cover lid to a connected tygon tube attached to a water filled, graduated burette (Figure 2.5).

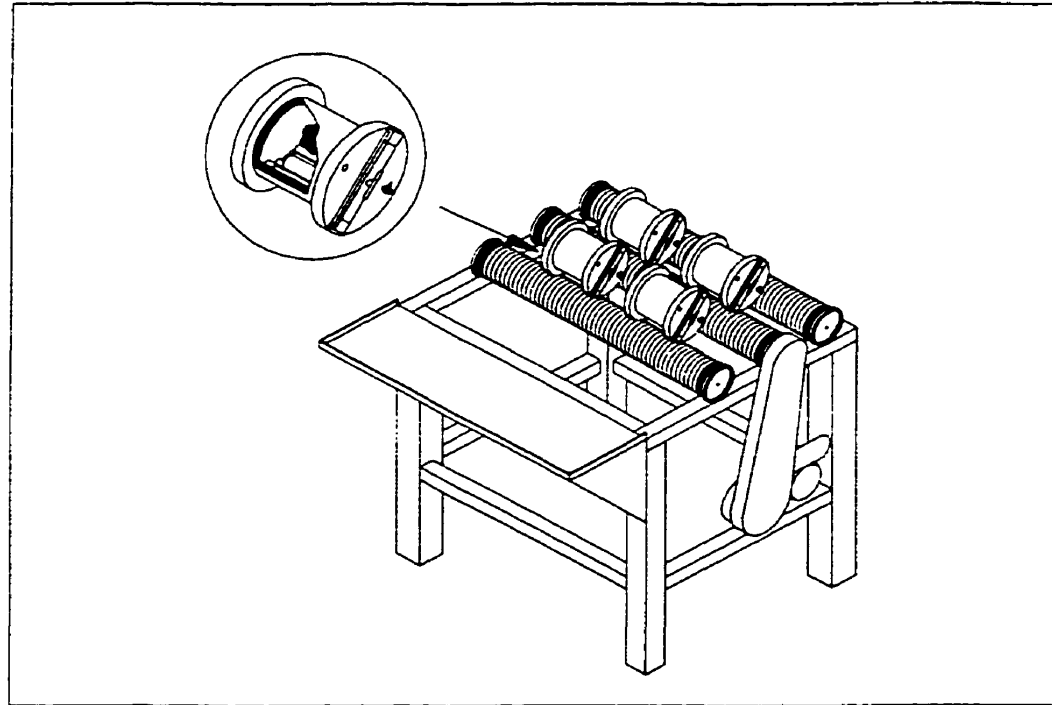


GAS TESTING LABORATORY – WATER DISPLACEMENT APPARATUS

Figure 2.4 Water displacement apparatus used to measure desorbed gas

As the gas flowed and displaced the water downward in the column, a leveling bulb connected via a tube to the base of the burette with plastic tubing collected the displaced water flowing from the base of the burette. The water level in the burette was matched with that in a water-leveling flask to maintain a pressure balance within the burette and outside air. When sufficient displacement of water had occurred, the valve was closed. The volume of water displaced, gas temperature in the burette, and laboratory barometric pressure was recorded.

This procedure was followed until desorption slowed to an imperceptible flow rate. The sample was immediately removed from the jar, weighed and placed in a rod mill, which was then closed. The internal free space of the mill was then inerted with nitrogen, and sealed. The sample was then pulverized in the mill to ~ -150 to -200 mesh on the roller apparatus where the remaining (residual) gas was released from the coal sample and its volume determined as described above (Figure 2.5).



GAS CONTENT OF COAL – MILLS AND ROLLER APPARATUS

Figure 2.5 Gas content of coal – mills and roller apparatus

Corrections were made to measured gas volumes for the expansion due to changes in temperature and pressure between the site and laboratory and for similar changes in the mill before and after crushing (Young, 1989). The final gas content is expressed in STP conditions (760 mm Hg and 0° C) in units of (cc/g) or equivalent (m^3/tonne).

2.2.6 Methane isotherm of coal

In 1994, CSL mine environment group began developing a method for conducting a methane isotherm test on a pulverized coal sample. A methane isotherm is a measure of the capacity of coal to physically adsorb methane under controlled temperature and pressure conditions.

Over the last several years CSL has measured the volume of methane contained in coal samples taken from mines located in the Sydney Coalfield. This data indicates that the

quantity of gas contained in these samples is a result of the confining gas pressure and temperature. Methane isotherms can be used to estimate the pressure of the confining gases and the capacity of in-seam coal to adsorb these gases. Along with gas content, diffusivity, and permeability, methane sorption isotherms provide one of the most critical, fundamental characteristics required for understanding, modeling and predicting the behavior of a coalbed reservoir (International Coalbed Methane Symposium, 1993).

Mining in the Sydney Coalfield has a long history and indicates that methane emissions increase with the depth of mining. It is assumed that both in-situ gas pressure and the geothermal gradient in the coalfield have a direct bearing on these emissions since both affect the capacity of the coal to physically adsorb methane. Since this relationship was essentially unknown for these coals, CSL developed its own procedure to more closely study this relationship.

A methane sorption isotherm is a measure of the coal's capacity to physically adsorb methane at a constant temperature and varying gas pressure conditions.

Volumetric techniques determine the amount of gas adsorbed by a coal sample by first determining the void of the empty cylinder and sample with helium which does not adsorb. The difference between the gas placed in the cell with and without the sample present is a measure of the coal's sorption capacity at an equilibrium pressure (Law, B.E. and Rice D.D., AAPG, 1993b). The gravimetric methods actually measure the weight change of the coal sample due to sorption. Other methods report the use of chromatographic columns but to a much lesser extent (Law and Rice, AAPG, 1993b).

The method used to test borehole H₂ sample is a combination of the volumetric and gravimetric techniques. In this method, helium is used to determine the void space of the sample container and a high capacity balance (5000 ±0.001 g) is used to measure the mass gained between successive pressurizations of the coal sample with methane. No correction is made to calculate the absolute gas content during successive measurements; therefore, the method calculates the Gibbs gas content only which only deals with the

original equilibrium state. Despite the many applications, most gas sorption data on coal rarely include or mention any corrections for sorbed phased volume. The value for sorbed volume for methane is reported as 0.375 g./cc when the gas is over its critical temperature which is the case most of the time (Law,.B.E. and Rice, D.D., AAPG, 1993b).

2.2.7 New methane isotherm method

In the usual tests for methane isotherms a standard sample size of a few grams or less is used. CSL realised that coal samples collected and tested for gas content typically weigh between 100 - 500 g. Once the gas content of one of these samples was determined, then the entire sample could be placed in the isotherm test cylinder and tested. This allows for direct comparison of the sample's gas content with the isotherm test results, eliminating any bias from sample preparation. Therefor, a new test procedure and precision built equipment were made for larger sample sizes of 100 to 500 g's (Young D.A. and Chipman D.G., 1996). Because of the large sample size, the amount of methane adsorbed onto the sample could be determined with the comparator balance which measures sample mass from 0 - 5 kg to the nearest milligram. A control cylinder allows for accurate correction of the effects of changes in air buoyancy in the balance chamber. This eliminates the need to calculate these changes from temperature, barometric pressure and humidity changes as required with other methods (Figure 2.6).

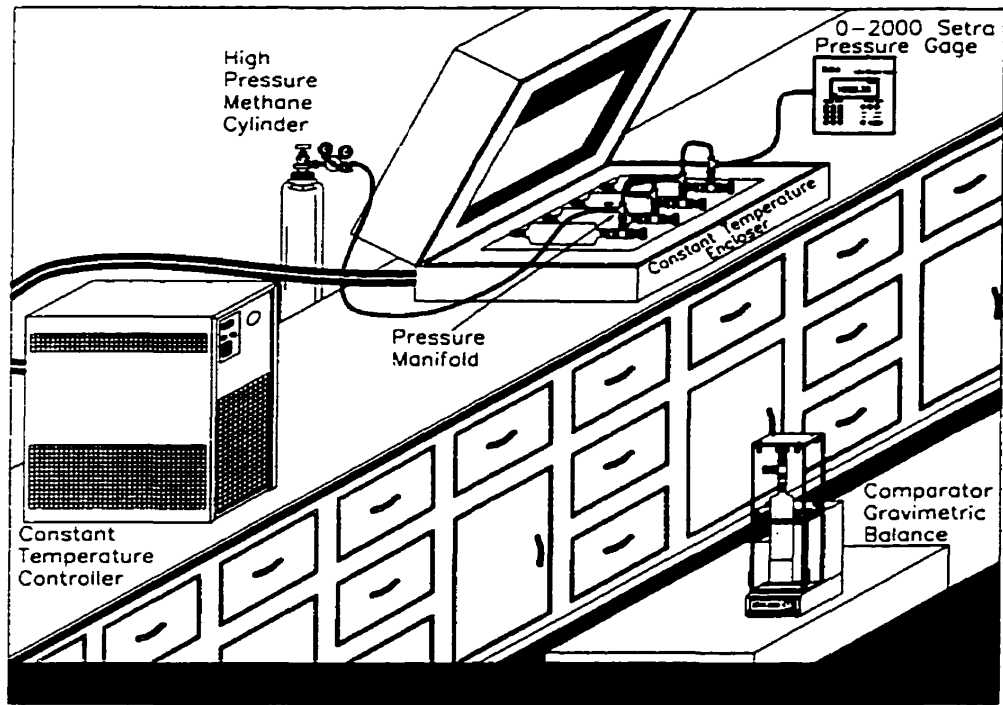


Figure 2.6 Methane isotherm apparatus

The test consists of weighing approximately a 500 g sample of coal to the nearest 0.001 g and placing it in a 1 litre steel cylinder. The sample cylinder and an identical reference cylinder of known volume, are then placed in a controlled temperature enclosure and are pressurized with methane through a common manifold. After equilibrium pressure has been established, both cylinders are weighed and the relative mass gain of each is determined. The difference between the relative weight gains of methane in relation to the void space in each cylinder is a measure of methane adsorbed by the sample. This is repeated for other pressure ranges in order to determine a methane adsorbed versus pressure relationship. The cylinder is then evacuated and purged with helium to remove residual gases, and then pressurized with helium to determine its internal void space. Figure 2.7 shows the void measuring device with the vacuum, helium gas supplies and the sample cylinder.

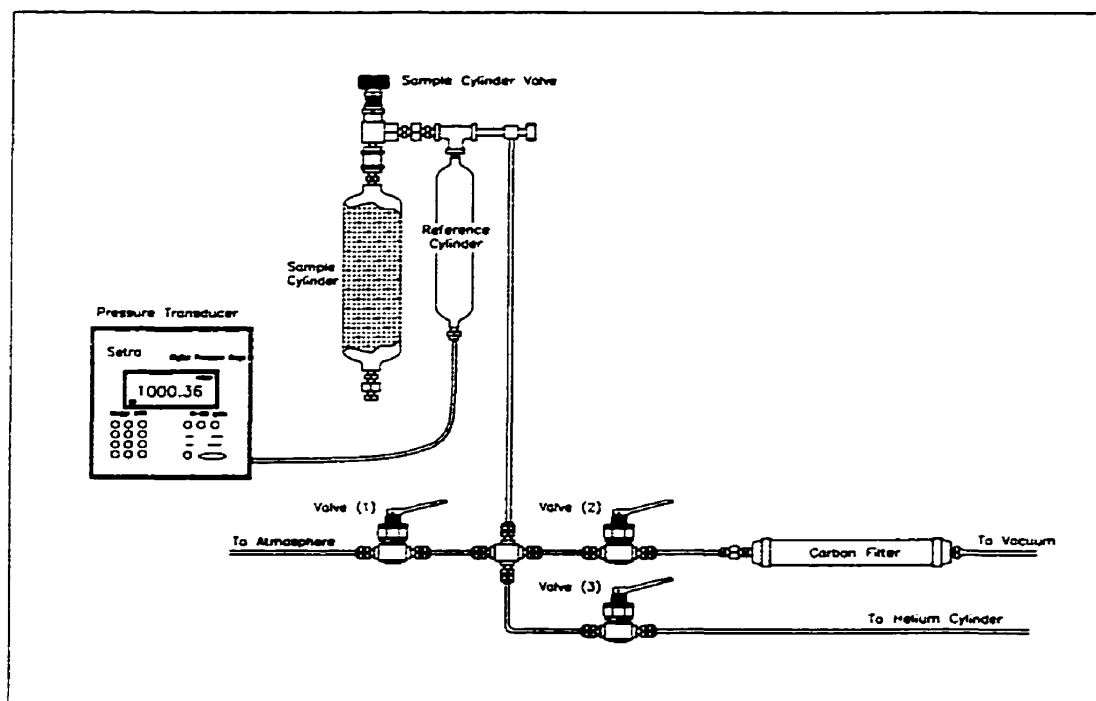


Figure 2.7 Void measurement apparatus

It is very important at this step to vent the methane contained in the sample cylinder from the isotherm test in a slow and controlled manner to an area outside the lab, preferably out of an open window away from any sources of ignition.

The cylinder is evacuated and purged with helium to remove residual gases, and then pressurized with helium to determine its internal void space. The void space is determined by measuring the pressure drop from the sample cylinder to a known volume cylinder at constant temperature. Prior to conducting this test the sample cylinder is evacuated for several hours to remove residual methane. Helium is used to purge the cylinder after the methane has been removed and is then used as the gas to conduct the pressure drop test.

Next, a cylinder of known volume is evacuated. Its temperature is monitored until it is within 0.1°C of the sample cylinder's temperature which has been pressurised with helium.

The sample cylinder valve is opened allowing the helium pressure in the sample cylinder and reference cylinder to equilibrate. This pressure is measured when the temperature of the two cylinders has also equilibrated.

The following formula allows the void volume of the sample cylinder to be calculated once the test is complete:

Where: V = the void volume in the sample cylinder (cc).
 V_c = the volume of the reference cylinder and connectors (525 cc).
 P_s = the helium pressure that the sample cylinder was raised to before equilibrium 40 psia (276 kPa).
 P_c = the pressure in the reference cylinder before equilibrium 1 psia (7 kPa).
 P_{sc} = the equilibrium pressure.

therefore, the void volume equation is:

$$V = \frac{V_c * (P_{sc} - P_c)}{(P_s - P_{sc})}$$

Note: Because the void determination requires evacuation of the sample, there is an associated moisture loss. Once the void test is completed the sample should be tested for moisture content and the results compared to the initial moisture content of the sample in order to correct the void for the volume of moisture lost. The volume of moisture lost (V_m) is subtracted from the void volume V :

$$V_s = V - V_m$$

Where: V_s is the corrected void volume
 V is the void volume
 V_m is the volume of moisture loss

Methane Isotherm Calculations: The amount of methane adsorbed on the sample at each pressure is measured by the increase in weight of the sample minus the weight of methane that occupies the void space at that temperature and pressure.

Any change in the control cylinder weight is caused by changes in air density during the weighing process. This allows calculation of a correction factor which is applied to the weights of the other cylinders at every step in the weighing process.

The mass of CH₄ in the void space in the sample cylinder is determined from the void space measurement and the density of methane calculated from the mass gained and known void volume in the comparison cylinder (M).

The following calculates the volume of methane adsorbed by the coal sample under standard conditions:

$$\text{Volume CH}_4 \text{ (STP)} = \text{Mass CH}_4 / \text{mwt (CH}_4) * (\text{SMV/mol}) \quad (1)$$

Where: Volume CH₄ (STP) = the volume of methane at 760 mm Hg and 0°C expressed in units cc/g or equivalent m³/Tonne

Mass CH₄ is the mass of methane adsorbed by the coal sample

mwt = 16 g/mol = the molecular weight of methane

SMV = 22517 cc mol⁻¹ = Standard molar volume of a gas STP (0° C, 1 atm)

2.2.8 Modeling adsorption on coal, Langmuir analysis

Methane Isotherms on coal samples are commonly modelled using Langmuir analysis. (Castellan, G.W.) speaks of physical adsorption when adsorption of a gas (adsorbate) on a solid (adsorbent) by Van Der Waals forces occurs. The adsorbed molecules are weakly bound to the surface and the 'heats of adsorption' are low (a few kilo-joules at most). For this reason an isotherm of the Langmuir type, which predicts a molecular monolayer and nothing more, is well suited for interpreting data. The Langmuir isotherm predicts a 'heat of

adsorption' that is independent of the mole fraction of adsorbate on the adsorbent for specific values of coverage. In the following discussion the adsorbate is methane and adsorbent is coal.

We can represent the process of methane adsorption by the following chemical equation:



Where $\text{CH}_4(\text{g})$ is the gaseous adsorbate, coal is an unoccupied site on the coal sample, and $\text{CH}_4.\text{Coal}$ is an occupied site on the coal sample. Langmuir's equation can be written as follows:

$$K = x_{\text{CH}_4.\text{Coal}}/x_{\text{Coal}} \quad (3)$$

Where K is an equilibrium constant representing rate of adsorption, $x_{\text{CH}_4.\text{Coal}}$ is the mole fraction of occupied sites on the coal sample, x_{Coal} is the mole fraction of vacant sites on the coal sample, and P is the pressure of the gas. It is more common to use V/V_i for $x_{\text{CH}_4.\text{Coal}}$ the fraction of occupied sites on the coal sample where V is the volume of methane adsorbed at a gas pressure, and V_i is the volume of gas adsorbed when a full monolayer of methane occupies all available sites in the coal sample. Conversely, x_{Coal} becomes $1-(V/V_i)$ the fraction of unoccupied sites on the coal sample. Substituting these variables in equation (1).

$$K = V/V_i / (1-(V/V_i)) * P \quad (4)$$

and after rearranging, the equation becomes:

$$P/V = P/V_i + 1/K * V_i \quad (5)$$

A plot of P/V vs P gives a slope $1/V_i$ where V_i is equal to the volume of gas in one monolayer on the sample and the intercept equals Langmuir's pressure.

Figure 2.8 presents a typical methane isotherm of Phalen coal samples retrieved from 8 East Bottom Development Face.

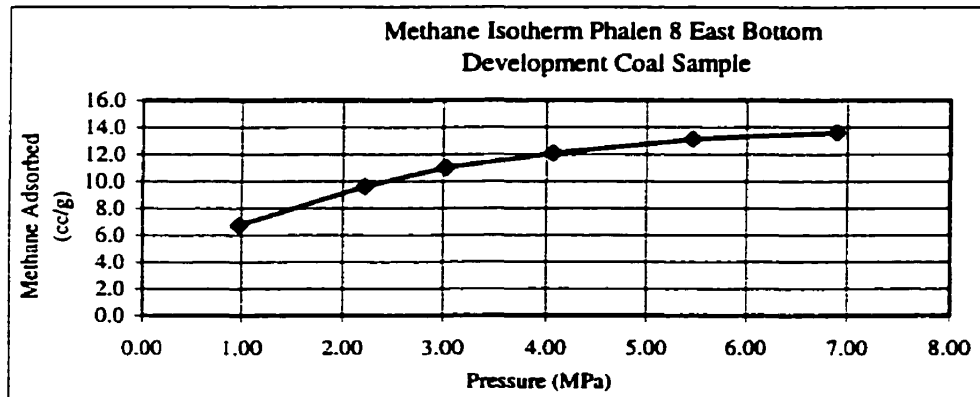


Figure 2.8 Methane isotherm of Phalen 8 East Bottom coal sample

This sample was tested using the methane isotherm methods described above. It shows that the rate of methane adsorbed by Phalen mine coal decreases with increasing gas pressure. The isotherm was conducted at 25 °C.

2.2.9 Methane isotherm of Geological Survey of Canada coal samples A and B

In June of 1995, the Geological Survey of Canada (GSC) contacted CSL to carry out methane isotherm tests on two coal samples identified as A and B. The purpose of the tests was to compare the results obtained to those of other labs in order to assess methodologies and to begin a process of identifying a common method.

A comparison of the findings of testing on similar samples from other laboratories will be used to discuss each laboratory's methodologies and possibly identify a common method for conducting a methane isotherm test on coal. Preliminary GSC results from other laboratories show very good agreement with CSL's results and will be subject to a GSC report.

Estimate of in-situ gas content

3.0 Estimate of in-situ gas content of a coal seam

In order to find a relationship between in-situ gas content of a coal seam and of a large number of gas content test results, statistical analysis is required. The following describes the method selected for determining an estimate of the in-situ gas content of a coal seam from the gas contents of coal face lump samples collected as previously described.

3.1 Creedy's method for estimating in-situ gas content of coal

Statistical methods have been developed by the British Coal Headquarters Technical Department to provide an estimate of the in-situ gas content of a coal seam from face samples collected in a similar method as above (Technical Coal Research, 1986). In this method it was assumed that values of gas content of a large group of coal samples collected from the active wall faces followed a normal distribution and from this distribution the 96.93 probability level represented an estimate of the in-situ gas content of the coal seam by the following equation:

$$E = 1.87 \cdot \sigma + X$$

Where: E = estimate of seam gas content (m³/tonne)

X = $\Sigma x_i / (n-1)$ = statistical average of n number of gas contents

σ^2 = standard deviation of gas content distribution = $(\Sigma (x_i - X)^2 / (n-1))^{1/2}$

3.2 Creedy's estimate of Harbour and Phalen coal seams

Tables 3.1, 3.2, and 3.3 present the gas contents as tested and the Creedy estimate of in-situ seam gas content for coal lump samples collected from Phalen mines 4, 5 and 6 East and Lingan mines 12 and 13 East wall faces.

Phalen 4 East Gas Contents			
Sample ID	x_i	$x_i - X$	$(x_i - X)^2$
1	7.7	-0.6	0.33
2	6.2	0.9	0.85
3	8.6	-1.5	2.18
4	5.8	1.3	1.75
5	6.7	0.4	0.18
6	7.7	-0.6	0.33
7	7.6	-0.5	0.23
8	8.0	-0.9	0.77
9	7.6	-0.5	0.23
10	7.7	-0.6	0.33
11	7.4	-0.3	0.08
12	7.1	0.0	0.00
13	6.9	0.2	0.05
14	7.5	-0.4	0.14
15	6.8	0.3	0.10
16	7.3	-0.2	0.03
17	6.9	0.2	0.05
18	6.1	1.0	1.05
19	6.3	0.8	0.68
20	6.6	0.5	0.27
21	7.0	0.1	0.02
22	7.4	-0.3	0.08
23	6.4	0.7	0.52
24	7.1	0.0	0.00
25	5.8	1.3	1.75
26	5.9	1.2	1.50
27	7.4	-0.3	0.08
28	6.0	1.1	1.26
29	6.1	1.0	1.05
30	6.2	0.9	0.85
31	6.8	0.3	0.10
32	6.5	0.6	0.39
33	6.4	0.7	0.52
34	7.2	-0.1	0.01
35	7.2	-0.1	0.01
36	7.4	-0.3	0.08
	$X = \sum x_i / (n-1)$		$\sigma^2 = \frac{\sum (x_i - X)^2}{(n-1)}$
	$X = 7.1$		$\sigma = 0.71$
Creedy =	$(\sigma \cdot 1.87) + X = 8.4 \text{ m}^3/\text{tonne}$		
Estimate	In-situ gas content for Phalen 4 east.		

Table 3.1 Creedy's estimate of in-situ gas content for Phalen mine 4 East coal seam

Phalen 5 East Gas Contents			
Sample ID	$x_i - X$	$(x_i - X)^2$	$(x_i - X)^2$
1	6.4	1.0	0.93
2	6.3	1.1	1.14
3	7.3	0.1	0.00
4	7.1	0.3	0.07
5	6.9	0.5	0.22
6	7.1	0.3	0.07
7	6.1	1.3	1.60
8	6.5	0.9	0.75
9	7.2	0.2	0.03
10	6.9	0.5	0.22
11	6.8	0.6	0.32
12	6.5	0.9	0.75
13	6.7	0.7	0.44
14	6.3	1.1	1.14
15	6.9	0.5	0.22
16	7.2	0.2	0.03
17	7.0	0.4	0.13
18	7.4	0.0	0.00
19	7.5	-0.1	0.02
20	7.7	-0.3	0.11
21	7.2	0.2	0.03
22	7.5	-0.1	0.02
23	7.8	-0.4	0.19
24	6.5	0.9	0.75
25	7.0	0.4	0.13
26	7.6	-0.2	0.05
27	7.0	0.4	0.13
28	9.1	-1.7	3.00
29	7.2	0.2	0.03
30	6.7	0.7	0.44
31	7.7	-0.3	0.11
32	6.9	0.5	0.22
33	7.6	-0.2	0.05
34	7.7	-0.3	0.11
35	7.9	-0.5	0.28
36	7.9	-0.5	0.28
37	7.1	0.3	0.07
38	8.2	-0.8	0.69
39	7.5	-0.1	0.02
40	7.4	0.0	0.00
$X = \sum x_i / (n-1)$		$\sigma^2 = \frac{\sum (x_i - X)^2}{(n-1)}$	
$x =$	7.4	$\sigma =$	0.62
Creedy = Estimate	$(\sigma \cdot 1.87) + x = 8.6 \text{ m}^3/\text{tonne}$		
In-situ gas content for Phalen 5 east.			

Table 3.2 Creedy's estimate of in-situ gas content for Phalen mine 5 East coal seam

Phalen 6 East Gas Contents			
Sample ID	x_i	$x_i - X$	$(x_i - X)^2$
1	8.6	-1.2	1.52
2	8.5	-1.1	1.28
3	8.3	-0.9	0.87
4	7.8	-0.4	0.19
5	8.8	-1.4	2.05
6	7.2	0.2	0.03
7	6.6	0.8	0.59
8	7.1	0.3	0.07
9	7.8	-0.4	0.19
10	7.8	-0.4	0.19
11	8.1	-0.7	0.54
12	7.3	0.1	0.00
13	6.9	0.5	0.22
14	7.0	0.4	0.13
15	5.9	1.5	2.15
16	7.0	0.4	0.13
17	6.7	0.7	0.44
18	5.8	1.6	2.45
19	7.0	0.4	0.13
20	6.1	1.3	1.60
21	8.1	-0.7	0.54
22	7.0	0.4	0.13
23	8.9	-1.5	2.35
24	8.2	-0.8	0.69
25	8.3	-0.9	0.87
26	8.5	-1.1	1.28
27	8.7	-1.3	1.78
28	8.7	-1.3	1.78
29	8.2	-0.8	0.69
30	7.5	-0.1	0.02
31	9.1	-1.7	3.00
32	8.4	-1.0	1.07
33	9.6	-2.2	4.99
34	8.4	-1.0	1.07
35	7.3	0.1	0.00
36	8.0	-0.6	0.40
37	7.8	-0.4	0.19
38	8.1	-0.7	0.54
39	7.5	-0.1	0.02
$X = \sum x_i / (n-1)$		$\sigma^2 = \frac{\sum (x_i - X)^2}{(n-1)}$	
$x =$	7.8	$\sigma =$	0.96
Creedy = Estimate	$(\sigma * 1.87) + x = 9.6 \text{ m}^3/\text{tonne}$		
In-situ gas content for Phalen 6 east.			

Table 3.3 Creedy's estimate of in-situ gas content for Phalen mine 6 East coal seam

Lingan 12 East Gas Contents			
Sample ID	x_i	$x_i - X$	$(x_i - X)^2$
1	7.4	-0.5	0.3
2	7.1	-0.8	0.6
3	6.6	-1.3	1.7
4	6.5	-1.3	1.8
5	6.5	-1.3	1.8
6	7.8	-0.1	0.0
7	7.8	-0.1	0.0
8	5.9	-2.0	4.1
9	7.9	0.0	0.0
10	8.7	0.9	0.8
11	6.6	-1.3	1.6
12	6.2	-1.7	2.8
13	7.1	-0.8	0.6
14	6.9	-1.0	1.0
15	7.7	-0.2	0.0
16	8.5	0.7	0.4
17	7.9	0.0	0.0
18	7.0	-0.9	0.8
19	9.0	1.2	1.4
20	6.5	-1.4	1.8
21	9.0	1.1	1.2
22	7.6	-0.2	0.1
23	7.7	-0.2	0.0
24	8.5	0.6	0.4
25	8.3	0.4	0.1
26	8.8	0.9	0.8
27	8.8	1.0	0.9
28	9.2	1.3	1.7
29	8.9	1.0	1.0
30	9.0	1.1	1.3
31	8.8	1.0	0.9
32	8.3	0.4	0.2
33	7.1	-0.8	0.6
34	5.3	-2.6	6.6
35	6.7	-1.2	1.4
36	9.0	1.1	1.2
37	8.6	0.7	0.5
38	7.5	-0.4	0.1
39	7.3	-0.6	0.4
40	8.2	0.3	0.1
41	7.4	-0.4	0.2
42	9.0	1.1	1.3
43	7.7	-0.2	0.0
44	5.2	-2.6	7.0
45	5.7	-2.2	5.0
46	7.7	-0.2	0.0
47	6.8	-1.1	1.3
48	8.6	0.7	0.5
49	9.5	1.6	2.6
50	8.2	0.4	0.1
51	8.8	0.9	0.8
52	9.2	1.3	1.7
$X = \sum x_i / (n-1)$		$\sigma^2 = \frac{\sum (x_i - X)^2}{(n-1)}$	
$X = 7.9$		1.10	
Creedy = $(\sigma \cdot 1.87) + X = 10.0$			
Estimate			
In-situ gas content for Lingan 12 East.			

Table 3.4 Creedy's estimate of in-situ gas content for Lingan mine 12 East coal seam

Lingan 13 East Gas Contents			
Sample ID	x_i	$x_i - \bar{X}$	$(x_i - \bar{X})^2$
1	7.9	0.6	0.32
2	7.2	1.3	1.60
3	9.0	-0.5	0.29
4	7.8	0.7	0.44
5	8.9	-0.4	0.19
6	8.7	-0.2	0.05
7	7.8	0.7	0.44
8	6.9	1.6	2.45
9	7.9	0.6	0.32
10	7.9	0.6	0.32
11	8.5	0.0	0.00
12	6.0	2.5	6.08
13	7.2	1.3	1.60
14	6.6	1.9	3.48
15	8.5	0.0	0.00
16	7.9	0.6	0.32
17	6.6	1.9	3.48
18	7.5	1.0	0.93
19	8.5	0.0	0.00
20	8.3	0.2	0.03
21	9.2	-0.7	0.54
22	8.6	-0.1	0.02
23	7.8	0.7	0.44
24	8.5	0.0	0.00
25	9.3	-0.8	0.70
26	9.8	-1.3	1.78
27	6.1	2.4	5.60
28	9.6	-1.1	1.29
29	10.8	-2.3	5.45
30	10.2	-1.7	3.01
$\bar{X} = \sum x_i / (n-1)$		$\sigma^2 = \frac{\sum (x_i - \bar{X})^2}{(n-1)}$	
$\bar{X} =$	8.5	$\sigma =$	1.19
Creedy =	$(\sigma * 1.87) + \bar{X} = 10.7 \text{ m}^3/\text{tonne}$		
Estimate			
In-situ gas content for Lingan 13 East.			

Table 3.5 Creedy's estimate of in-situ gas content for Lingan mine 13 East coal seam

Table 3.6 shows Creedy's gas content estimates and determinations of the gas content for borehole samples (Feng, K.K., Cheng K.C, and Augsten R., 1983) from the Phalen seam at 806m and sample depth for all samples.

Mine	District	Coal seam	Estimated In-situ Gas Content	Depth (m)	Method
Lingan	12 east	Harbour	10.0	685	Creedy
Lingan	13 east	Harbour	10.7	722	Creedy
Phalen	4 east	Phalen	8.4	425	Creedy
Phalen	5 east	Phalen	8.6	476	Creedy
Phalen	6 east	Phalen	9.6	530	Creedy
Phalen	Borehole 140	Phalen	11.0	806	Direct
Phalen	Borehole H2	Phalen	14.8	1077	Isotherm

Table 3.6 In-situ gas content estimates for Harbour and Phalen coal Seams

As evident from the statistical analysis (Tables 3.1 to 3.5), the standard deviation among sample sets is large enough to show that even though there is a general increase in estimated gas content, the data sets overlap to a large degree and this casts some concern in stating that there is indeed a trend of increasing gas content with depth. More evidence was required to support this conclusion that indeed the gas content of Phalen and other coal seams were increasing with depth and some estimate of the gas pressure associated with this increase was required for its proof. This evidence could be gained from previous borehole pressure measurements recorded directly from Phalen strata and/or indirectly from estimates using methane isotherm data.

3.3 Previous measurements of in-situ gas pressure of the Phalen coal seam

Table 3.7 shows a summary of the principal in-situ gas pressure measurements of coal and non-coal strata as measured at Phalen mine.

Mine	Location	Hole ID	Date	Gas Pressure (MPa)	Depth (m)	CH4 %	C2H6 %	C3H8 %	C4H10+ %	N2 %	O2 %	CO2	H2 ppm
Phalen	2 centre bottom	PH102	Dec.13/93	5.1	-613	-	-	-	-	-	-	-	-
Phalen	3 slope face	PH104	Feb.9/94	3.1	-699	88.4	5.4	2.2	0.4	3.4	0.0	0.2	-
Phalen	3 Slope coal rib	CBCRL	Jan 16/95	1.6	-695	93.5	2.7	0.4	0.1	3.3	0.0	0.0	<100

Table 3.7 In-situ gas pressures and composition of the Phalen coal seam and Lower Sandstone Unit

The highest pressure recorded to date in the Phalen coal seam is 1.6 MPa (225 psia). All other pressure estimates have been derived from Lower Sandstone Unit that have intersected the coal seam in the Phalen colliery. The highest value equals 5.0 MPa (725 psig) measured at borehole PH-162 at 2 center top at a depth of ~613 m. In all these measurements, high pressure gas leakage was suspected from within the boreholes, although PH-162 appeared to be sealed the most effectively.

3.4 H2 borehole methane isotherm temperature and pressure corrections

In order to improve the accuracy and range of the relationship between the gas content and depth (rank) for the Phalen, Harbour and associate coal seams, a gas content determination of a coal sample was required, preferably from a greater depth in the Phalen seam. It was decided to retrieve a retained coal sample from the 1970's drilling program for methane isotherm testing, since it was very improbable that any other borehole sample from the required depths would be provided in the foreseeable future. This would provide the only means for obtaining an in-situ gas content and pressure information.

The Nova Scotia Department of Natural Resources was contacted and provided some retained coal from H2 borehole that was drilled from ocean level above the Phalen mine coal reserve block in 1978. The sample represented the Phalen coal seam at a depth of 1077 m. The sample was prepared and tested according to CBCRL's isotherm procedure (Young, D.A. and Chipman, D.G., 1996) and for proximate analysis. A portion of the sample was sent to Global Geo-energy Co. for vitrinite reflectance testing, for a comparison with previous recorded vitrinite values and to determine whether significant sample oxidation had occurred. Only slight oxidation had been reported and vitrinite reflectance was close to the value reported for the sample tested in 1978 (Table 3.8).

Borehole H2 Composite Sample	Moisture Content %	Volatile Matter Content %	Ash Content %	Fixed Carbon %	Vitrinite Reflectance $R_{o,vit}$
Pe -1028-78	0.58	25.28	9.50	64.64	1.23
Isotherm no. 23	1.75	26.29	8.06	63.90	1.18
Isotherm no. 24	0.67	26.48	8.61	64.24	1.18

Table 3.8 Proximate and vitrinite reflectance test results for H2 coal sample for 1978 and present

Upon initial testing of the sample at CSL, it was determined that the moisture content of the sample had increased compared to 1978 moisture results. Moisture content has a direct effect on reducing sorption capacity of coal; therefore, to make the sample more representative for isotherm testing, it was dried in a heating pad with a stream of argon passing over it for a period of time to reduce the moisture content. Once the sample moisture content was close to that previously reported in 1978, it was tested again in the isotherm apparatus.

The results indicate that the sorption capacity of the sample increased with gas pressure as expected. However, because the isotherm was conducted at 25 °C, a means for correcting the isotherm for original geothermal gradient was needed. The sorption capacity of coal for methane decreases with increase in temperature.

The geothermal gradient of the Phalen seam has been estimated from boreholes drilled 8-10 m into four coal faces of the Phalen mine and from an exploratory drill hole on three slope bottom. At each test site, a long plastic probe fitted with a calibrated thermister and wire cable was inserted into the bottom of each hole. Each was then filled with water to insulate the probe and packing was placed in the collar of the hole to prevent ventilation air from entering. The probe was left in the test hole for a 24 hour period to reach temperature equilibrium and read with appropriate readout the following day.

Figure 3.1 shows the geothermal gradient plot for the Phalen seam.

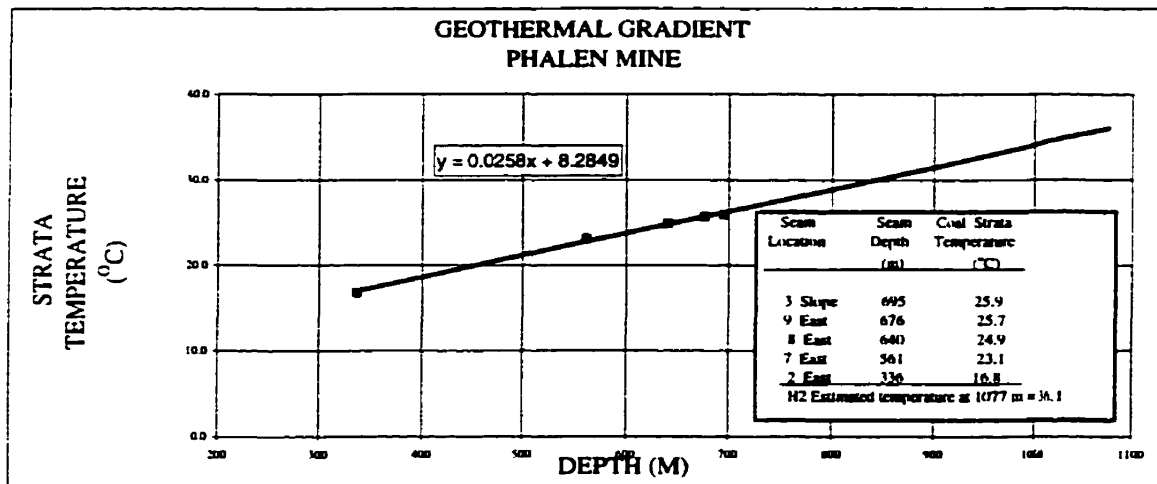


Figure 3.1 Geothermal gradient of the Phalen coal seam

The geothermal gradient is 2.28 per 100 m of depth. From this gradient, the temperature of borehole sample H2 was estimated to be 36.1 °C. The original methane isotherm temperature conducted on H2 borehole sample was at 25 °C; therefore, a correction factor was required to project an estimate of the H2 isotherm at 36.1 °C.

Patching, T. and Mikhail, M., 1981 have derived some correction factors to reduce an isotherm to its equivalent at 21 °C. The factors record a % reduction in the sorption capacity of bituminous coal per °C between 0 and 4.1 MPa (600 psig) gas pressure. These factors were plotted versus pressure (MPa) in Figure 3.2 to show that the reduction in the sorption capacity of coal at higher temperatures is not constant and decreases exponentially with increase in gas pressure per °C.

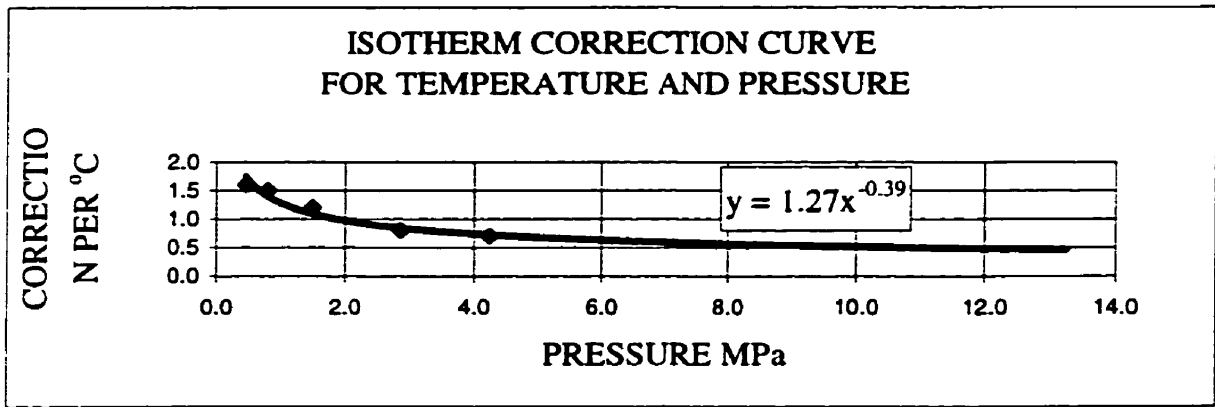


Figure 3.2 Extrapolation of Patching's and Mickhail's temperature and pressure correction factors for bituminous coal

This plot was extended to 12.8 MPa (1870 psig) the maximum pressure used in the sorption study of H₂ borehole sample. Assuming that the reduction in sorption capacity followed this trend for H₂ borehole sample, the original isotherm values were corrected and reduced on a percentage basis to a new sorption capacity at the projected geothermal temperature of 36.1 °C (Tables 3.9 and 3.10).

Pressure MPa	Correction per °C *	Correction 25.0 °C a	Correction 36.1 °C b	Correction H2 Isotherm b-a
2.1	0.96	3.8	14.4	10.6
4.1	0.73	2.9	11.0	8.1
6.2	0.62	2.5	9.4	6.9
8.4	0.55	2.2	8.4	6.2
10.1	0.51	2.1	7.8	5.7
12.9	0.47	1.9	7.1	5.2

Table 3.9 Calculation of the percentage reduction in adsorption capacity for methane isotherm on H₂ borehole coal based on Patching's and Michail's extrapolated temperature and pressure correction curve of Figure 3.2

Methane Pressure MPa	Original Isotherm m ³ /tonne (STP)	Correction H2 Borehole Isotherm % Reduction	Corrected H2 Borehole Isotherm (STP)
2.1	8.9	10.6	7.9
4.1	11.5	8.1	10.6
6.2	13.6	6.9	12.6
8.4	14.4	6.2	13.5
10.1	16.0	5.7	15.1
12.9	16.2	5.2	15.4

Table 3.10 Final results of methane isotherm correction for H2 borehole isotherm

Figure 3.3 shows the original and corrected methane isotherms for H2 borehole sample.

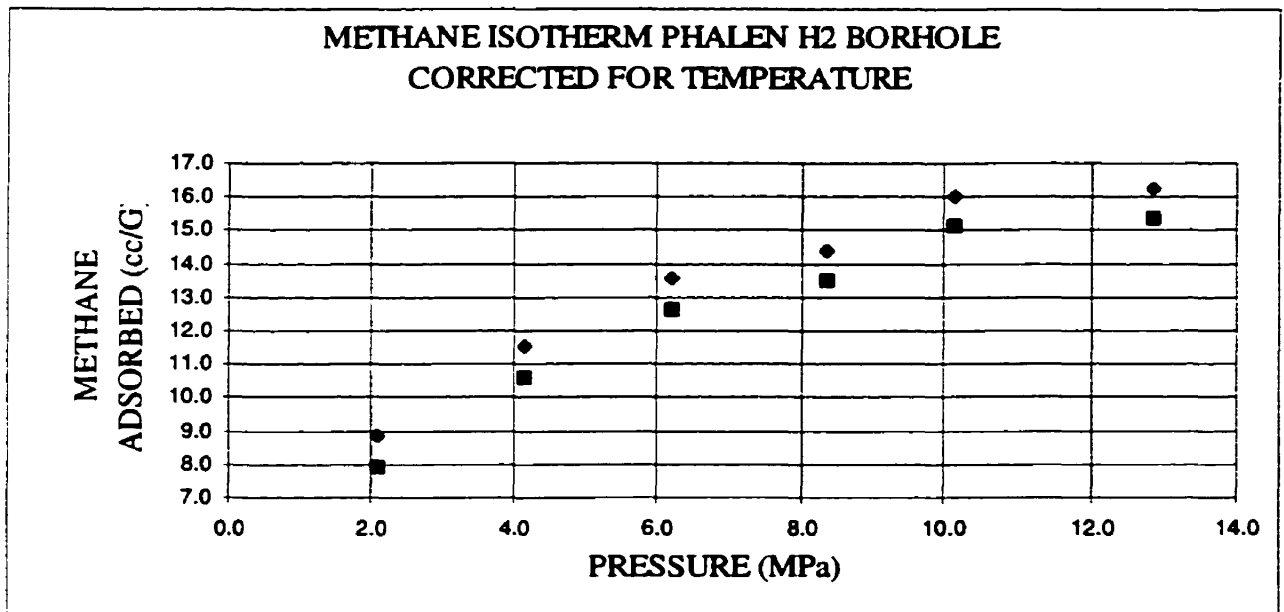


Figure 3.3 Methane isotherm for H2 borehole sample before and after application of temperature and pressure corrections

Figure 3.4 shows Langmuir's P/V versus P for the corrected isotherm data and indicates that at an assumed hydrostatic gas pressure of 10.56 MPa, the gas content equals 14.8 m³/Tonne.

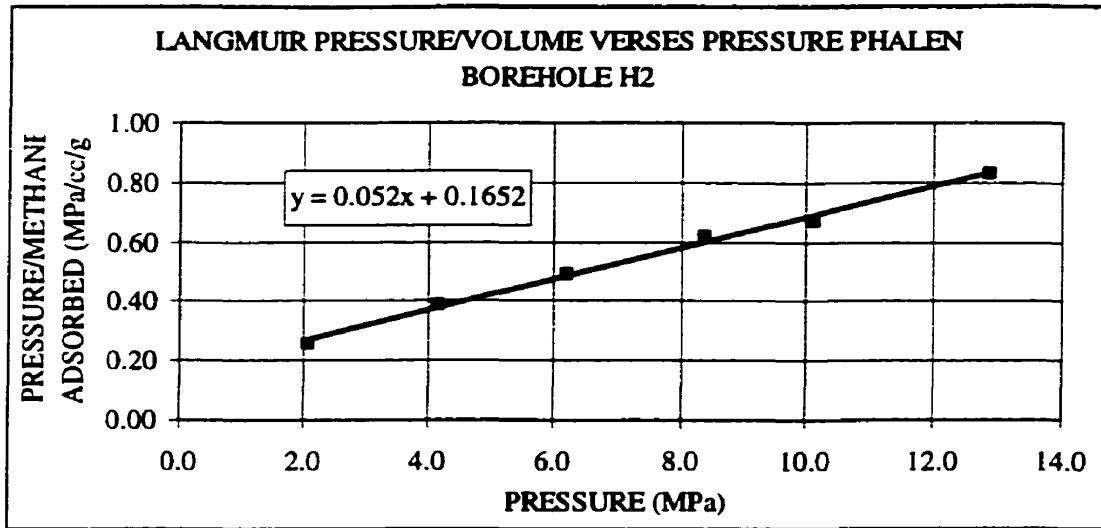


Figure 3.4 Langmuir pressure/volume versus pressure plot for H2 borehole sample

3.5 Estimate of in-situ gas pressure for the Phalen coal seam by isotherm analysis

A plot of the data from Table 3.6, indicates that at a depth of 1077 m, H2 gas content estimate of 14.8 m³/Tonne falls above the projected curve's trend line (Figure 3.5).

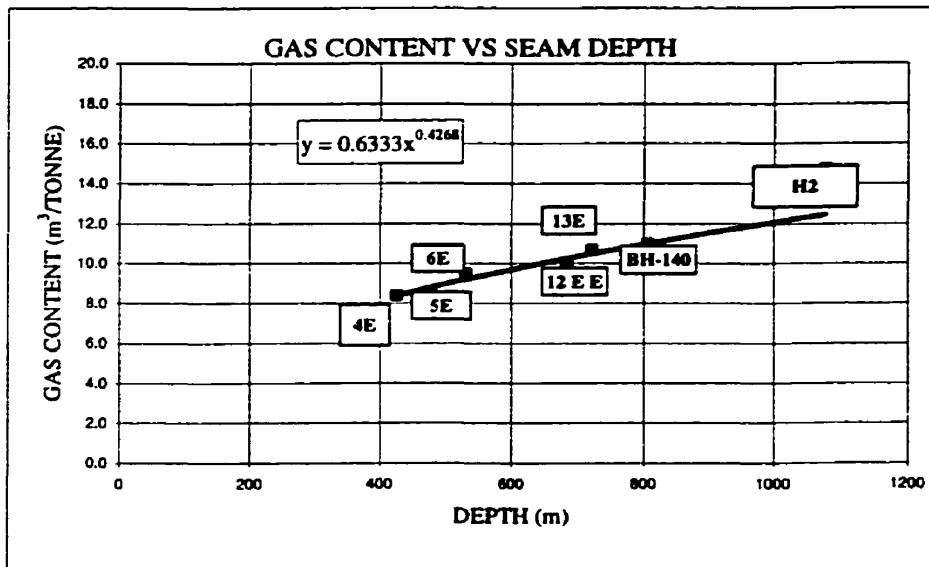


Figure 3.5 Gas content estimates Phalen mine's 4, 5, 6 East and Lingan 12 and 13 East districts, borehole 140 and H2 methane isotherm estimate from Figure 3.4 versus depth

The reasons for this could be as follows:

- (1) The original sample had changed and the sorption isotherm was not representative. This could be disputed by the proximate and reflective R_o results (Table 3.8). The sample appeared to be similar to the original in terms of rank and physical condition.
- (2) The reduction in sorption capacity with temperature as presented is flawed and is not representative of the sample.
- (3) Sorption testing with methane is not indicative of the adsorption of the natural components of gas in-situ.
- (4) The hydrostatic head consists of both gas and other fluids and the actual gas pressure in equilibrium with the coal seam is lower than hydrostatic head.
- (5) The isotherm measures adsorbed gas, not free gas that may occupy the pore space of coal. This would increase the in-situ gas content of the sample.

It is most likely that the largest factor affecting the sorption capacity of coal is item 4, and it will be assumed at this point in the discussion that the gas pressure at 1077 m is less than hydrostatic pressure. As mentioned previously, the quantity of methane in equilibrium with coal during late thermogenic methane generation is much less now than in the past. In time this results in a lower equilibrium gas pressure, and as a result, other fluids such as water replace and reduce the quantity of methane adsorbed on the coal. If the curve fit line in Figure 3.5 is extended to 1077 m, the projected gas content for a H₂ borehole sample at 1077 m depth equals 12.5 m³/tonne. The in-situ gas pressure can be estimated as follows. Dividing 12.5 m³/tonne, under pressurized gas content estimate at 1077 m depth, by 14.58 m³/tonne, fully pressurized gas content estimate as determined from the corrected isotherm at the equivalent hydrostatic head at 1077 m depth, equates to 0.84 or the percentage of hydrostatic head that is gas pressure.

If we assume that the pressure measured in borehole PH-102 is gas pressure only as presented in Table 3.7 equates to 5.0 MPa. The hydrostatic head at 613 m depth equals 6.0 MPa; therefore, 5.0/6.0 equals 0.833 hydrostatic head in terms of gas pressure only.

These two results are virtually the same value and without any other information to improve this estimate, it will be assumed that $(0.84 * \text{hydrostatic head})$ equals Phalen in-seam gas pressure.

3.6 In-situ gas content versus depth of coal seams in the Phalen mine

If we apply Langmuir's P/V versus P plot to the data as shown in Figure 3.5 versus the estimate of in-seam gas pressure from above, we derive a linear equation, and this equation can be projected from lower to higher depths. At this point it should be stated that the use of Langmuir's analysis is purely intuitive and is being used to simply arrive at an equation to derive a model relating gas content with depth (Figure 3.6).

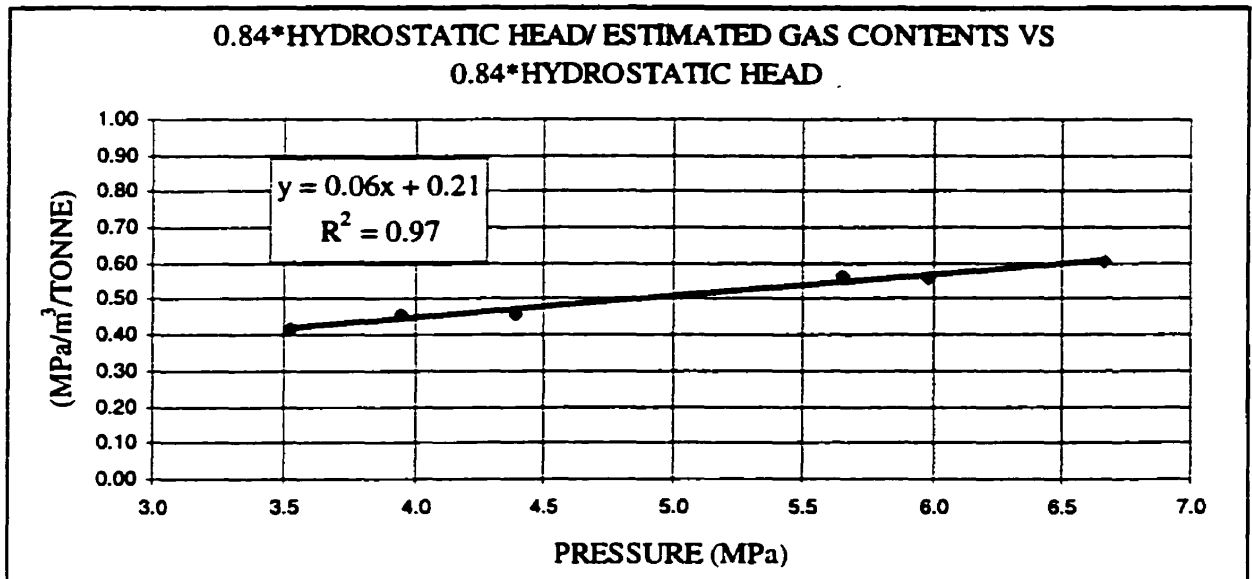


Figure 3.6 Langmuir type analyses plot of $0.84 * \text{hydrostatic head} / \text{in-situ gas content}$ versus $0.84 * \text{hydrostatic head}$

3.7 An in-situ gas content curve for the Phalen coal seam

The equation for relating gas content with depth is shown in (Figure 3.7) as plotted with the in-situ gas content estimates of Table 3.4. This equation assumes that the in-situ gas pressure estimate is uniform through out the Phalen coal seam and adjacent coal seams. This equation can be used to estimate the gas content of the Phalen coal seam at Phalen mine which is required for methane prediction using Airey's method.

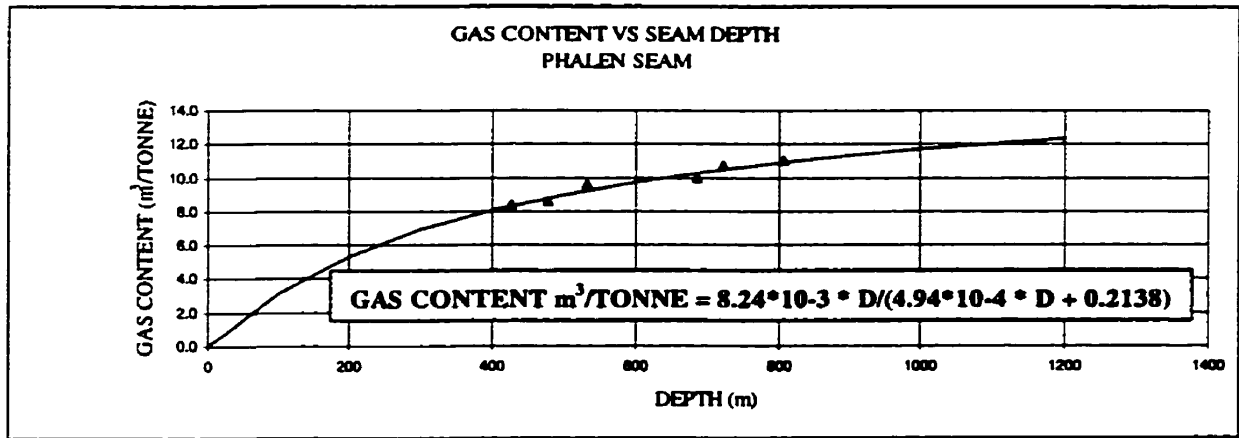


Figure 3.7 In-situ gas content versus depth model for coal seams adjacent to the working Phalen district derived from the equation in Figure 3.6

Methane Prediction Methods

4.0 Methane prediction methods

Methane prediction methods developed in Europe and North America have followed two different pathways. The following gives a historic review of these methods and focuses on the Airey's method which will be used later in this report to compare predicted and measured methane flow from two previously mined Phalen longwall gobs. The reason for focusing on gobs only is an attempt to determine the amount of methane, based on predicted methane flow, for Phalen's 7 East district. 7 East was being affected by gob emissions entering the return airway. An assessment of the performance of the present ventilation system based on predicted gob emission was carried out and will provide a bases for decisions on future mine ventilation plans.

4.1 European

The European methods have used the same basic approach and were aimed at specifically longwall operations. The parameters investigated were as follows:

- The stratigraphic profile above and below the worked seam
- The desorbable gas content of the worked seam and adjacent seams
- The zones of gas emission in both the roof and floor
- The degree of gas emission from these zones

An understanding of the stratigraphic column above and below the worked seam is very important since most of the gas entering a mine during longwall mining comes from adjacent strata. In a large number of cases, the extent of this zone depends on the degree of gas emission from the other coal measures. The degree of gas emission depends on what percentage of the gas contained in a zone at a specific level is available to flow to the mine area.

Each European country prediction method differs in both definition of the zone of horizon and the degree of emission within that zone. However, most methods define

variations of degree with height within a zone which was represented by a rectangular prism.

Each method requires a knowledge of gas content which in many countries is rarely available because exploration programs have been inadequate with respect to the assessment of methane, and for most calculations are based on:

- the gas content of the worked seam
- the gas content in the worked seam is the same as in adjacent strata except where measurements are available
- the assumption that the adjacent strata contains a percentage of the worked seam's gas content

All the methods address the following:

- the seam being worked
- the adjacent seams and strata
- coal in transit

Degree of Methane Emission: is calculated based on the height of the seam in the adjacent strata to the seam being worked. The degree of emission is given by both mathematical and graphical methods.

Strata Emissions: relates the methane emission from the adjacent seams and strata to the coal produced in the seam being worked. This is the ratio of the thickness of each seam or stratum to the thickness of the worked seam. This ratio is multiplied by the seam's gas content to give the strata emission per tonne of coal from the working face. The sum of the separate emissions gives the total emission emitted from adjacent seams and strata.

Methane from the seam being worked: by multiplying a percentage factor to the gas content of the seam being worked. The rate of face advance being the most important factor to consider in this case.

Gas emission during coal transportation: this is calculated from the time it takes the coal to leave the mine and the residual gas content of the coal.

The Total gas emission: is the sum of the above elements. The value can be presented in m^3/tonne of coal mined, m^3/day or m^3/sec .

Most methods claim ~ 20 % to 30 % accuracy which is close enough for mine planning purposes (Norwest Resource Consultants Ltd., 1985).

4.2 North American methods

In the United States most models are based on computer modeling of the various parameters that affect methane flow. Apart from the European methods, the determination of gas contents and emission curves are simply used to calibrate models and are not needed for actual predictions. The accuracy of the model must be compared to individual cases.

Most of the work has included the development of a computer model MINEAD for the flow of methane and water in coal strata based on geometry and corresponding to an advancing face and coal pillar (Norwest Resource Consultants Ltd., 1985).

In phase two of the work, the development of a two dimensional model had been undertaken. The simulations included finite element methods and consider the vertical section to the center of the workings.

Anisotropic permeability is taken into account in addition to the compressibility of the gas. The flow of methane through the boundaries is calculated, allowing for storage and desorption effects.

Similar programs have been developed for methane degassification (Norwest Resource Consultants Ltd., 1985).

The major limitation to existing models concerns the application of solving practical mine problems, and proper model verification and field testing. There are some expected gaps in applying mathematical models in that no consideration is given to gases from adjacent seams.

Because of the expense and overall difficulty of obtaining data to define the multi-phase and three dimensional parameters and running costs of finite element models, it is still a research tool and may be too expensive for mine planning purposes (Norwest Resource Consultants Ltd, 1985).

4.3 Airey's Prediction model

The following is a theory on gas emission from broken coal proposed by (E.M, Airey, 1968). His empirical equation can be used to describe the flow of methane from coal of any size, pressure, and moisture content.

$$V(t)=A[1-\exp\{-(t/t_0)^{1/3}\}]$$

Where: $V(t)$ =volume of methane released at time t

A = gas content of the coal

t_0 = a time constant with $t_0 = 1/2$ being proportional up to a mesh size of 1/4 inch

n = an index used in the equation

In a comparison with a theoretical equation describing gas flow through a cracked solid it was found that the index n was related to the degree of fracturing in the coal sample; therefore, n could take on values of $n=1/2$ for smaller particles and values of $1/3$ for larger ones. The constant t_0 was found to be independent of the initial gas pressure but proportional, in theory, to the square of the particle size e.g. meshes size (Lobbe Technologies Ltd., 1987). Figure 4.1 presents Airey's equation curve fit to desorption data collected from testing on a Harbour seam core sample from Donkin mine.

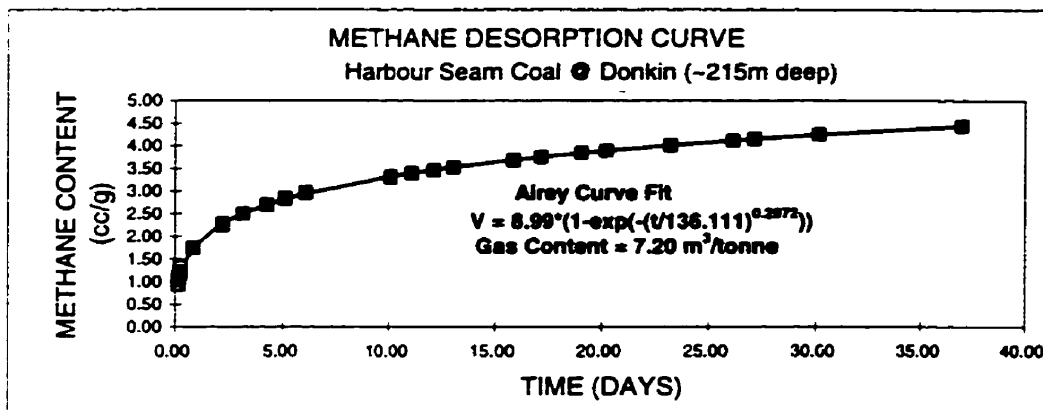


Figure 4.1 Airey model of gas desorption measurements from Donkin Harbour seam coal core sample

The equation describes almost perfectly the desorption of gas from the core.

The development of Airey's prediction model for methane flow from coal is based on an empirical equation shown above.

The assumptions underlying the equation are:

- (1) At the initial time the rate of gas release is infinite. In a strict sense this can't be true; since, the rate has to be finite all the time.
- (2) The coefficient n is a constant value and cannot be correlated directly to any set of variables such as particle size, properties, etc.

(3) The time constant t_0 is a function of particle size up to 0.1 inch, above which it increases non-linearly and assumes a constant value of 140 hours for large coal lumps (Lobbe Technologies Ltd., 1987).

Overall (Airey, 1971) proposed a phenomenological model for methane emission which incorporated the theoretical equation to describe the methane emission process according to the following assumptions:

(1) A coal seam consists of an assembly of closed packed "coal lumps" (grains) with the spaces (fissures) between the grains offering negligible resistance to methane flow. The permeability of the fissures is unaffected by the stress distribution.

The assumption of stress independent permeability is incorrect for most coal seams. (Lobbe Technologies Ltd., 1987 after McPherson, M.J., 1975).

(2) The size of lumps varies with the distance into the solid from the coal surface. The size of lumps is represented by a characteristic time $t_0(t)$, which is assumed to vary in a prescribed fashion:

$$\text{for } x > 0 \quad t_0(t) = t_0 \exp. (x/x_0)$$

$$x < 0 \quad t_0(t) = t_0$$

Where: x_0 and t_0 are further defined in Figure 4.2.

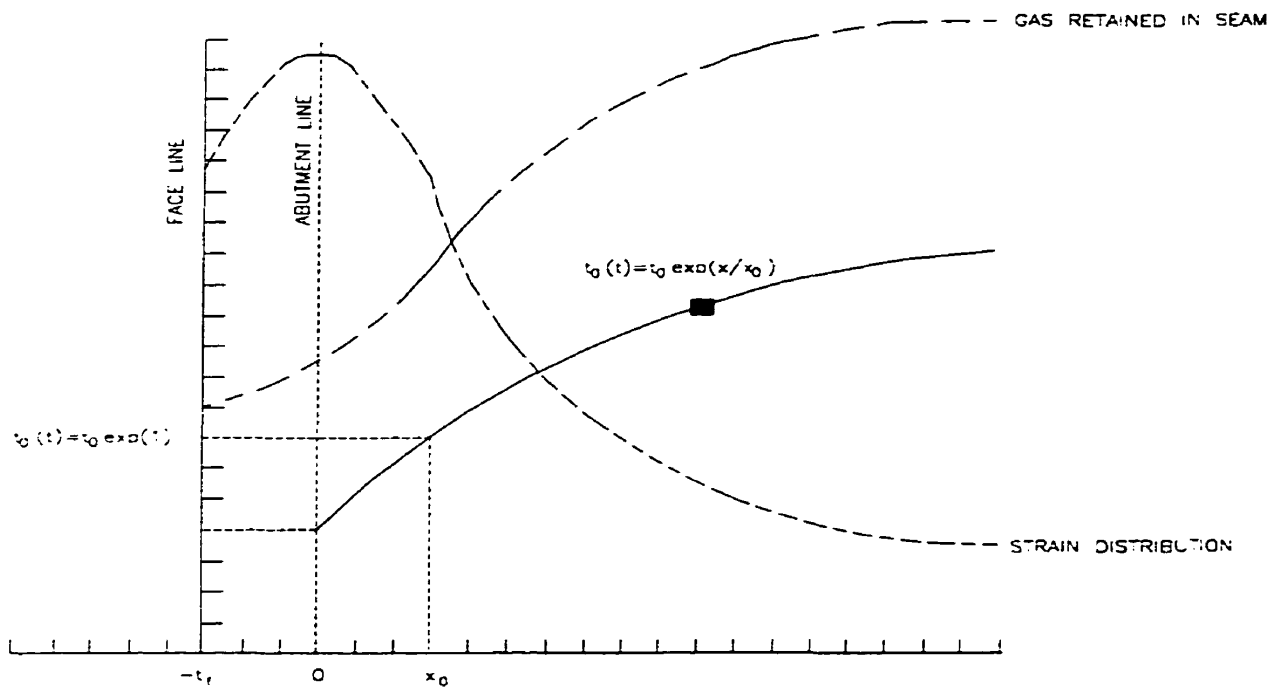


Figure 4.2 Distribution of gas, strain and t_0 in coal seam

(3) Gas emission per unit mass of coal is determined by the empirical equation so that a low emission from the coal away from the face is associated with a large lump size. For example, gas emission at a distance of $x = x_0$ would have a characteristic time $t_0(t) = 2.7 t_0$, or $2.7 * 140$ hours = 378 hours. The characteristic time at $t_0(t) x = 5 x_0$ would be equal to $150 * 140$ hours = $2.1 * 10^4$ hours.

This model depends on the face moving in the x direction with a reduction in coal grain size with time, and $t_0(t)$ decreasing in time. The difficulty with this approach is that methane emission from different grain sizes change as a function of time values as each grain moves along the solid toward the open face.

Assuming a uniform rate of face advance, the rate of gas emission at the face is given by Airey equation:

$$dv(t)/dt = dw/dt A(t) r \{ 1 - \exp[-(x_0 + L_{fs})/(r t_0)^{1/2}] \}$$

Where: dw/dt = the weight of coal removed per unit advance rate (m/s)

$A(t)$ = gas content in the seam (m^3 /tonne)

L_{fs} = the distance between the face and the position of maximum abutment load (x_0)

This equation is a weak function of L_{fs} and (x_0) and for small values in terms in the parenthesis () can be approximated as follows:

$$dv/dt = \text{constant } r^{0.8}$$

Gas emission from the cut coal can be calculated using a modified empirical equation:

$$V(T) = 1 - \exp [-(CT^3)^n]$$

Where: $V(t)$ = fraction of gas lost, $V(t) / A$

c and n = parameter dependent on the lump size distribution $T = t_0(t) / t_0$

For a narrow size distribution $n = 0.33$ and $C = 1$, and for a normal size distribution $c = 0.82$ and $n = 0.24$.

Later (Airey, 1979) derived an expression for $t_0(t)$ based on stress distribution within the seam. The proposed functional form is:

$$t_0(t) = T(\sigma_1 / \sigma_3)$$

Where T = a function of a principal stress σ_1 and σ_3 in x and y directions

The value of $t_0(t)$ can be calculated numerically from the stress distribution in the worked and adjacent seams, and as a function of depth of the worked seams. It is assumed that the lines of equal (σ_1 / σ_3) values correspond to lines of equal time constant $t_0(t)$.

The values of L_{fs} , L_{fa} , and L_{ga} , (the distance between the face and the position of maximum abutment, and the length of gob,), were found to be not critical and were assumed to be:

- for the worked seam face, $L_{fs} = 2$ m
- for the adjacent seams methane emission into the face, $L_{fa} = 10$ m

- for the adjacent seams emission into the gob, $L_{fa} = 100$ m

The value of x_0 is defined as the characteristic length at which $t_0(t) = t_0 \exp(-t/x_0)$. In practice, this correlation constant determines how steep the pressure gradient is in the vicinity of the maximum load abutment. A value of $x = 4$ was found to yield a satisfactory fit of the model equations to experimental emission.

Figure 4.3 presents Airey's emission curves for coal seams adjacent to the working seam and depth correction values.

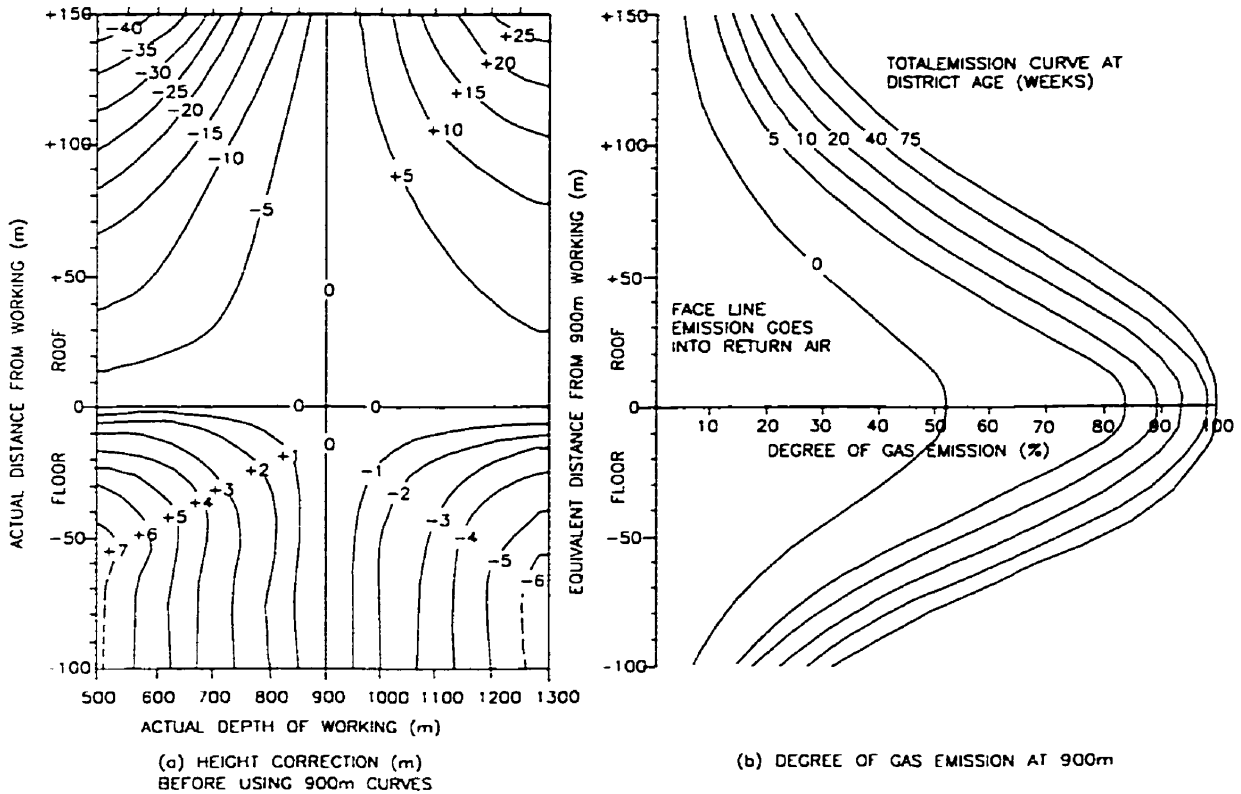


Figure 4.3 Degree of gas emission function for MRDE prediction method with correction for depth of working

From the previous discussion it is clear that Airey's model provides the means for determining the emissions from all sources in a longwall mine. Its largest weakness is dealing with stress related methane flow which it essentially ignores. Research has shown that methane flow is stress dependent (Harpalani, S., and McPherson, M.J., 1988).

It was confirmed in this report that no single equation can adequately define the complete process of desorption.

Airey assumes that a coal seam consists of an assembly of closed packed "coal Lumps" (grains) with the spaces (fissures) between the grains offering negligible resistance to methane flow. The permeability of the fissures is unaffected by the stress distribution. The flow of gas from coal depends not only on joint structure and natural permeability but on the shape and conductivity of the surrounding strata which encompasses the seam. Upon the disturbance of the coal, gas flow is controlled by diffusion and can be described according to Fick's law where the flow is dependent on concentration gradients within the pore system of the coal. Once the gas finds the cleat systems, the Darcy system of flow takes over. In coal, the amount of water present and the degree of water depressurization that must proceed to gas flow control Darcy flow. In coal, the face cleat is the dominant flow system, and extends for several meters and cuts the bedding planes. The size and extent of both cleat systems play an important role in the flow of gas through a coal seam. For example, gas flow is much higher in the main cleat direction (Law.B.E. and Rice D.D., AAPG, 1993c).

In terms of the model, no mention is made of the effects of coal thickness in adjacent seams and in a sense treats the larger lumps in the x direction as being the same height. This can have the effect of predicting lower emissions than might be measured in a real situation (Lobbe Technologies Ltd., 1987).

In a retreat longwall panel, considerable amount of degassing can be expected to have occurred from the panel prior to coal production due to the long development time (1- 2 years). The degassing of the perimeter can occur up to three times the drivage width which can represent 10 to 20 % of the coal present. This coal's contribution to actual emissions can be considerably lower than predicted because of the absence of this gas.

Finally, (Creedy, 1981) has indicated that as a result of testing on coal core samples retrieved from the floor of a previously mined out area, the emissions as predicted from floor coal seams using Airey's prediction method might be over estimated. Every

prediction model has its limitations and a few have been touched on above in regards to Airey's method.

4.4 Simplified Airey's method

The MRDE model, which is based on a set of computer programs to calculate all the various parameters, presented in Airey's prediction model is not available for this report. An abridged program of the model presented by (Creedy and Kershaw, 1988) was evaluated and later used with some modifications.

The model on which the simplified method is based considers that all seams within 200 m in the roof and 100 m in the floor release gas, the quantity depending on the thickness of coal, proximity to the workings, and inseam gas content. Coal seams in the zone disturbed by mining are considered to be the only sources of gas. This will be followed in this report.

The model considers a mature district of 50 weeks in age thus yielding a reasonable estimate of the maximum methane flow that the ventilation must be designed to deal with. The model determines methane flow (l/s) on a weekly basis and this will be followed except with methane flow being expressed in units of m³/s.

In this report, Airey emission factors (MRDE, 1976) will be presented in this model as deduced according to the emissions the curves of Figure 4.3. This Figure provides worked seam depth correction factors, if its depth is lower or higher than 900 m. These correction values are added to the height interval of coal seams in the adjacent strata relative to the worked seam. Once the corrected seam height is determined, than a degree of emission factor is deduced from Figure 4.3, which takes into consideration the age of the district.

Example: In the abridged program, the emission factor at coal seam height of 100m in the roof, at worked seam depth of 600 m, and a district age of 50 weeks equals 0.56.

This is arrived at by placing a straight edge on Figure 4.3 at the 600 m depth mark and drawing a line perpendicular to this axes to the + 100 m mark, the distance between the roof seam and the working district. A second line drawn perpendicular to the ordinate from this 100 m mark intersects the height correction curve at -20 m. The value of -20 m is added to the height of 100 m to give a corrected height of 80 m for this seam at a working district depth of 600 m. This 80 m value is used in the second emission curve (Figure 4.3), and is matched with the 80 m mark on the ordinate axes and a perpendicular line from this point on the axes is drawn to the district age curve of 50 weeks. At the point of intersection between the intersection of this line and the district age curve, a second line is drawn perpendicular to and down to the X axis where it intersects the degree of emission factor of 0.56 for the coal seam at corrected height of 80 m. All emission factors for coal seams adjacent to the Phalen seam were derived as described.

In the abridged model a geological cross section showing the thickness and depths of all seams from 200m and 100 m below the proposed working is required. It also requires clean coal thickness which are not available for this report (seam height is assumed to be clean coal height or thickness), although the uniformity and quality of the coal measures has been stated.

4.5 Model limitations

The calculations are made in the following two stages of which two will be presented in this report each occupying a separate pro-forma.

Calculation of Specific Emissions from Adjacent Gas Sources

Assumptions

(1) In the abridged program, the gas from the adjacent coal seams is much greater than the worked seam; therefore, the simplifying assumption has been made that the degree of emission of face coal, cut coal in the district, and any uncut coal sources are constant.

In this report actual measurements of coal face gas will derive this worked seam gas emission and Airey's face emission curve will not be used. Inspection of this curve clearly indicates that it would over estimate specific emissions for the worked seam and this will not be pursued. Specific emission is the total gas make from all gas sources divided by the tonnes mined from the working seam for that same time period.

Table 4.1 presents the results of four borehole logs describing a cross section of coal seams through the Phalen mine resource block and detail the coal seam sequence - 200 m above and 100 m below the Phalen seam.

Borehole No.	Harbour Coal Seam Thickness (m)	Depth (m)	Upper Boutillier Coal Seam Thickness (m)	Depth (m)	Boutillier Coal Seam Thickness (m)	Depth (m)
C 125	2.00	138	0.50	73	0.88	55
B 162	2.13	136	0.31	73	1.00	52
BH- 140	2.13	137	0.30	86	0.90	56
B-162	2.13	133	0.00		0.45	53
Average	2.10	136	0.28	77	0.81	54
Borehole No.	Backpit Coal Seam Thickness (m)	Depth (m)	Phalen Coal Seam Thickness (m)	Depth (m)	Emery Coal Seam Thickness (m)	Depth (m)
C 125	1.13	29	2.40	-	1.05	-42
B 162	0.46	31	2.19	-	1.05	-42
BH- 140	0.60	35	2.10	-	1.05	-42
B-162	0.10	36	2.00	-	1.05	-42
Average	0.57	33	2.17*	-	1.05	-42

Table 4.1 Borehole log data of the Harbour, Boutillier, Backpit, Phalen and Emery coal seams

Note that the Emery seam values are estimated based on Figure 2.1; since, the boreholes did not provide information for this seam down to the -40 m mark. To simplify calculations, it is assumed that the distance interval for each coal seam to the worked seam, and seam thickness is the same; since, it covers a relatively small area with respect to Phalen 4 and 5 each districts. Depth correction factors deduced from Figure 4.3 are based on averaged borehole log data that are virtually the same for each seam;

therefore, an average depth correction value will be used and does not alter calculations of methane flow significantly (Table 4.2).

District	Depth (m)	Harbour (m)	Upper Boutillier (m)	Boutillier (m)	Backpit (m)	Phalen (m)	Emery (m)
4 East	425	-	-20	-14	-9	-	7
5 East	475	-	-18	-13	-9	-	7
6 East	525	-	-18	-13	-9	-	7
7 East	575	-	-15	-11	-8	-	6

Table 4.2 Depth correction values for coal seams in table 4.1 (Derived from Figure 4.2)

Table 4.3 presents the Airey emission factors for coal seams adjacent to the working seam of Phalen 4, 5 and 7 East districts.

Airey Emission Factors Coal Seams in Adjacent Strata				
Districts Age(Wks)	Upper Boutillier	Boutillier	Backpit	Emery
17	58.8	72.9	84.9	75.6
18	59.7	73.6	85.6	76.4
19	60.5	74.3	86.3	77.2
20	61.3	75.0	87.0	78.0
21	61.7	75.4	87.3	78.3
22	62.2	75.7	87.6	78.7
23	62.6	76.1	87.9	79.0
24	63.0	76.4	88.2	79.3
25	63.4	76.8	88.5	79.7
26	63.8	77.1	88.8	80.0
27	64.2	77.5	89.1	80.3
28	64.7	77.8	89.4	80.6
29	65.1	78.2	89.7	81.0
30	65.5	78.5	90.0	81.3
31	65.9	78.9	90.3	81.6
32	66.3	79.2	90.6	82.0
33	66.7	79.6	90.9	82.3
34	67.2	79.9	91.2	82.6
35	67.6	80.3	91.5	83.0
36	68.0	80.6	91.8	83.3
37	68.4	81.0	92.1	83.6
38	68.8	81.3	92.4	83.9

Table 4.3 Airey emission factors for coal seams adjacent to the working seam of Phalen 4, 5 and 7 East districts (continued)

Airey Emission Factors Coal Seams in Adjacent Strata				
Districts Age(Wks)	Upper Boutillier	Boutillier	Backpit	Emery
39	69.2	81.7	92.7	84.3
40	69.7	82.0	93.0	84.6
41	69.9	82.2	93.1	84.8
42	70.1	82.4	93.2	85.0
43	70.4	82.6	93.3	85.1
44	70.6	82.8	93.5	85.3
45	70.9	83.0	93.6	85.5
46	71.1	83.2	93.7	85.7
47	71.3	83.4	93.8	85.9
48	71.6	83.6	93.9	86.1
49	71.8	83.8	94.0	86.2
50	72.0	84.0	94.1	86.4
51	72.3	84.2	94.3	86.6
52	72.5	84.4	94.4	86.8
53	72.8	84.6	94.5	87.0
54	73.0	84.8	94.6	87.2
55	73.2	85.0	94.7	87.3
56	73.5	85.2	94.8	87.5
57	73.7	85.4	94.9	87.7
58	73.9	85.6	95.1	87.9
59	74.2	85.8	95.2	88.1
60	74.4	86.0	95.3	88.3
61	74.7	86.2	95.4	88.4
62	74.9	86.4	95.5	88.6
63	75.1	86.6	95.6	88.8
64	75.4	86.8	95.7	89.0
65	75.6	87.0	95.9	89.2
66	75.8	87.2	96.0	89.4
67	76.1	87.4	96.1	89.5
68	76.3	87.6	96.2	89.7
69	76.6	87.8	96.3	89.9
70	76.8	88.0	96.4	90.1
71	77.0	88.2	96.5	90.3
72	77.3	88.4	96.7	90.5
73	77.5	88.6	96.8	90.6
74	77.8	88.8	96.9	90.8
75	78.0	89.0	97.0	91.0

Table 4.3 Airey emission factors for coal seams adjacent to the working seam of Phalen 4, 5 and 7 East districts

(3) The Harbour seam is not considered in the calculation; since, it has been worked out of the sequence of seams by previous mining. Moreover, it is assumed that little degassing of the coal seams below the Harbour has not occurred; therefore, the unworked coal is assumed to be in its original gassy state.

(4) It is assumed that the average methane flow from sealed gobs for the 1 East Bleeder comparison = $0.120 \text{ m}^3/\text{s}$ for 4 East, and = $0.198 \text{ m}^3/\text{s}$ for 5 East. These have been determined from previous surveys prior to 4 and 5 East going into production.

(5) The gas content of coal seams in adjacent strata will be found by the equation in Figure 3.7 as derived.

4.6 Methane prediction for Phalen mine 4 and 5 East districts

Calculation of Specific Emission from the Adjacent Coal Seams

The calculation of specific emission for each coal seam adjacent to Phalen 4 and 5 East is presented in Tables 4.4 and 4.5. These are arrived at by multiplying the emission factor for the seam of interest from Table 4.3 by the seams estimated gas content derived from Figure 3.7. These emission values will be used in section 6 to calculate predicted methane versus measured flow for Phalen 4, 5 and 7 East district gobs. 7 East Sewergate will use the predicted methane flow for 7 to estimate the methane captured and performance.

Phalen 4 East						
Predicted Specific Emissions						
	(U) Boutillier	Boutillier	Backpit	Phalen	Emery	
Thickness (cm)	30	81	57	263	105	
Relative Thickness	0.11	0.31	0.22	1.00	0.40	
Depth (m)	348	371	392	425	467	
Gas Content (m ³ /Tonne)	7.5	7.7	8.0	8.3	8.7	
Weeks	Specific Emissions (m ³ /Tonne)					Total Strata Emissions
17	0.50	1.74	1.46		2.62	6.32
18	0.51	1.75	1.48		2.65	6.39
19	0.51	1.77	1.49		2.68	6.45
20	0.52	1.79	1.50		2.71	6.51
21	0.53	1.79	1.51		2.72	6.54
22	0.53	1.80	1.51		2.73	6.57
23	0.53	1.81	1.52		2.74	6.60
24	0.54	1.82	1.52		2.75	6.63
25	0.54	1.83	1.53		2.76	6.66
26	0.54	1.84	1.53		2.78	6.69
27	0.55	1.84	1.54		2.79	6.71
28	0.55	1.85	1.54		2.80	6.74
29	0.55	1.86	1.55		2.81	6.77
30	0.56	1.87	1.55		2.82	6.80
31	0.56	1.88	1.56		2.83	6.83
32	0.56	1.88	1.56		2.84	6.86
33	0.57	1.89	1.57		2.86	6.89
34	0.57	1.90	1.57		2.87	6.91
35	0.58	1.91	1.58		2.88	6.94
36	0.58	1.92	1.58		2.89	6.97
37	0.58	1.93	1.59		2.90	7.00
38	0.59	1.93	1.59		2.91	7.03
39	0.59	1.94	1.60		2.92	7.06
40	0.59	1.95	1.60		2.94	7.08
41	0.59	1.96	1.61		2.94	7.10
42	0.60	1.96	1.61		2.95	7.12
43	0.60	1.97	1.61		2.96	7.13
44	0.60	1.97	1.61		2.96	7.15
45	0.60	1.98	1.61		2.97	7.16
46	0.61	1.98	1.62		2.97	7.18
47	0.61	1.98	1.62		2.98	7.19
48	0.61	1.99	1.62		2.99	7.21
49	0.61	1.99	1.62		2.99	7.22
50	0.61	2.00	1.62		3.00	7.24
51	0.62	2.00	1.63		3.01	7.25
52	0.62	2.01	1.63		3.01	7.27
53	0.62	2.01	1.63		3.02	7.28
54	0.62	2.02	1.63		3.03	7.30
55	0.62	2.02	1.63		3.03	7.31

Table 4.4 Airey predicted specific emissions factors for coal seams adjacent to the 4 East district

Phalen 5 East Predicted Specific Emissions (U) Boutillier Boutillier Backpit Phalen Emery						
Thickness (cm)	30	81	57	263	105	
Relative Thickness	0.11	0.31	0.22	1.00	0.40	
Depth (m)	399	422	443	476	518	
Gas Content (m ³ /Tonne)	8.0	8.3	8.5	8.8	9.1	
Weeks	Specific Emissions (m ³ /Tonne)					Total Strata Emissions
17	0.54	1.86	1.56		2.75	6.71
18	0.55	1.87	1.57		2.78	6.78
19	0.55	1.89	1.58		2.81	6.84
20	0.56	1.91	1.60		2.84	6.91
21	0.57	1.92	1.60		2.85	6.94
22	0.57	1.93	1.61		2.87	6.97
23	0.57	1.94	1.61		2.88	7.00
24	0.58	1.95	1.62		2.89	7.03
25	0.58	1.95	1.62		2.90	7.06
26	0.58	1.96	1.63		2.91	7.09
27	0.59	1.97	1.64		2.93	7.12
28	0.59	1.98	1.64		2.94	7.15
29	0.60	1.99	1.65		2.95	7.18
30	0.60	2.00	1.65		2.96	7.21
31	0.60	2.01	1.66		2.97	7.24
32	0.61	2.02	1.66		2.99	7.27
33	0.61	2.03	1.67		3.00	7.31
34	0.62	2.03	1.67		3.01	7.34
35	0.62	2.04	1.68		3.02	7.37
36	0.62	2.05	1.69		3.03	7.40
37	0.63	2.06	1.69		3.05	7.43
38	0.63	2.07	1.70		3.06	7.46
39	0.63	2.08	1.70		3.07	7.49
40	0.64	2.09	1.71		3.08	7.52
41	0.64	2.09	1.71		3.09	7.53
42	0.64	2.10	1.71		3.10	7.55
43	0.64	2.10	1.71		3.10	7.56
44	0.65	2.11	1.72		3.11	7.58
45	0.65	2.11	1.72		3.12	7.60
46	0.65	2.12	1.72		3.12	7.61
47	0.65	2.12	1.72		3.13	7.63
48	0.66	2.13	1.72		3.14	7.65
49	0.66	2.13	1.73		3.14	7.66
50	0.66	2.14	1.73		3.15	7.68
51	0.66	2.14	1.73		3.16	7.69
52	0.66	2.15	1.73		3.16	7.71
53	0.67	2.15	1.73		3.17	7.73
54	0.67	2.16	1.74		3.18	7.74
55	0.67	2.16	1.74		3.18	7.76

Table 4.5 Airey predicted specific emissions factors for coal seams adjacent to the 5 East district

Phalen 7 East Predicted Specific Emissions (U) Boutillier Boutillier Backpit Phalen Emery						
Thickness (cm)	30	81	57	245	105	
Relative Thickness	0.12	0.33	0.23	1.00	0.43	
Depth (m)	498	521	542	575	617	
Gas Content (m ³ /Tonne)	9.1	9.2	9.4	9.7	10.0	
Weeks	Specific Emissions (m ³ /Tonne)					Total Strata Emissions
17	0.65	2.23	1.86		3.23	7.97
18	0.66	2.25	1.88		3.26	8.05
19	0.67	2.27	1.89		3.30	8.13
20	0.68	2.29	1.91		3.33	8.21
21	0.68	2.30	1.91		3.35	8.25
22	0.69	2.31	1.92		3.36	8.28
23	0.69	2.32	1.93		3.37	8.32
24	0.70	2.34	1.93		3.39	8.35
25	0.70	2.35	1.94		3.40	8.39
26	0.71	2.36	1.95		3.42	8.43
27	0.71	2.37	1.95		3.43	8.46
28	0.72	2.38	1.96		3.45	8.50
29	0.72	2.39	1.97		3.46	8.53
30	0.73	2.40	1.97		3.47	8.57
31	0.73	2.41	1.98		3.49	8.61
32	0.74	2.42	1.98		3.50	8.64
33	0.74	2.43	1.99		3.52	8.68
34	0.74	2.44	2.00		3.53	8.71
35	0.75	2.45	2.00		3.54	8.75
36	0.75	2.46	2.01		3.56	8.79
37	0.76	2.47	2.02		3.57	8.82
38	0.76	2.49	2.02		3.59	8.86
39	0.77	2.50	2.03		3.60	8.89
40	0.77	2.51	2.04		3.61	8.93
41	0.77	2.51	2.04		3.62	8.95
42	0.78	2.52	2.04		3.63	8.97
43	0.78	2.52	2.04		3.64	8.99
44	0.78	2.53	2.05		3.65	9.01
45	0.79	2.54	2.05		3.65	9.03
46	0.79	2.54	2.05		3.66	9.05
47	0.79	2.55	2.05		3.67	9.06
48	0.79	2.56	2.06		3.68	9.08
49	0.80	2.56	2.06		3.68	9.10
50	0.80	2.57	2.06		3.69	9.12
51	0.80	2.57	2.06		3.70	9.14
52	0.80	2.58	2.07		3.71	9.16
53	0.81	2.59	2.07		3.72	9.18
54	0.81	2.59	2.07		3.72	9.20
55	0.81	2.60	2.07		3.73	9.22

Table 4.6 Airey predicted specific emissions factors for coal seams adjacent to the 7 East district (continued)

Phalen 7 East						
Predicted Specific Emissions						
(U) Boutillier Boutillier Backpit Phalen Emery						
Thickness (cm)	30	81	57	245	105	
Relative Thickness	0.12	0.33	0.23	1.00	0.43	
Depth (m)	498	521	542	575	617	
Gas Content (m ³ /Tonne)	9.1	9.2	9.4	9.7	10.0	
Weeks	Specific Emissions (m ³ /Tonne)					Total Strata Emissions
56	0.81	2.60	2.08		3.74	9.24
57	0.82	2.61	2.08		3.75	9.25
58	0.82	2.62	2.08		3.76	9.27
59	0.82	2.62	2.08		3.76	9.29
60	0.82	2.63	2.09		3.77	9.31
61	0.83	2.64	2.09		3.78	9.33
62	0.83	2.64	2.09		3.79	9.35
63	0.83	2.65	2.09		3.79	9.37
64	0.84	2.65	2.10		3.80	9.39
65	0.84	2.66	2.10		3.81	9.41
66	0.84	2.67	2.10		3.82	9.43
67	0.84	2.67	2.10		3.83	9.45
68	0.85	2.68	2.11		3.83	9.46
69	0.85	2.68	2.11		3.84	9.48
70	0.85	2.69	2.11		3.85	9.50
71	0.85	2.70	2.11		3.86	9.52
72	0.86	2.70	2.12		3.86	9.54
73	0.86	2.71	2.12		3.87	9.56
74	0.86	2.71	2.12		3.88	9.58
75	0.86	2.72	2.12		3.89	9.60

Table 4.6 Airey predicted specific emissions factors for coal seams adjacent to the 7 East district

Coal Mine Ventilation

5.0 Coal mine ventilation

The basic objective of ventilation is to provide airflows of sufficient quantity and quality to (i) sustain life and activity and (ii) to dilute contaminants to safe concentrations in all parts of the mine where personnel work or travel.

5.1.0 Phalen mine ventilation

Phalen mine is ventilated by an exhaust fan which is located on the surface at the top of a shaft which meets the junction of the two main returns airways underground (Figure 5.1).

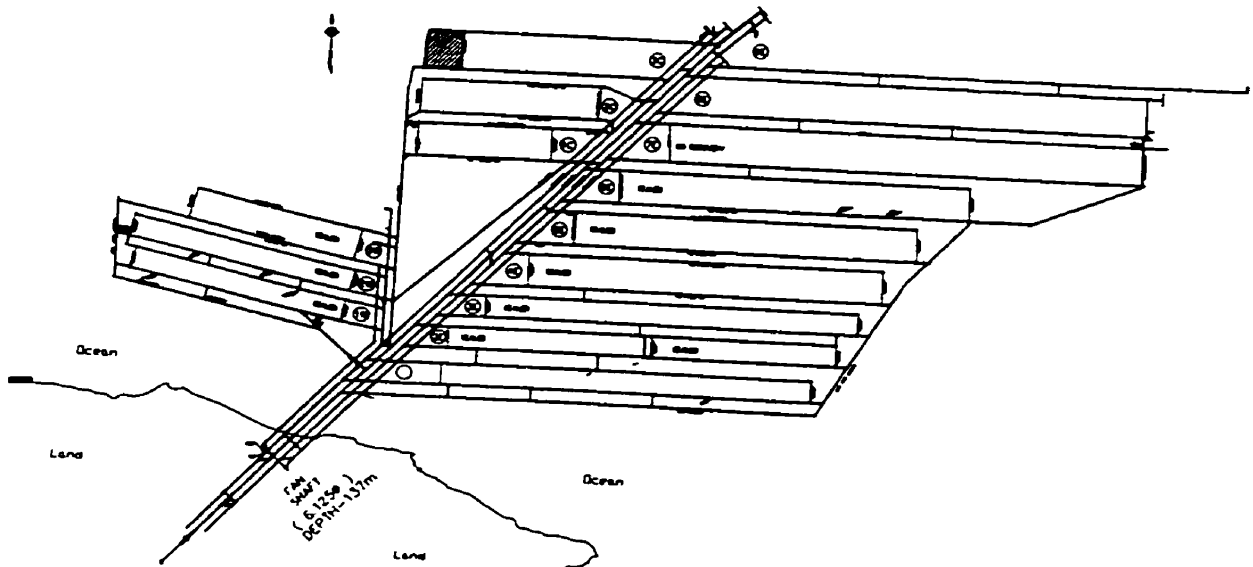


Figure 5.1 Phalen mine layout

Phalen mine is considered gassy (specific emissions $> 10 \text{ m}^3$ tonne mined) where concentrations of methane desorbed from both the cut coal and surrounding strata about the seam are high. As a result, special design considerations must be practiced during mine layout to ensure adequate quantities of fresh air are available for mine gas dilution to keep concentrations well below the explosive range (Macdonald R.J., D.A.Payne, 1992).

5.1.1 Z and Bleeder Deep U ventilation

Earlier in its life, Phalen mine used two forms of ventilation layouts to control methane emissions. During the early stages of wall production a 'Z' system was practiced where air was coursed in the top and bottom levels of the wall and returned on the supported top gate to a backbleeder roadway (Figure 5.2).

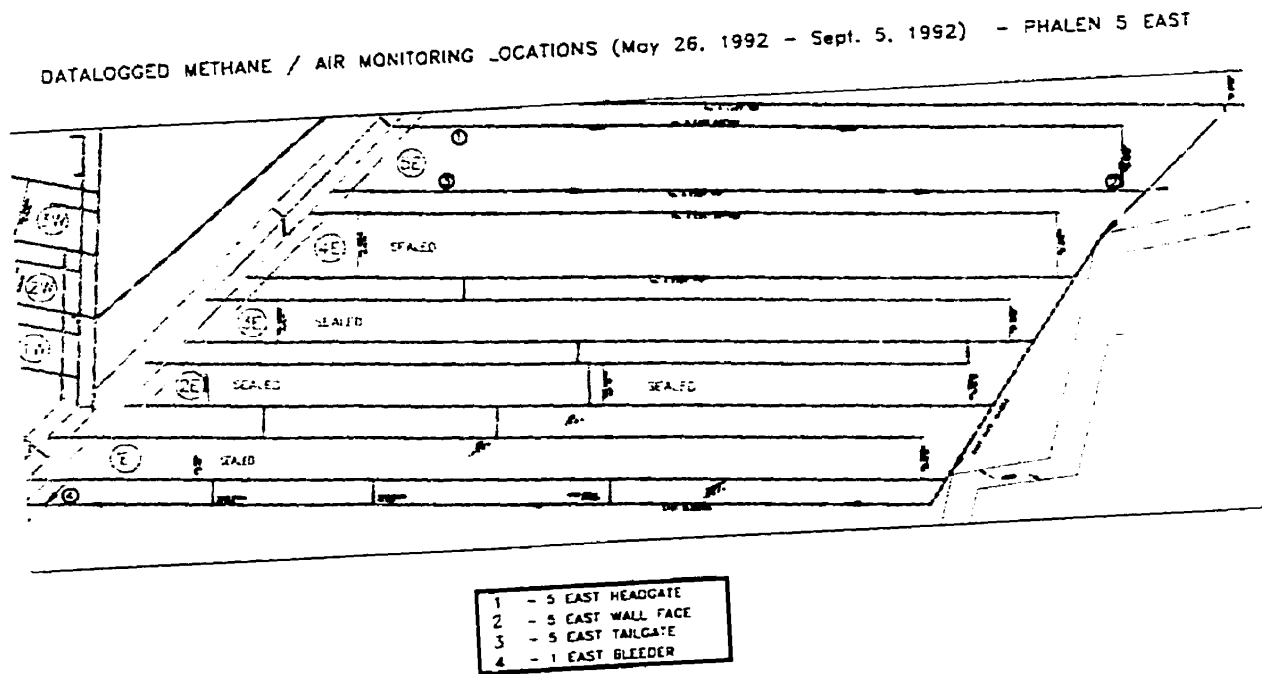


Figure 5.2 Phalen mine Z type ventilation layout and methane monitoring locations

When the wall had retreated to a point where the development of the next lower section broke through than ventilation was changed to a Bleeder Deep U system (Figure 5.3).

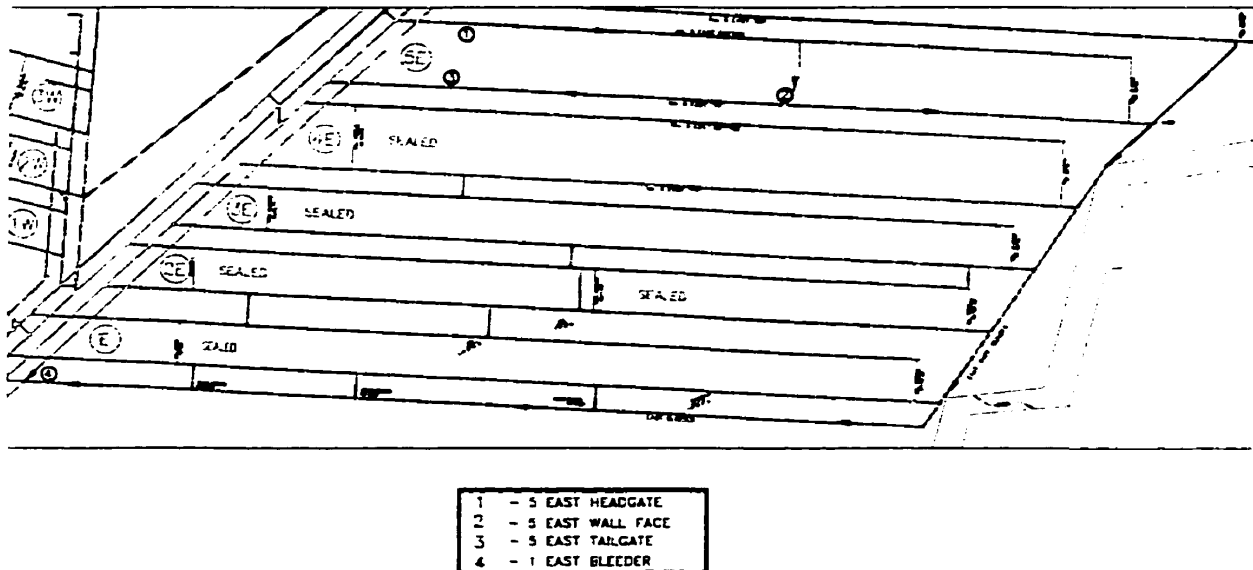


Figure 5.3 Phalen mine Bleeder Deep U ventilation layout and methane monitoring locations

These systems suffered from the following problems. Firstly, the Z system suffered from air leaving the face which could result in a deficiency of air at the top return end of the face and thus a potential rise in concentration of methane which would automatically shut down power to face equipment should it exceed 1.25%. Also, the coursing of air through such tight restrictions in the supported level behind the face gave rise to a high water gauge on the main surface fan and decreased its operating efficiency. Thirdly, the Bleeder Deep development could not continue until the next lower section broke through and this delayed development of this drivage.

The problem with the Bleeder Deep U system was viewed similar to those mentioned for the Z-system, although ventilation of the top face was adequate. Some concern was expressed in regards to gas slippage along the highside rib, return side of the face. The biggest problem with the system was waiting for the top level of the next wall to break through in order to provide additional air to the bleeder roadway. Through the transition from Z to Bleeder Deep U system due to water gauge restrictions placed on the main surface, a period of time may have existed when there was less air coursing the back

bleeder, therefore difficulty with dilution of methane below the statutory 2 % for this roadway. In the long term, concern was expressed that the coursing of air in an ever lengthening Bleeder Deep assigned to dilute increased methane emissions from the wall at greater depths, would eventually consume most of the available pressure drop required across the gob in the supported top level of the wall. At this point, the insufficient pressure drop and airflow across the constantly lengthening and restricting supported top level would make dilution of methane below 2% difficult.

5.1.2 Sewergate ventilation system

The Sewergate ventilation concept (Figure 5.4) was introduced to CBDC in a report by (AMCL, 1991) of Calgary.

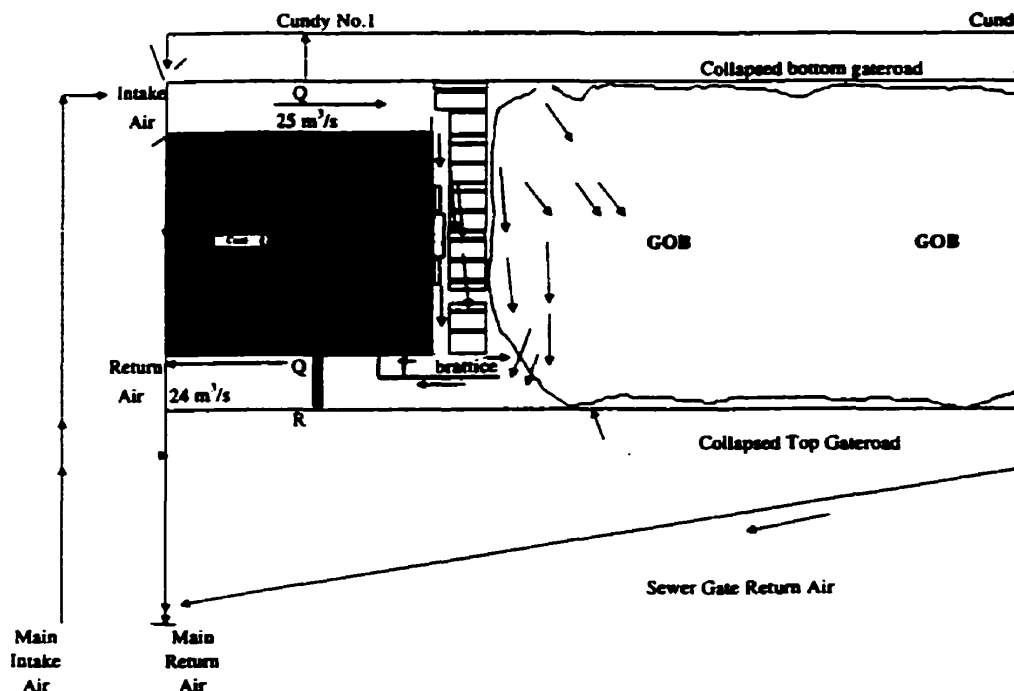


Figure 5.4 A Sewergate ventilation layout

The system, which is well tried in United Kingdom and is used in at least one mine in Australia, is that the gob area behind the face and the adjacent old gob, are kept at a pressure lower than the absolute pressure at the working face (Macdonald and Payne,

1992). Methane desorbed from adjacent strata will migrate to positions of lower pressure, and not to the working face. In all systems, including the bleeder system, the vital factor is the pressure distribution. In a bleeder system, the pressure is a result of high airflow behind the face. In the Sewergate, the pressure is achieved by a different means, but the effect on the methane is the same (Macdonald R.J., D.A. Payne, 1992). It is not necessary to have significant airflow behind the face with the Sewergate, indeed such airflow is undesirable, firstly because it reduces airflow at the coal front, and secondly it creates a pressure loss in the Sewergate and reduces its efficiency. All pressures on the face and in the face return must be at a higher pressure than the Sewergate.

CBDC decided to abandon pillarless workings at a later date, so the original Sewergate concept was changed but nevertheless still practiced. In this case, the face start line was point of lower absolute pressure, the top gate road was allowed to fully cave, and it was expected that a sufficient pressure gradient of at least 500 Pa would develop across the gob. In practice, the Sewergate has suffered some major drawbacks from its earlier concept due to poor gob consolidation and air leakage problems related Lower Sandstone Unit.

5.1.3 BM Methane sensor locations

Figures 5.2, 5.3 and 5.5 present the location of methane monitoring during the data collection phase for Phalen 4, 5 and 7 East walls. The locations of these detectors posed some problems in interpreting methane flow calculated from these data as follows:

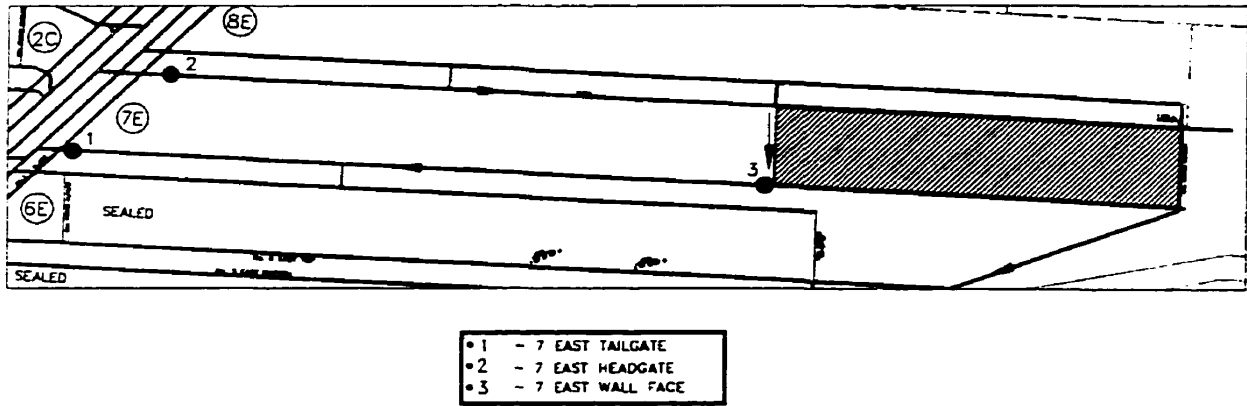


Figure 5.5 Phalen 7 East Sewergate ventilation layout and methane monitoring locations

- (1) Phalen 4 and 5 East operated on a bleeder ventilation system, and it was not possible to locate a permanent methane monitor in the East Bleeder Deep, outside the return airway because of electrical requirements (Figure 5.1, no.3) but was placed in the bleeder airway's outside end which was being contaminated by emissions from previously worked walls. This was further complicated by the emissions from the soon to be operating adjacent panels and as a result Phalen 4 and 5 East walls Bleeder Deep emissions could not be isolated from each other on a real time basis. Two surveys of the East Bleeder prior to the start-up of both 4 and 5 East walls determined that the methane flow was 0.120 (AMCL, 1991) and 0.198 m³/sec (Author) respectively from old gobs (Figure 5.1).
- (2) When Phalen switched to Sewergate ventilation on 6 and 7 East wall, methane monitors were removed from the East Bleeder and placed outside a fenced off area on 5 slope return airway to measure the methane content in air from the East Bleeder. No provision was made to monitor methane flow directly from the East Bleeder (except for spot samples) or from a location up-stream on 5 slope where sufficient mixing of the mine air occurred to get a good methane measurement. This location too would have suffered since it would be measuring methane emissions for the whole Eastside of the mine. Overall, no estimates of the methane flow from the East Bleeder (hence, from 6 and 7 East gobs) could be accurately made on a real time basis.

5.2.0 Methane patterns databases

Presently data bases have been created for Phalen 2 West and 4, 5, 6 and 7 Eastside districts and for Lingan 12 East and 13 East districts (the mine flooded in 1992 and was permanently closed in 1993). Data analysis of methane emissions have been provided on an on going basis since 1989 via CANMET Steering Committee Reports 14 to 44 under the subtitles Mine Environment - Ventilation of High Output Retreat Walls and Methane Studies. The data have has been reduced and reported on an 8 hour shift basis, because of the shear quantity of the information collected from BM monitors.

5.2.1 BM Methanometer sensitivity

Another source of error in the determination of methane flow is the sensitivity of the BM type methane sensor itself. Its accuracy is $\pm 0.1\%$, methane content in air between 0 and 1.25%. CSL on occasions have conducted calibration checks of these sensors on site using standard CSE calibration gases (0 %, 1%, and 2.5 % methane in dry air) and have found that with the 0 % methane in air standard, the sensor typically reads 0.1 %. (Table 5.1).

Using the 1 % methane in air standard, the sensor gives a reading of 1.03 %. These units work within the manufacturer's specifications; however, $\pm 0.1\%$ is a relatively high error when looking at methane contents that are typically on average between 0 and 1 % in the mine airway. However, all things equal, methane readings on average should be consistent and representative of the methane content in the mine airway.

Mine	Date	Location	CSE Gas Calibration Standards (% CH ₄ in dry air)		
			0%	1%	2.5%
Lingan	10/4/90	12 East Top (Outside end)	0.08	0.90	-
Phalen	10/10/90	12 East intake	0.08	1.06	-
		2 West intake	0.04	1.08	-
		2 West Face	0.08	0.95	-
Lingan	10/23/90	2 West bleeder	0.20	0.89	-
		12 East Top (Outside end)	0.04	0.97	-
		12 East Face	0.06	1.03	-
Phalen	10/25/90	12 East intake	0.08	1.06	-
		2 West intake	0.04	1.08	-
		2 West Face	0.03	0.97	-
Phalen	10/25/90	2 West bleeder	0.16	0.85	-
		2 West intake	0.04	1.08	-
		2 West Face	0.03	0.98	-
Phalen	11/30/90	2 West bleeder	0.16	0.85	-
		2 West intake	0.04	1.08	-
		2 West Face	0.02	1.01	-
Phalen	12/17/90	2 West bleeder	0.21	1.01	-
		2 West intake	0.03	1.07	-
		2 West Face	0.23	1.01	-
Lingan	11/8/90	12 East Top (Outside end)	0.04	0.97	-
		12 East Face	0.06	1.03	-
		12 East intake	0.08	1.06	-
Lingan	11/30/90	12 East Top (Outside end)	0.01	1.03	-
		12 East Face	0.05	1.00	-
		12 East intake	0.09	0.98	-
Lingan	12/19/90	12 East Top (Outside end)	0.01	1.03	-
		12 East Face	0.04	1.00	-
		12 East intake	0.09	0.98	-
Phalen	1/7/91	2 West intake	0.01	1.01	-
		2 West Face	0.04	1.01	-
		2 West bleeder	0.22	0.98	-
Lingan	1/8/91	12 East Top (Outside end)	0.09	0.98	-
		12 East Face	0.09	1.02	-
		12 East intake	0.05	0.97	-
Phalen	1/29/91	2 West intake	0.01	1.01	-
		2 West Face	0.04	1.01	-
		2 West bleeder	0.22	0.98	-
Lingan	1/30/91	12 East Top (Outside end)	0.17	1.02	-
		12 East Face	0.13	0.96	-
		12 East intake	0.05	0.97	-
Lingan	1/30/91	12 East Top (Outside end)	0.09	1.02	-
		12 East Face	0.10	0.99	-
		12 East intake	0.05	0.97	-
Prince	9/19/94	Surface Fan - shaft bottom	0.15	1.00	-
Prince	3/25/95	Surface Fan - shaft bottom	0.07	0.90	-
Prince	2/13/96	-	0.10	1.11	-
Phalen	9/15/94	Surface fan duct	0.20	1.02	-
Phalen	4/19/95	Surface fan duct	0.26	1.05	-

Table 5.1 BM methane sensor calibration checks and sensitivity (continued)

Mine	Date	Location	CSE Gas Calibration Standards (% CH ₄ in dry air)		
			0%	1%	2.5%
Lingan	3/1/90	12 East Top (Outside end)	0.07		2.06
		12 East Face			
		12 East intake	0.19		
Phalen	3/2/90	2 West Bleeder	0.08		2.50
		2 West Face	0.05		2.45
		2 West intake			2.19
Lingan	3/14/90	12 East Top (Outside end)	0.10		2.19
		12 East Face			
		12 East intake	0.09		2.10
Phalen	3/15/90	2 West Face	0.18		2.25
		2 West intake	0.00		2.49
Lingan	4/3/90	12 East Top (Outside end)	0.00		2.36
		12 East Face	0.00		
		12 East intake	0.09		2.04
Phalen	4/6/90	2 West intake	0.17		2.33
Lingan	4/18/90	12 East Top (Outside end)	0.08		2.39
		12 East Face	0.08		2.26
Phalen	4/19/90	2 West bleeder	0.17		2.30
Lingan	5/1/90	12 East Top (Outside end)	0.06		2.46
		12 East Face	0.01		
		12 East intake	0.07		2.28
Phalen	5/2/90	2 West intake	0.12		2.47
		2 West bleeder	0.18		
Lingan	5/23/90	12 East Top (Outside end)	0.06		2.27
		12 East intake	0.10		2.34
Phalen	5/24/90	2 West bleeder	0.18		2.22
Lingan	6/12/90	12 East Top (Outside end)	0.04		1.55
		12 East Face	0.03		
Phalen	6/13/90	2 West intake	0.14		2.57
		2 West Face	0.13		
		2 West bleeder	0.18		2.14
Lingan	7/4/90	12 East Top (Outside end)	0.07		2.41
		12 East Face	0.12		
		12 East intake	0.12		2.42
Lingan	7/25/90	12 East Top (Outside end)	0.04	1.04	
		12 East intake	0.12	0.95	
Phalen	7/26/90	2 West intake	0.15	1.31	
		2 West Face	0.01	1.03	
		2 West bleeder	0.19	0.98	
Lingan	8/15/90	12 East Top (Outside end)	0.03	1.02	
		12 East Face	0.03	1.02	
		12 East intake	0.13	1.04	
Phalen	8/17/90	2 West intake	0.16	1.13	
		2 West Face	0.12	1.07	
		2 West bleeder	0.18	0.90	
Summary			CSE Gas Calibration Standards (% CH ₄ in dry air)		
			0%	1%	2.5%
Number of calibrations			92	61	25
Statistical Average % CH ₄			0.10	1.03	2.38
Standard Deviation			0.07	0.07	0.21

Table 5.1 BM methane sensor calibration checks and sensitivity

5.2.2 Ventilation measurements

CSL employed Ba 5 air velocity detectors readings during the study period. The information obtained from the detectors could only be used on a qualitative basis because of the sensors location which purpose is only to detect air speed. To a lesser extent, but to some certain degree, the methane flow data is weakened because it is calculated from ventilation measurements made and reported by CBDC ventilation staff. These quantities are reported in a ventilation log and the frequency of the measurements usually depends on the need to determine ventilation system changes and/or for regulatory requirements

5.2.3 Anemometry versus tracer gas

Although reasonably accurate ventilation measurements were made by CBDC staff (normally one measurement per week airway), CSL must assume that these air flows remain constant between readings, which is unlikely; since, air flow varies during the week and corresponds with the opening and closing of the wall face cross section during mining (McPherson, 1993). Table 5.2 shows a comparison between ventilation measurements as determined by anemometer and tracer gas techniques. In terms of airflow measurements, errors are associated with routine measurements of mine airflow with anemometers. This is a second source of error to consider in the calculation of methane flow in airways in the data bases.

Anemometry Versus Tracer Gas Airflow Measurements			
Location	Air quantity (Tracer gas)	Air quantity (Anemometry)	% Difference
	(m ³ /s)	(m ³ /s)	
Phalen 2 West Bottom Intake	20.9	22.9	9.6%
Phalen 2 West Intake	18.0	18.3	1.7%
Lingan 12 East Top	23.3	25.1	7.7%
Lingan 12 East Top	25.6	27.3	6.6%
Lingan 12 East Top	29.0	31.7	9.3%
Phalen East Bleeder (outside end)	67.1	75.1	11.9%
Phalen East Bleeder (3rd cundy)	63.8	71.9	12.7%
Phalen East Bleeder (5 east back)	61.6	65.3	6.0%
Phalen East Bleeder (6 east back)	57.7	62.7	8.7%
Phalen Mine Surface Fan	194.6	209	7.4%
Prince Mine Surface Fan	91.7	101	10.1%
Phalen Mine Surface Fan	170.5	187.8	10.1%
Prince Mine Surface Fan	98.4	101.3	2.9%
Phalen Main East + West Main Return	170.5	187.8	10.1%
5 Slope Above 1 East Bleeder	100.8	106.7	5.9%
5 Slope Below 1 East Bleeder	104.4	109	4.4%
Phalen Main Surface Fan	155.8	175.5	12.6%
Phalen 2 East Intake	24.5	28.0	14.6%
Phalen 2 East Return	17.0	20.3	19.3%
Phalen Mine East Return at Shaft	116.0	133.9	15.4%
Phalen Mine West Return at Shaft	40.1	40.8	1.8%
Average % Difference			9.0%

Table 5.2 Anemometry versus tracer gas determined air quantities

Firstly, tracer gas is considered the more accurate measurement; since, it does not suffer from the effects of structures in airways which interfere with the measurements and affect the accurate determination of the airway's cross section needed in the anemometry's calculation. Secondly, anemometry measurements were not made with an extension handle; consequently, localized increases in air velocity due to the close proximity of the ventilation technologist was suspected. Thirdly, extension handles aid in making measurements in hard to reach areas where air velocities were different than in the main air stream. Comparison of anemometry and tracer gas measurements of ventilation flow consistently have shown that anemometry presents higher measurements, 9 % on average than those determined with tracer gas.

5.2.4 Methane flow and specific emissions calculations

Methane flows for airways in this report were calculated from the manufacturer's specifications for the BM methanometer system and from CBDC air flow measurements. The variations in the calculated flows may be as much as +/-10 to 15 % of the real value; therefore, in this context, any comparison with prediction techniques should be qualified to take this into account. When planning mine ventilation requirements this should be kept in mind and an allowance for such a variation to be taken into consideration.

Z Ventilation - Wall Face: - Methane flow from the wall face has been calculated by subtracting the average shift intake air methane content from the average shift wall face air methane content recorded by the methanometers multiplied by the difference in CBDC airflow measurements made between the top and bottom intakes for the Z-ventilation system. Methane flow units is given in the unit m^3/s .

Bleeder Deep U ventilation - Face: Methane flows from the wall face have been calculated by subtracting average shift intake air methane content from the average shift face air methane content and then multiplying this difference by the CBDC airflow measurements made for the return airway for both the Bleeder Deep U and Sewergate ventilation systems. Methane flow units is given in the unit m^3/s .

Return airway (outside end) methane flow: Methane flow in the return airway of the top level outside end (including the face emissions) has been calculated by subtracting the average shift intake air methane content from the average shift return air methane content then multiplying this difference by the CBDC airflow measurements made for the return airway for both Bleeder Deep U and Sewergate ventilation systems. Methane flow units is given in the unit m^3/s .

East Bleeder Methane Flow: The East Bleeder methane flow has been calculated from the average shift methane in air content for the East Bleeder roadway multiplied by CBDC airflow measurements made for the East Bleeder airway. Methane flow units is given in

the unit m^3/s . Note that 0.1 % methane content in air has been subtracted from the average shift methane content in air (noted on surveys and assumed constant) to account for background methane contamination from Phalen development sections.

Shift Specific Methane Emissions: Shift specific methane emissions have been calculated by multiplying the methane flow as calculated above by $8\text{hrs} \times 3600 \text{ s/hr}$ (units m^3) divided by the CBDC reported run of the mine tonnes per shift (tonnes). Specific emission is given in units of m^3/tonne .

Average Weekly Methane Flow: Average weekly methane flow has been calculated by averaging the shift average methane flow for 21 shifts (units m^3), starting Sunday at 23:00 hrs (backshift) to the following Sunday 23:00 hrs inclusive. Specific emission is given in units of m^3/tonne .

Average Weekly Methane Specific Emissions: Average weekly methane specific emissions for all areas has been calculated by averaging the shift average methane flow for 21 shifts, starting Sunday at 23:00 hrs (backshift) to the following Sunday 23:00 hrs inclusive and multiplying this by $7 \text{ days/wk} \times 24 \text{ hrs/day} \times 3600 \text{ s/hr}$ (units m^3) and dividing this value by the sum of all shift run of mine tonnes reported over the same period. Specific emission is given in units of m^3/tonne .

5.3.0 A comparison of the methane emissions and ventilation systems

Figures 5.5, 5.6 and 5.7 present the specific emission versus tonnes per shift basis for Phalen 4 and 5 East Face (Bleeder Deep U ventilation) and 7 East Face, Sewergate ventilation, respectively.

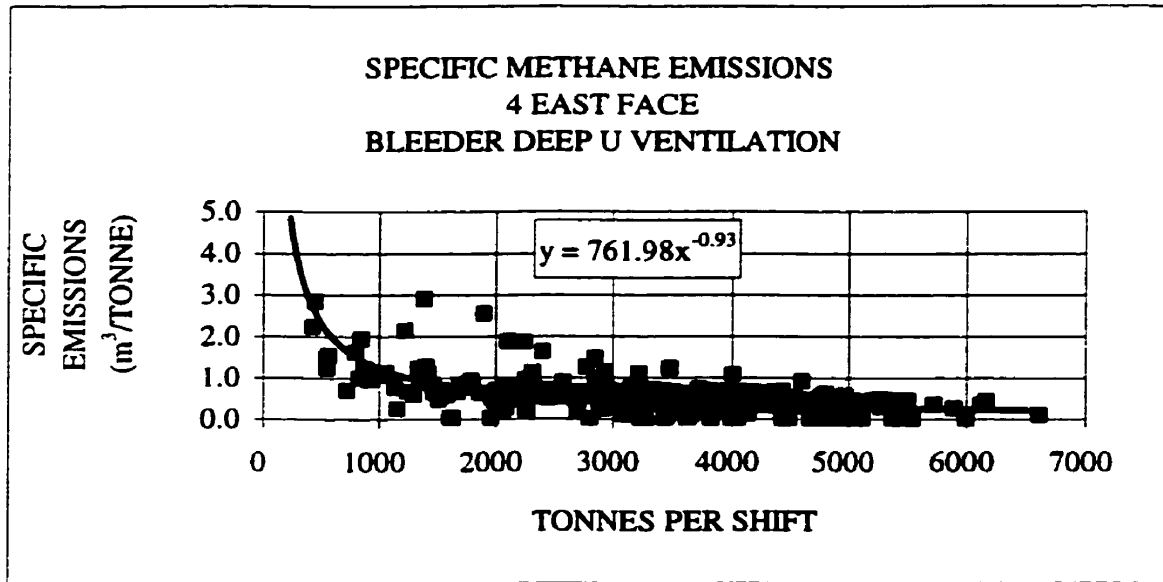


Figure 5.6 Specific emissions and and run of the mine tonnes per shift at Phalen 4 East Face, Bleeder Deep U ventilation

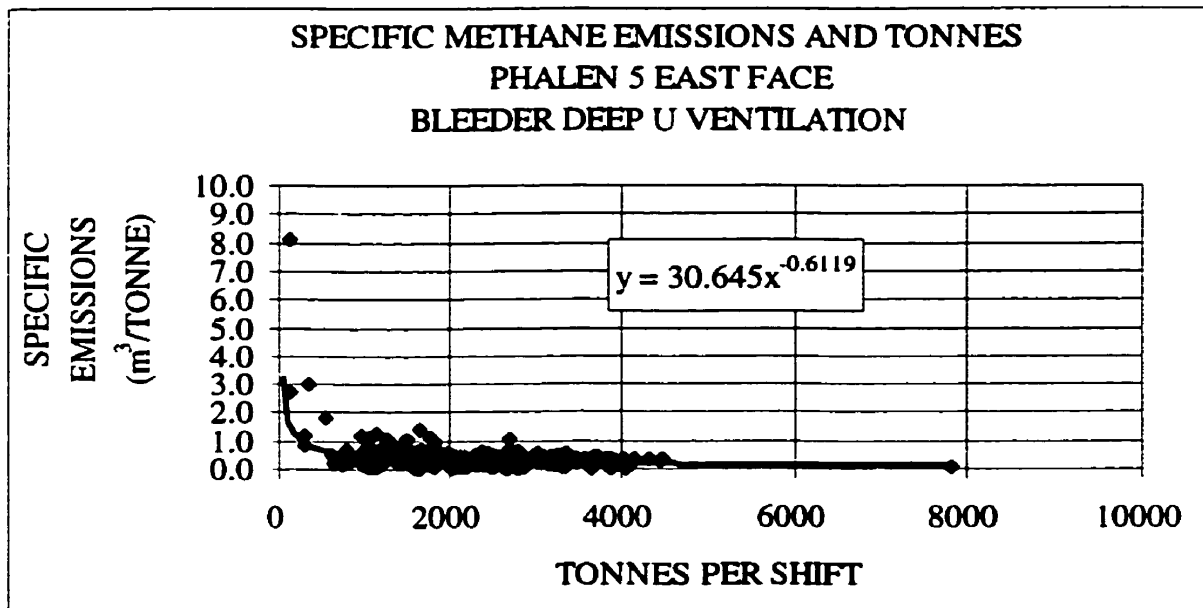


Figure 5.7 Specific emissions and and run of the mine tonnes per shift at Phalen 5 East Face, Bleeder Deep U ventilation

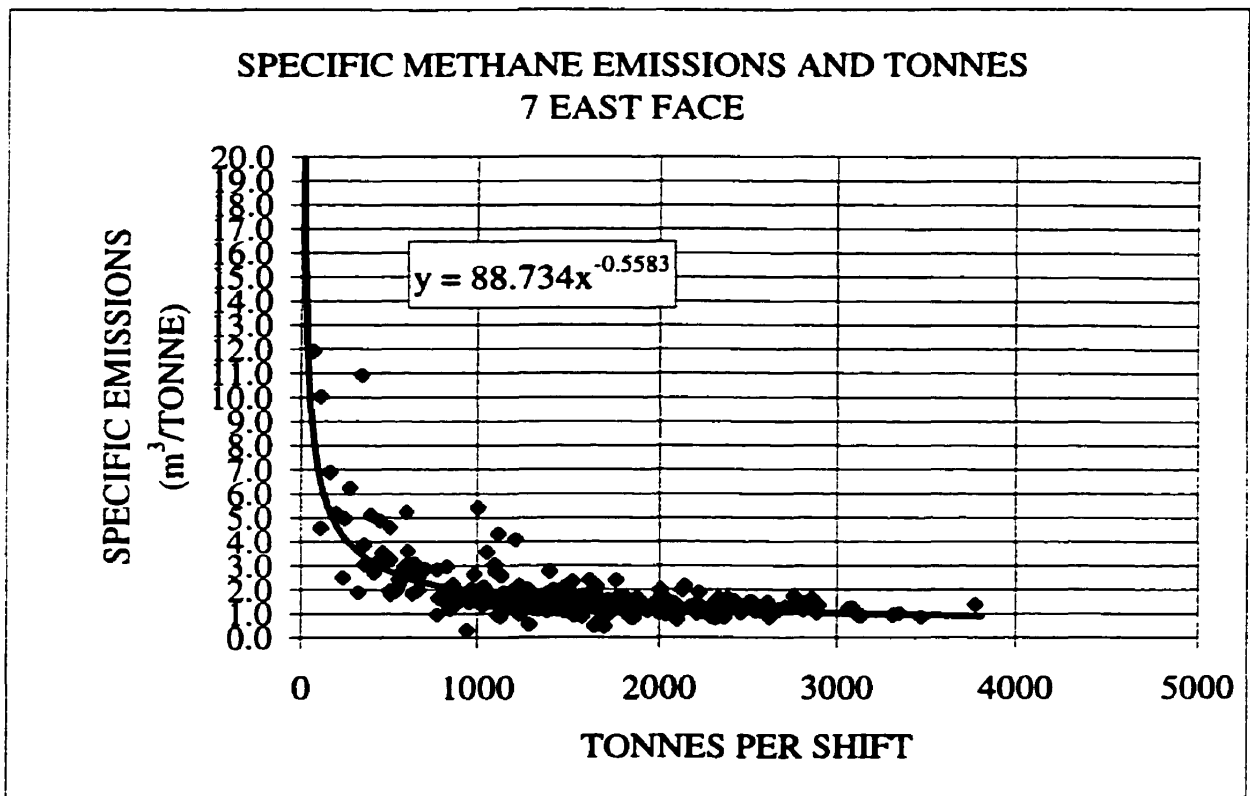


Figure 5.8 Specific emissions and and run of the mine tonnes per shift at Phalen 7 East Face, Sewergate ventilation

Figures 5.9, 5.10, 5.11 and 5.12 present the specific emissions versus tonnes per shift basis for Phalen 4 and 5 East Top (outside end), Bleeder Deep U ventilation and 6 and 7 East Top (outside end), Sewergate ventilation.

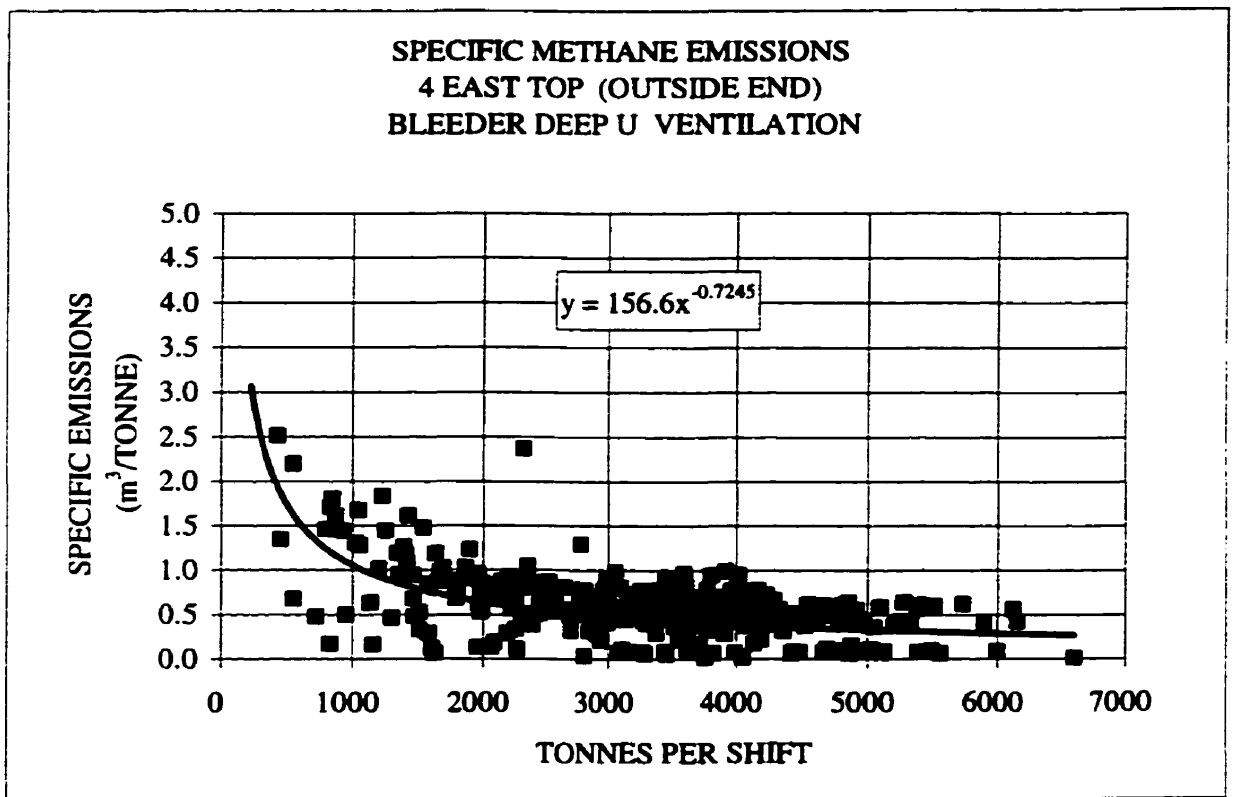


Figure 5.9 Specific emissions and run of the mine tonnes per shift at Phalen 4 East Top (outside end), Bleeder Deep U ventilation

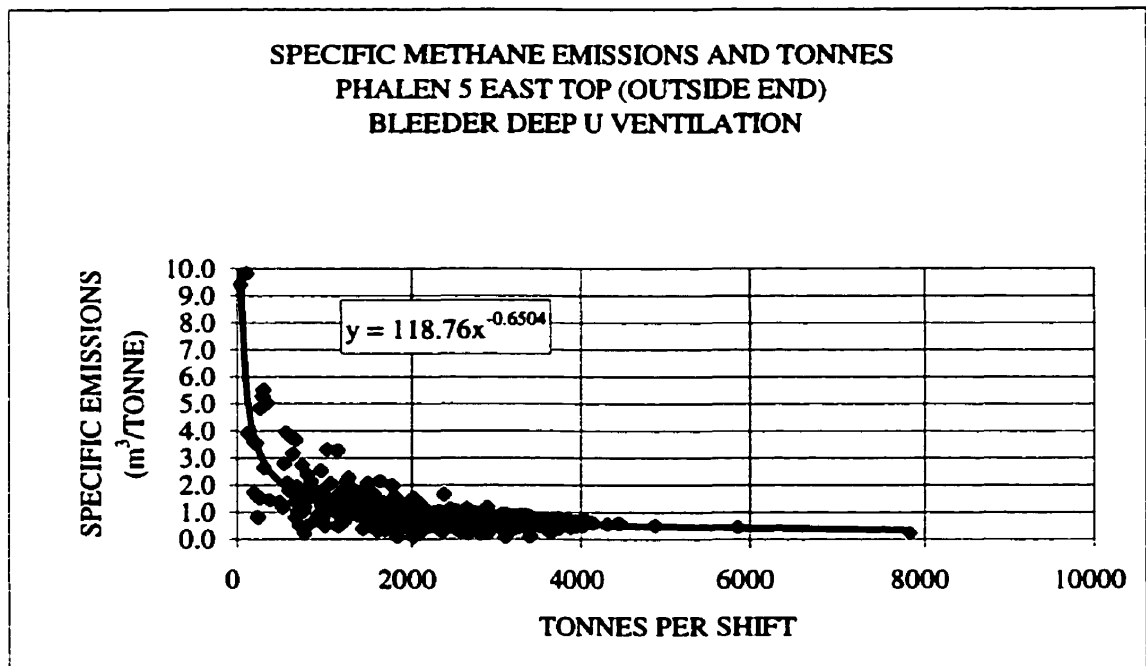


Figure 5.10 Specific emissions and run of the mine tonnes per shift at Phalen 5 East Top (outside end), Bleeder Deep U ventilation

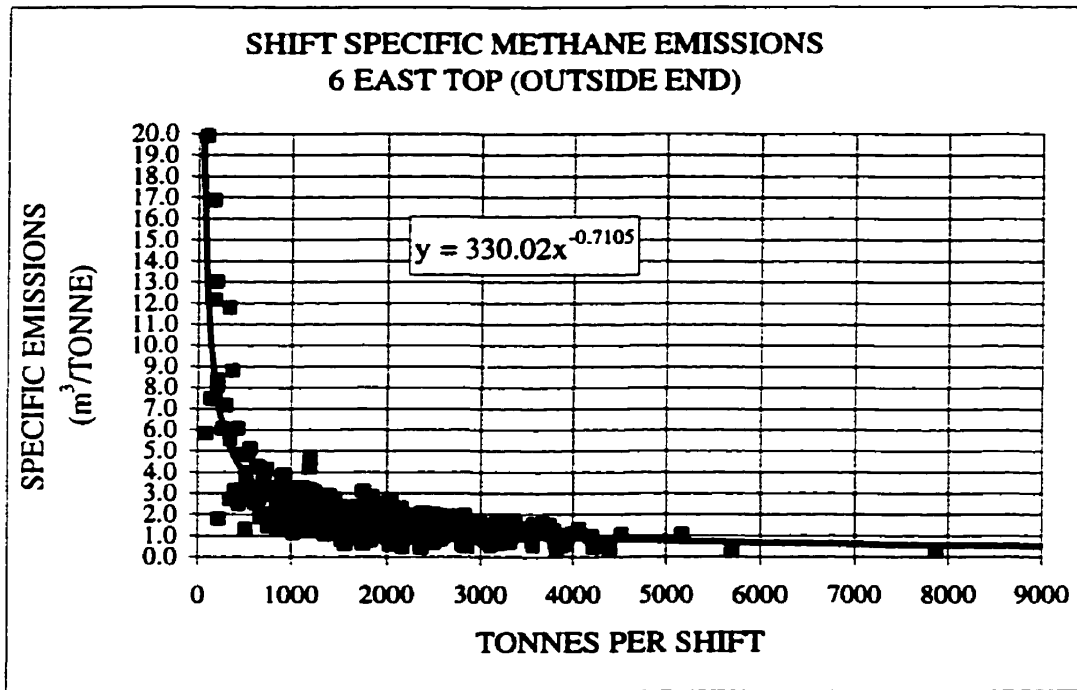


Figure 5.11 Specific emissions and run of the mine tonnes per shift at Phalen 6 East Top (outside end), Sewergate ventilation

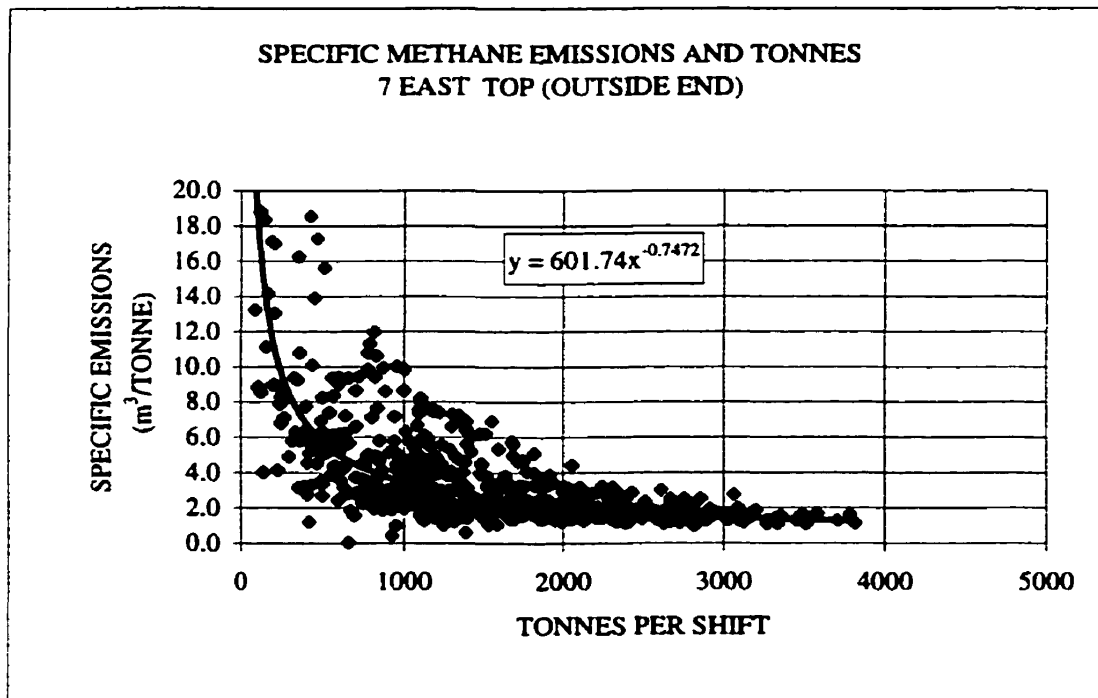


Figure 5.12 Specific emissions and run of the mine tonnes per shift at Phalen 7 East Top (outside end), Sewergate ventilation

From the curve fit equations presented (Figures 5.6 and 5.12) were used to construct and present a comparison of the average methane flow per shift as projected against tonnes per shift (Figures 5.13 and 5.14).

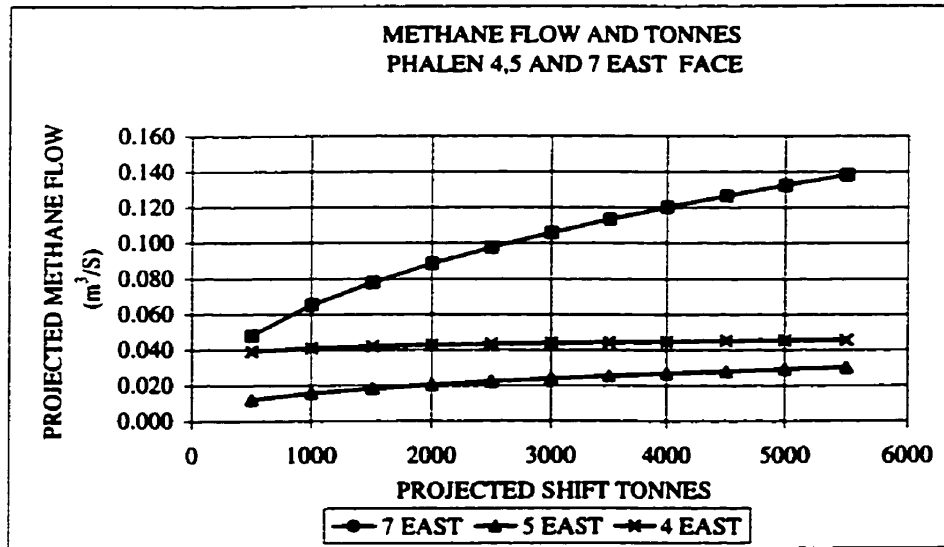


Figure 5.13 A comparison of methane flow for Phalen 4, 5 and 7 East Face emissions

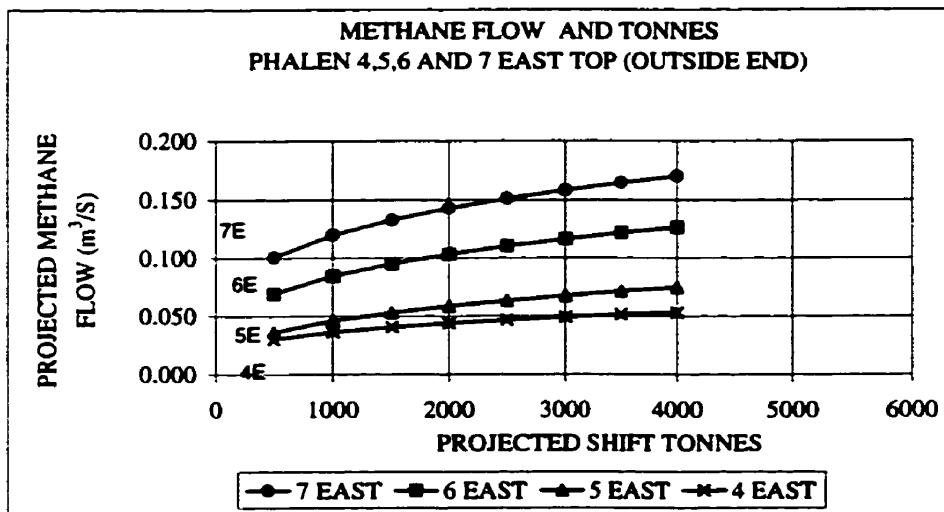


Figure 5.14 A comparison of methane flow for Phalen 4, 5, 6 and 7 East Top (outside end)

There is a considerable amount of data scatter in each of the figures and as a result the curve fit equations are statistically weak (in some cases $R < 0.5$); however, general trends are indicated.

5.3.1 Methane emissions from the worked seam face Bleeder Deep U and Sewergate ventilation

Figure 5.13 indicates a trend of increased face emissions between 4 and 5 East Faces and 7 East Face. However, it is important to point out that the methane seen by the methane sensor located over the top motor drive for the pan line for 7 East was quite different than for the other two walls. For much of half of the monitoring period of 7 East a brattice line had directed at least 80 to 90 percent of the wall face air past the motor, to an area along side the high side rib. The turbulence and improved mixing of mine air near this sensor would give a more representative methane content in air reading; therefore, a direct comparison with 4 and 5 East may be invalid. This also suggests that the methane content in air as seen by the sensors for 4 and 5 East may not be entirely indicative of well mixed airbody; therefore, face emissions should be viewed in this light.

Figure 5.14 presents the best comparison of methane flow from the Phalen Eastside Walls. Here the effects of both ventilation systems being used and increased wall face emissions with depth can be seen. Inspection of each of the curves shows that on average there has been an increase in methane of between 200 and 300 % in the top level return airways between 4 and 7 East walls. This far surpasses any reasonable increase in wall face emissions expected with depth for this mine. This is a direct result of the ventilation systems employed at each wall; since, it has been known and proven for some time now that methane leakage from the gobs of 6 and 7 East has increased greatly since the introduction of Sewergate ventilation. It shows that switching to Sewergate ventilation at Phalen has in effect directed some of the gob produced methane to the return airway for dilution. In effect, by switching to the Sewergate ventilation system, a trade off occurs between not ventilating the East Bleeder at the expense of using the wall face air to dilute additional gob methane reaching the return airway. Depending on the statutory methane

limits allowed in the return airway i.e. 1.25% or 2.0, a reduction in production will occur depending on the quantity of gob methane that can be successfully handled at the return end of the face. Increasing the airflow on the face does not necessarily improve conditions; since, this may also increase the flow of air through the gob and increase the capture of the methane fringe. Other factors may influence the performance of the Sewergate, especially, strata conditions which will be discussed in further sections. Studies have indicated that the compaction of gobs within the Sydney Coalfield were effected by the composition of the roof geology. In Lingan Colliery, leakage of air across the Westside advancing panel's gob was 30 % of intake air compared to 60% of the Eastside panel's gob intake air for a similar length of advance (Cain, P., Stokes, A., and Genter, D., 1984). Similar work indicated that good compaction of the gobs took at least 100 m of advance before high air resistance was developed. In Lingan mine, the overlying Eastside walls contained sandstone channels while the Westside walls were relatively free at the time of the above studies. It was believed that the sandstone channels provided lower air resistance gobs on the Eastside because of reduced compaction of gob material compared to the westside gobs. This implies that the Phalen mine gobs would also be of low air resistance because of the presence of the Lower Sandstone Unit which occupies most of the immediate roof area in Phalen mine.

Comparing Measured and Predicted Methane Emissions

6.0 Comparing measured and predicted methane emissions

The following discussion pertains to the comparison of 'gob produced' and 'predicted' methane flow from Phalen 4 and 5 East districts. Tables 6.1 and 6.2 present the predicted and measured methane flow for the gob of Phalen 4 and 5 East districts. The predicted flows have been calculated based on the predicted specific emissions presented in Tables 4.4 and 4.5. Predicted flow is calculated by multiplying the weekly tonnes per second by the methane total strata emissions column of Tables 4.4 and 4.5.

Phalen 4 East						
Airey Predicted and Measured Gas Flow from 4 East Strata						
Date	Week	Weekly Tonnes	Airey Emission m ³ /Tonne	Airey Flow m ³ /s	I East Bleeder m ³ /s	Difference %
8/17/91	23	37067	6.6	0.414	0.401	3.3%
8/24/91	24	35304	6.6	0.396	0.436	9.1%
8/31/91	25	34766	6.6	0.392	0.434	9.7%
9/7/91	26	47386	6.7	0.536	0.476	12.6%
9/14/91	27	39393	6.7	0.448	0.464	3.5%
9/21/91	28	41193	6.7	0.470	0.352	33.7%
9/28/91	29	44243	6.7	0.507	0.422	20.3%
10/5/91	30	48792	6.8	0.562	0.459	22.3%
10/12/91	31	37833	6.8	0.437	0.531	17.7%
10/19/91	32	52241	6.8	0.606	0.492	23.3%
10/26/91	33	49086	6.9	0.572	0.410	39.6%
11/2/91	34	55221	6.9	0.646	0.379	70.4%
11/9/91	35	25718	6.9	0.302	0.408	25.9%
11/16/91	36	26579	6.9	0.314	0.424	26.0%
11/23/91	37	38712	7.0	0.459	0.437	5.0%
11/30/91	38	31098	7.0	0.370	0.439	15.8%
12/7/91	39	31549	7.0	0.377	0.293	28.8%
12/14/91	40	31413	7.1	0.377	0.449	16.0%
12/21/91	41	0	7.1	-	0.465	-
12/28/91	42	16333	7.1	-	0.462	-
1/4/92	43	43318	7.1	0.524	0.464	6.0%
1/11/92	44	37026	7.1	0.449	0.473	2.4%
1/18/92	45	43325	7.1	0.526	0.477	4.9%
1/25/92	46	38107	7.2	0.464	0.613	14.9%
2/8/92	48	39176	7.2	0.479	0.553	7.4%
2/15/92	49	53321	7.2	0.653	0.523	13.1%
3/7/92	52	50529	7.3	0.623	0.523	10.0%
3/14/92	53	41922	7.3	0.518	0.513	0.4%
3/21/92	54	18154	7.3	0.225	0.442	21.8%
				Predicted Flow	Measured Flow	Average (absolute)
Average		37545		0.468	0.456	17.2%
Standard Deviation				0.107	0.063	

Table 6.1 Predicted and measured methane flow from coals seams in the adjacent strata of Phalen 4 East district

Phalen 5 East						
Airey Predicted and Measured Gas Flow from 5 East Strata						
Date	Week	Weekly Tonnes	Airey Emission m ³ /Tonne	Airey Flow m ³ /s	l East Bleeder m ³ /s	Difference %
8/24/92	17	25493	6.7	0.291	0.327	11.2%
8/31/92	18	14166	6.8	0.163	0.164	0.5%
9/7/92	19	31253	6.8	0.364	-0.034	-
9/14/92	20	40068	6.9	0.471	0.265	77.8%
9/21/92	21	37846	6.9	0.447	0.387	15.3%
10/5/92	23	29927	7.0	0.356	0.365	2.4%
10/26/92	26	25196	7.1	0.304	0.332	8.4%
11/2/92	27	24698	7.1	0.299	0.327	8.5%
11/9/92	28	22038	7.2	0.268	0.344	22.1%
11/16/92	29	27033	7.2	0.330	0.391	15.6%
11/23/92	30	0	7.2	-	0.352	-
11/30/92	31	0	7.2	-	0.326	-
12/7/92	32	22894	7.3	0.283	0.283	0.1%
12/14/92	33	30526	7.3	0.379	0.378	0.2%
12/21/92	34	3426	7.3	-	0.323	-
12/28/92	35	745	7.4	-	0.364	-
1/4/93	36	1864	7.4	-	0.302	-
1/11/93	37	2595	7.4	-	0.240	-
1/18/93	38	17745	7.5	0.225	0.331	32.0%
1/25/93	39	17676	7.5	0.225	0.397	43.4%
2/1/93	40	41604	7.5	0.532	0.460	15.5%
2/8/93	41	33399	7.5	0.428	0.470	9.0%
2/15/93	42	30375	7.5	0.390	0.532	26.7%
3/1/93	44	30977	7.6	0.399	0.526	24.0%
3/8/93	45	34894	7.6	0.451	0.579	22.2%
4/12/93	50	34000	7.7	0.444	0.614	27.8%
4/19/93	51	45573	7.7	0.596	0.658	9.4%
5/3/93	53	45657	7.7	0.600	0.434	38.1%
5/10/93	54	47728	7.7	0.628	0.522	20.4%
5/17/93	55	43949	7.8	0.580	0.498	16.3%
5/31/93	57	35588	7.8	0.471	0.456	3.4%
6/7/93	58	19477	7.8	0.258	0.439	41.1%
				Predicted Flow	Measured Flow	Average (absolute)
Average		24578		0.410	0.422	19.8%
Standard Deviation				0.133	0.108	

Table 6.2 Predicted and measured methane flow from coals seams in the adjacent strata of Phalen 5 East district

6.1 Phalen 4 and 5 East emissions from the adjacent strata of the worked seam

From Tables 6.1 and 6.2 the predicted versus the average weekly methane flow from the gobs of Phalen 4 and 5 East is presented in Figures 6.1 and 6.2.

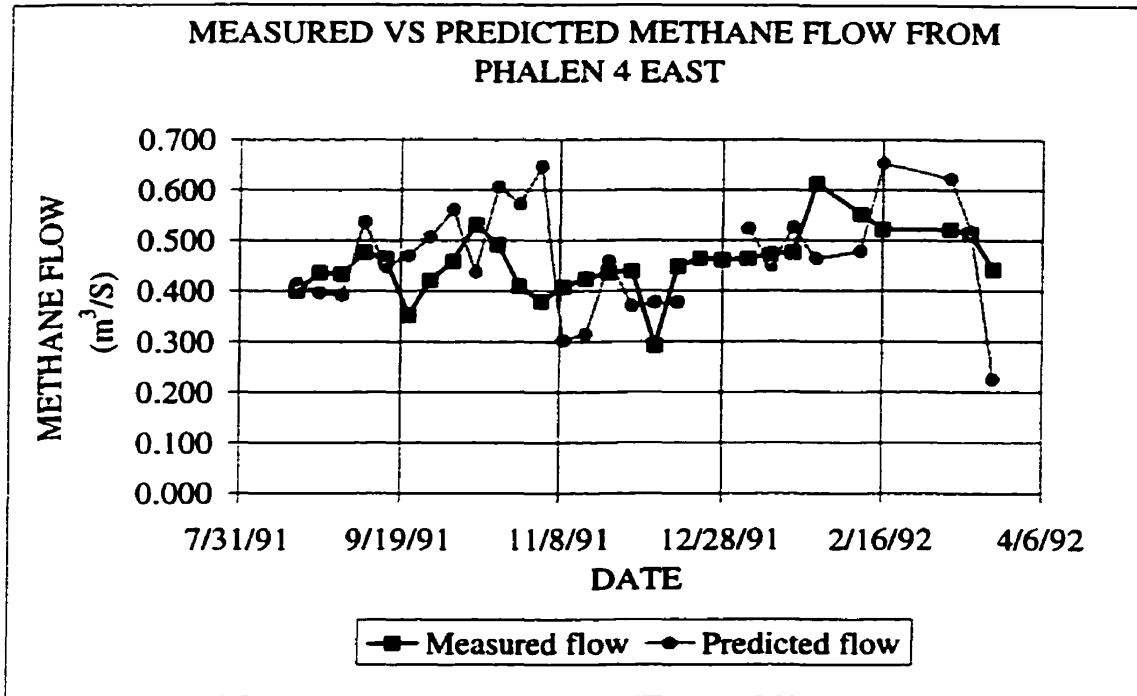


Figure 6.1 Measured versus predicted methane flow from coals seams in the adjacent strata of Phalen 4 East district

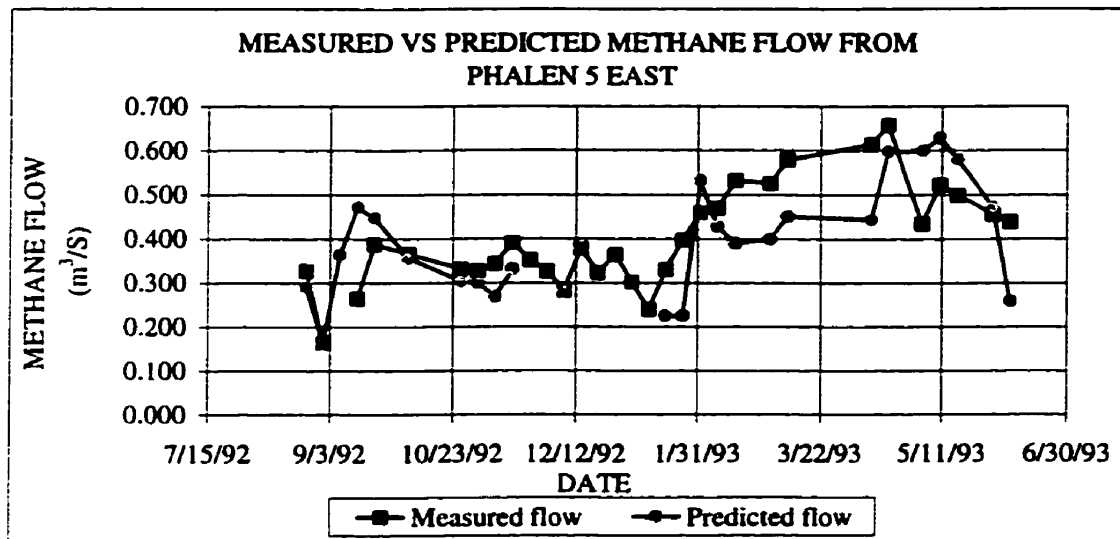


Figure 6.2 Measured versus predicted methane flow from coals seams in the adjacent strata of Phalen 5 East district

The predicted versus the measured methane flow are quite reasonable given the assumptions made along the way. Because the simplified method is extremely sensitive to the tonnes values, it predicts 0 methane flow at 0 production which is not the case in the real situation. However, given steady production weeks and ignoring down times such as vacation and holidays periods, the prediction method gives a mine ventilation planner an idea of methane emissions expected from mining. This method as used only predicts emissions from coal seams adjacent to the working seam and cannot predict emissions that are associated with other gas sources. Any changes in the geology that may occur at greater depths leading to changes in coal strata, or the introduction of another potential gas source such as a sandstone bed or channel must be accounted for at all times.

Sewergate Ventilation

7.0 Sewergate ventilation

A Sewergate (or bleeder) road system involves the provision of an additional route along which gas mixtures can flow away from the coalface. The usual approach is to connect an abandoned tailgate via the return end of the face startline to a return elsewhere in the network at a lower pressure. As the abandoned road does not need to be inspected, there is no statutory limit to the concentration of gas it carries. If high gas concentrations are involved, the gas can be discharged into a return airway through a stopping.

Sewergate roads are relatively straightforward to engineer where the practice is to reuse roadways and work skin to skin and in fact they are inescapable in such circumstances. The system requires careful planning monitoring, and regulation to work and may prove difficult to work where strata conditions lead to rapid convergence. In a gassy mine, the sewer road may mask shortcomings in methane drainage so it may not add to the overall effectiveness of the methane control system (Creedy, D.P., 1992).

The system at 7 East wall depends on the collapse of the gate to create the resistance for the necessary pressure drop to drive methane toward the return elsewhere in the system (East Back Bleeder). Secondly, the system is better suited to pillarless drivages which is not the case at 7 East where a solid coal pillar exists on the return side.

7.1 Principle of operation

The principle of operation of the present system is based on utilizing the influence of mine ventilation pressure. Historically it was observed that methane migrated across the gobs of advancing longwalls as expected due to a strong pressure gradient across the gobs. However, the collection of highly concentrated gas in boreholes near the face startline indicated that methane was being pulled from the strata without entering the gob and essentially happened without any measurable airflow (Farrell and Associates, 1995). In terms of a retreat panel, the same effect could be established if the face start line is connected to a point of sufficient pressure drop in terms of the face current position, that

methane would migrate from the shallow gob areas to the point of low pressure. The critical parameter to be maintained being the pressure gradient.

Large airflows in such systems are not good through the gob or old gates. The flow of air nullifies the pressure gradient available to draw methane from the immediate roof strata. Also, the flow of air from the gob or other connections to the back return must be sufficiently low in order to maintain the majority of the pressure drop across the active panel.

7.2 Phalen 7 East longwall - Case study

Phalen 7 East longwall utilizes a Sewergate ventilation system that depends largely on developing an effective pressure gradient across the face through the gob to the face start line by effectively minimizing the airflow leakage through the gob (Figure 5.4). The difficulty with the Sewergate has occurred when insufficient gob collapse in the unconsolidation area immediately behind the face supports removes the pressure gradient by removing the resistance factor, forming an uncontrolled zone. Any methane entering this zone will mix with wall face air which has penetrated the same low resistant area. Instead of migrating back to the startline, this gas eventually makes it way back to the return airway or maybe deflected out into the return airway by the pressure drop that occurs across the shearer as it diverts face air into the gob while cutting the coal face. Unacceptable levels of methane in air show up in the return end of the face especially along the highside rib portion at the T-junction.

Once this has occurred, remedial measures are necessary to control or at least dilute the high concentrations of methane at the return end of the wall. Air-movers and brattice lines can deal with minor influxes of methane by diverting a portion of the face air to the ribside and diluting the methane to acceptable levels. However, if the low resistance area in back of the face line is large enough, the situation arises where gob produced methane becomes entrenched with the penetrating wall face air. Unacceptable large volumes of methane laden air from the gob mix with coal front produced gas at the return and stop production, sometimes after only cutting a few meters.

The 7 East fabricated back return system (brattice line) was designed to produce a mixing area for all gases entering the return (Figure 7.1).

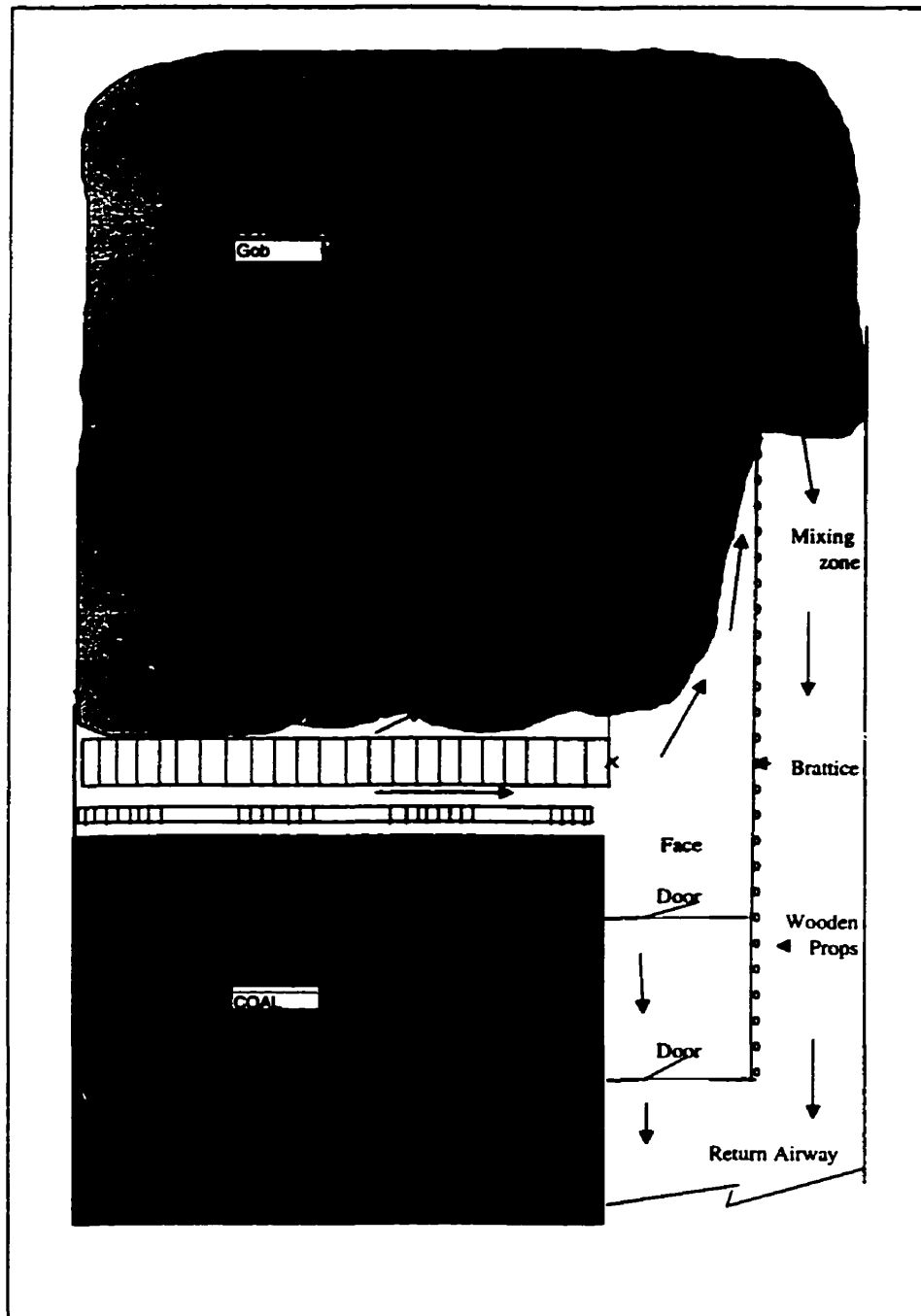


Figure 7.1 7 East fabricated back return system (not to scale)

The difficulty with this ventilation control at Phalen 7 East Wall was that face emissions (coal front) were mixed with gob emissions in the mixing area behind the face line (back

return). This total mixture was then passed through the airway between the highside rib and brattice line where a BM methane sensor was located and set to trip at 1.5% methane content in air, which shuts down the face electrical equipment. The regulatory trip point for electrical equipment in a coal mine face airway is 1.25% methane content in air. In this ventilation set-up, the face electrical equipment was often shut down by the highside rib BM monitor even when the methane content of face air above was less than 1.25% as determined by the BM sensor located above the wall's top motor. As a result full production was not realized.

7.3 Phalen 7 East Sewergate performance

The capture of methane by the Sewergate could not be measured directly because methane monitoring in the East Bleeder could not be conducted on a real time basis. Methane capture by the Sewergate in the following section was determined by comparing the predicted methane make from coal seams in the adjacent strata with the methane flow calculated from the methane patterns database. Methane from the gob was determined by multiplying the airflow through 7 East return airway by the difference between the methane concentration measured at the 7 East outside end from the methane concentration above the motor at the return end of the face. The percentage capture of methane by the Sewergate system or its performance was calculated by dividing the measured return airway methane flow from the gob by the predicted methane flow from strata (Figure 7.2).

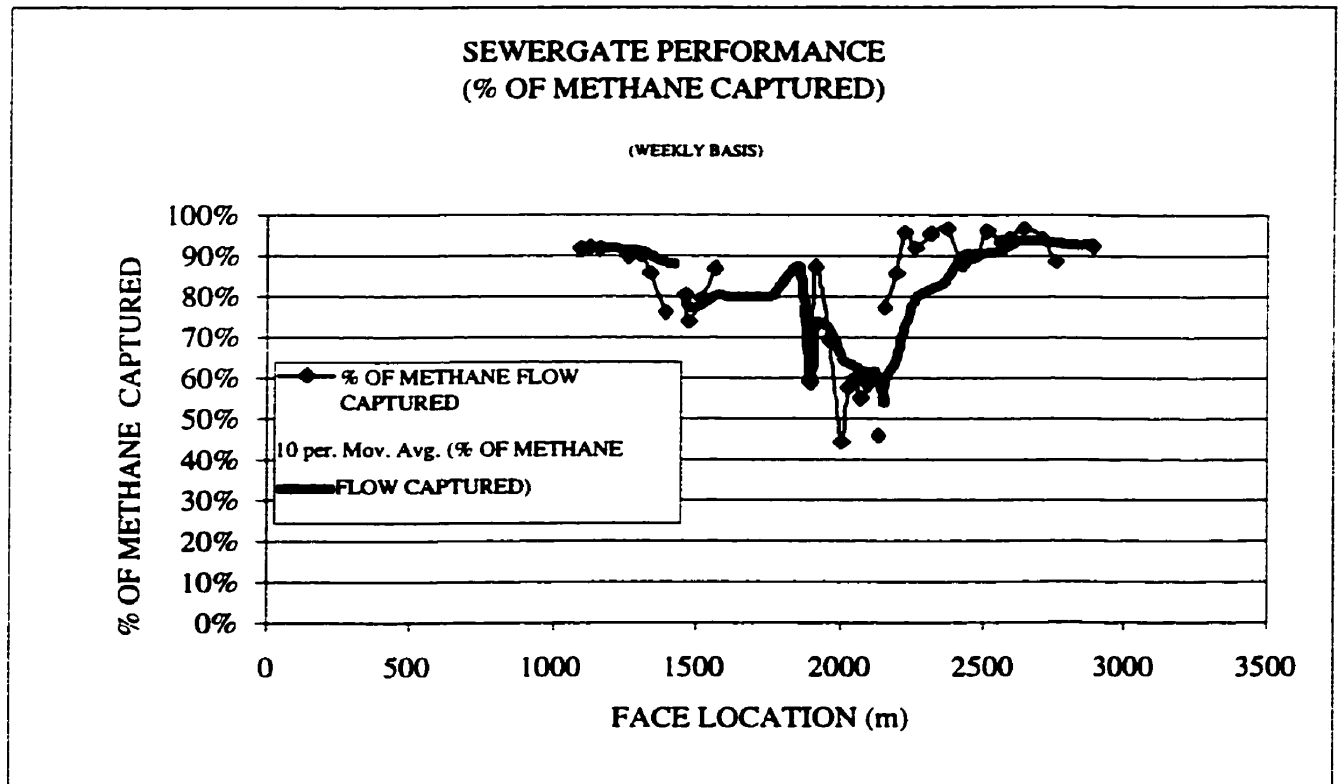


Figure 7.2.7 East Sewergate performance

Figure 7.2 indicates that on average the Sewergate captured 70% of the predicted methane emissions. The change in the performance of the Sewergate around 2100m mark was likely a result of a major change in roof geology with the rising and thinning of the Lower Sandstone Unit at this point in the panel. This change will be discussed further in section 7.61.

7.4 Lower Sandstone Unit as a gas source

The performance of the Sewergate was hampered by the effects of the Lower Sandstone Unit. Figure 7.3 presents the specific emissions (not captured by the Sewergate) from 7 East gob versus wall face location and proximity of the Lower Sandstone Unit to the top of the coal seam. The performance of the Sewergate was directly effected by the both the proximity and thickness of the Lower Sandstone Unit.

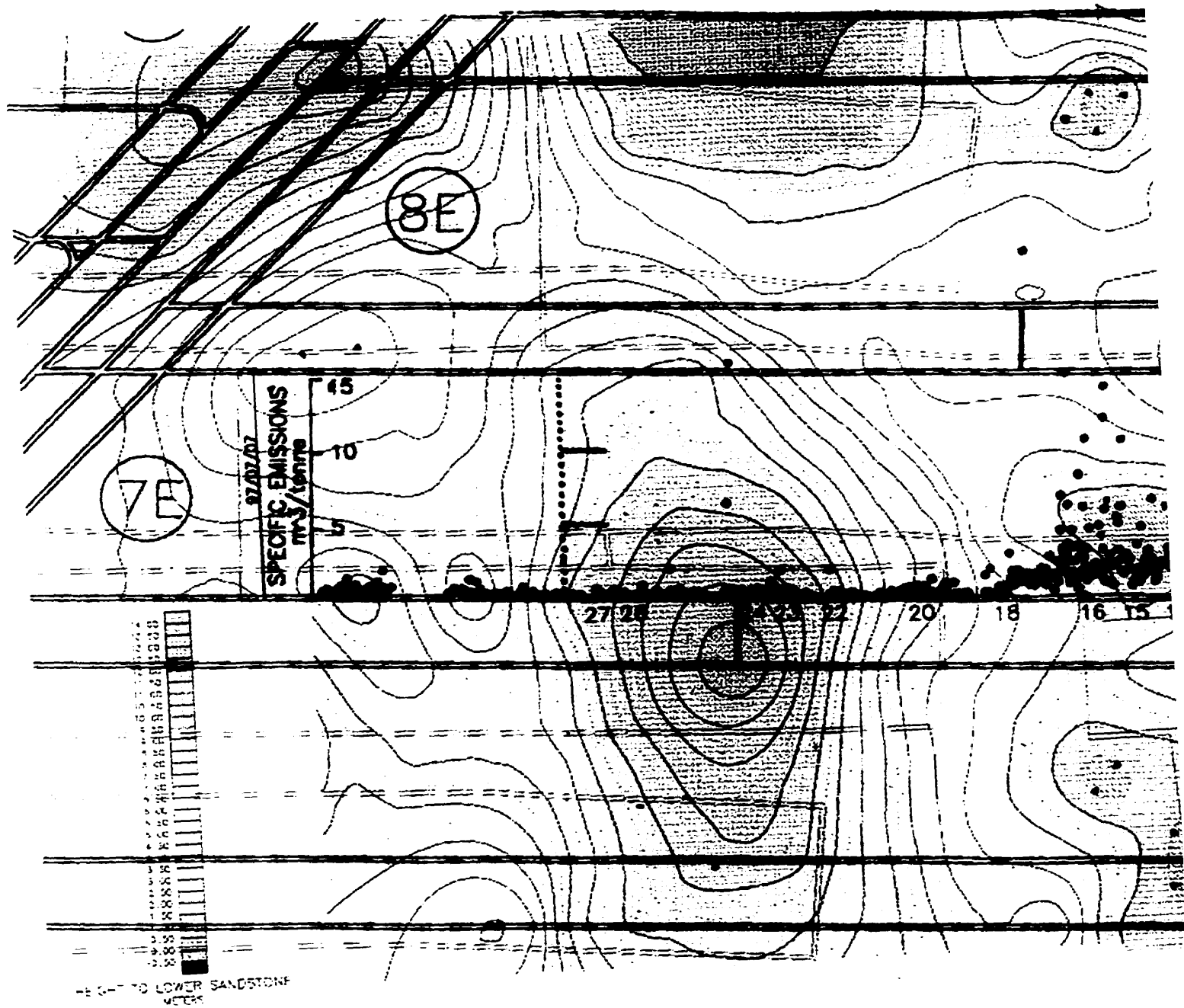
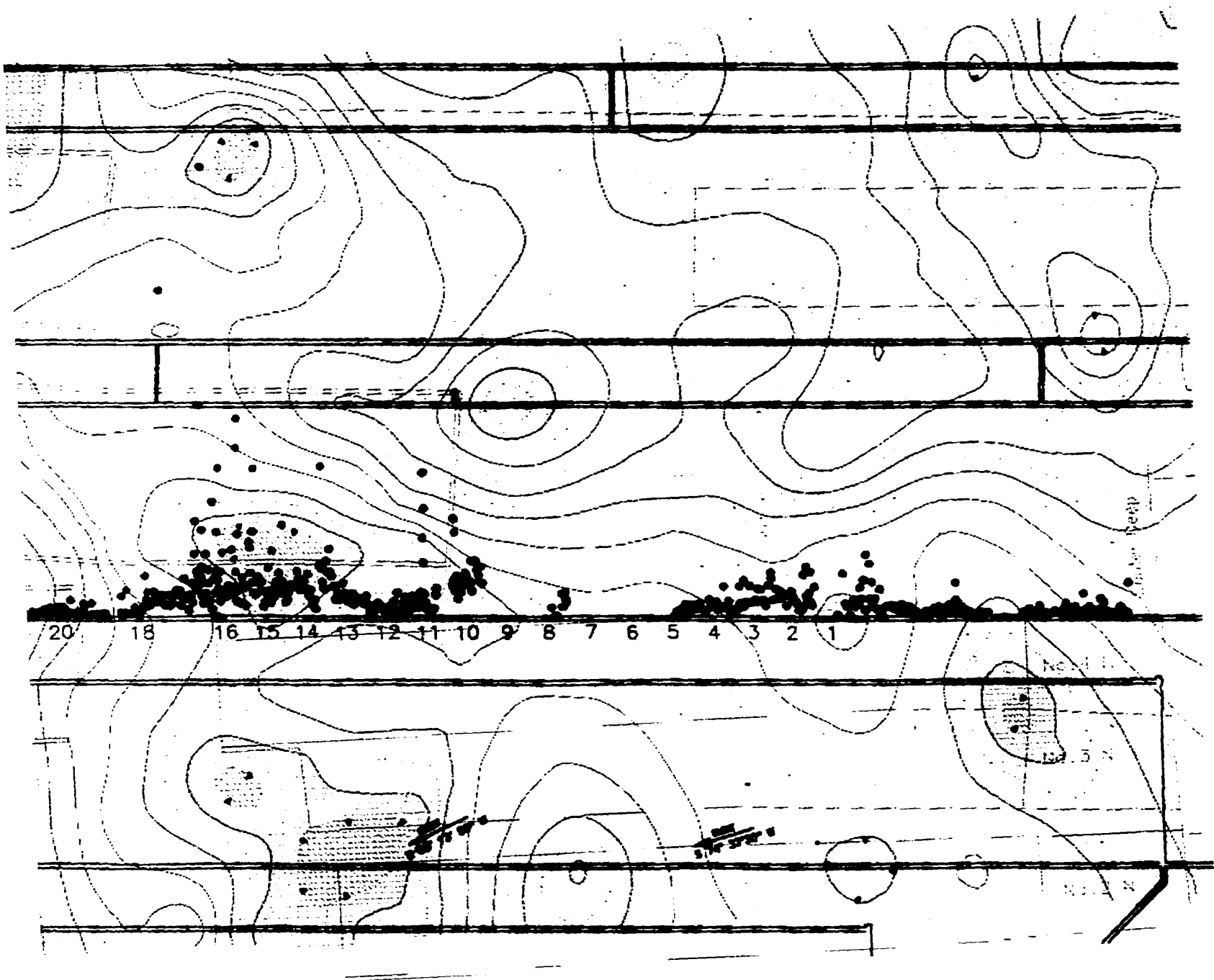


Figure 7.3 Specific gob emissions versus wall face location and Lower Sandstone Unit iso-pache





sandstone Unit iso-pache



What was not clear was whether the Lower Sandstone Unit was a significant gas source or whether it was pushing the neutral point back into the gob to such a large extent that in effect a huge area of the gob was under the direct influence of the face ventilation system and large quantities of gob gas were migrating back to the T-junction at relatively low concentrations (Liney, A., 1997).

One other factor possibly affecting the performance of the Sewergate came to light after the 7 East was complete. This was the discovery of the Stony coal seam at ~ 18 m below the Phalen seam. This seam was not believed to exist to any great extent in the geological cross section. The seam was discovered during 9 East Top Level Development when the floor ruptured in the level and a large quantity of gas was released. Consequent drilling indicated the presence of a ~0.6 m dirty coal seam at 18 m. This seam added more complications to the determination of why the Lower Sandstone Unit affected the Sewergate performance. In this case, the thickening of the Lower Sandstone Unit and an increase in weightings on the wall, may have resulted in the early release of methane from the floor to the uncontrolled zone in the gob and further complicated the gas mix in the gob.

Evaluating the performance of the Sewergate using a prediction method based on coal seams being the only source of gas, negates the fact that missing gas sources in effect makes the prediction of methane tentative. However, the ability to dilute this gob gas in a safe and yet productive manner remains the problem. In order to better understand how the methane migrates from the gob to the return airway, a series of experiments were conducted as described in section 7.6.

7.5 Water and gas emissions from the undermined Lower Sandstone Unit

The presence of the Lower Sandstone Unit and channels in the roof of Phalen 7 East wall has posed some serious restraints on production. Periodic weightings of the wall face and increases in gas emissions from the sandstone have been suspected. Increases in water flow associated with massive sandstone bodies can be linked to increases in CO₂ (formation water). CBDC have sampled and determined that the CO₂ content in the air

leaving the East Bleeder may rise proportionally to increase in strata water flowing into 7 East gob. This needs further investigation for verification, possibly when the East Bleeder is inspected before 8 East panel goes into production.

Figure 7.5 presents the methane flow as measured at 7 East Top (outside end) and total water flow as measured at 7 East Bottom for the period prior to the first major roof fall on Phalen 7 East Wall Face.

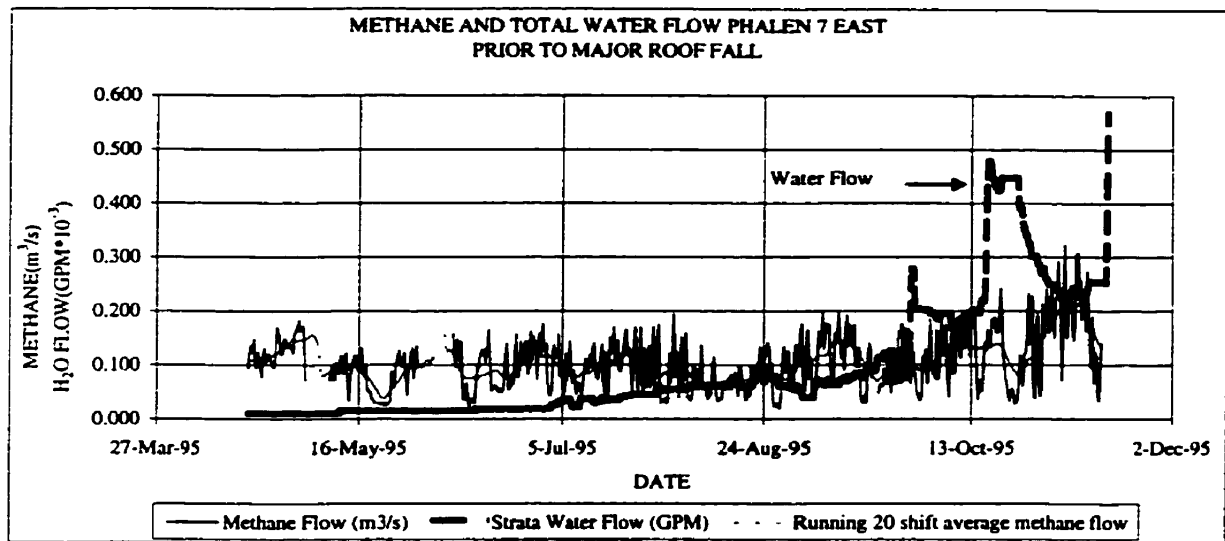


Figure 7.4 Methane emissions and water flow from roof strata of Phalen 7 East prior to first major roof fall

The water flow readings are not continuous and have been projected between readings to add some continuity to the plot; therefore, the two events are not happening simultaneously.

In Figure 7.4 a trend of increased methane with water flow is evident. The peak methane flows have increased ~ 30 percent in the period just after the first two major flow events. On the third water flow event, the first major roof fall occurred and a drop in methane flow was evident when the wall stopped production. What was still not clear is whether the increased methane flow was a product of the sandstone bed, or if it follows the water

flow event from other gas sources. Then spot water flow data was not accurate enough for such a determination. It is noted that where a prediction method, as used in this report, it could not possibly predict an extraneous methane flow event because the event was being controlled by factors not accounted for in the prediction model.

7.6.0 Tubebundle experiments - 7 East Top Level

A tubebundle was installed just prior to the restart of Phalen 7E wall on June 13, 1996. The first segment of the tubebundle was 1500 ft (468 m) in length and consisted of 10 individual tubes in an armoured casing (Figure 7.5).

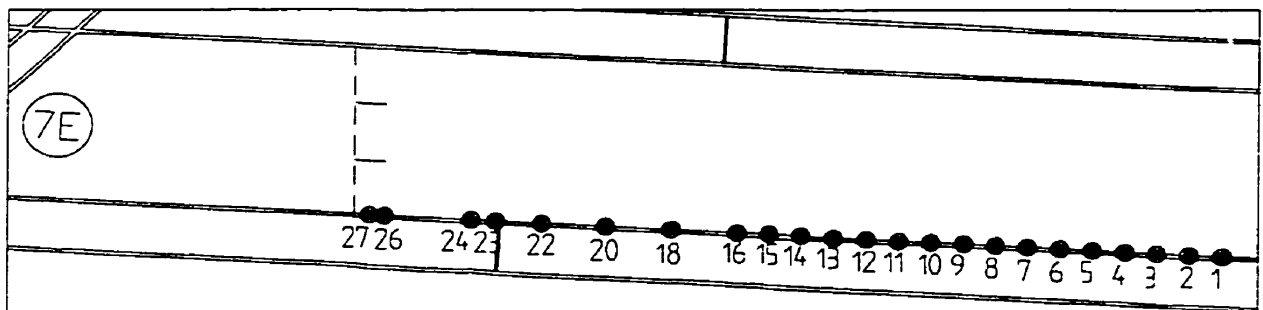


Figure 7.5 Tubebundle experiment Phalen 7 East Top Level

Ten sample stations along the high side rib were set up at 45 m intervals starting at the wall restart position (T-junction at the top of the wall). Two more 500 m segments of armored 10 core bundle were installed in the return airway and with face retreat covers a total length of ~1300m, 27 stations in-by the T-junction of the collapsed return gate. Pressure differentials and air samples were being routinely obtained.

7.6.1 Differential air pressure measurements

Phalen 7 East contains a very large and competent Lower Sandstone Unit located in the roof which runs parallel with the panel. It has led to a low resistance gob behind the supports which has been confirmed with differential air pressure measurements and tracer gas injections using a tubebundle system.

Figures 7.6 and 7.7 present differential air pressure measurements made over the first 450 m of retreat and show that the effective differential air pressure gradient does not exist in by the T-junction for at least the first 20-40 m.

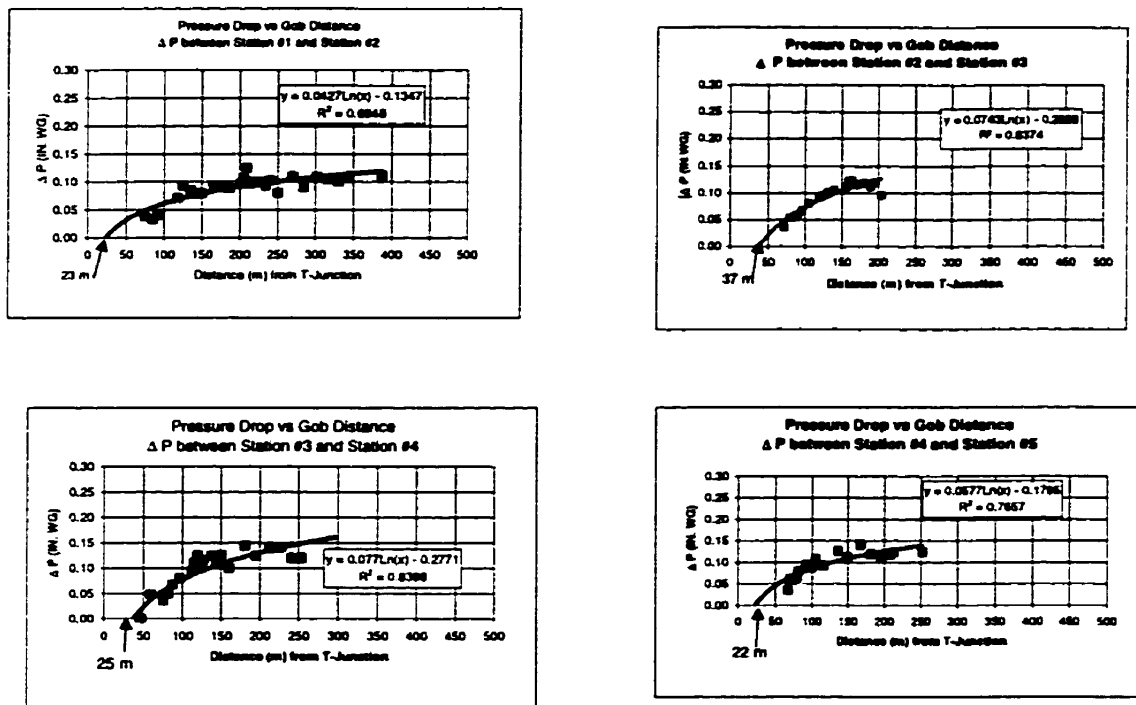


Figure 7.6 Differential air pressure measurements between stations no. (1 and 2), (2 and 3), (3 and 4), and (4 and 5)

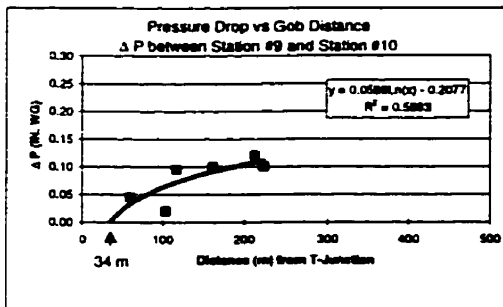
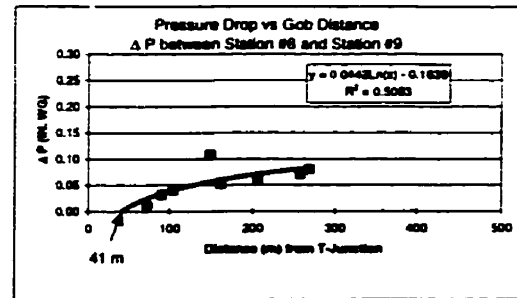
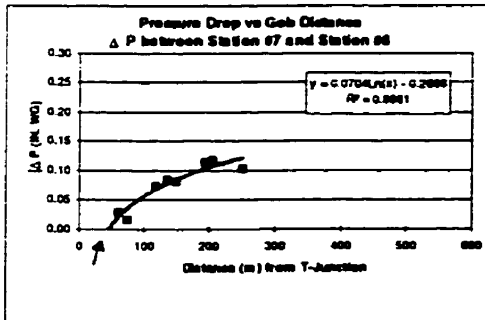
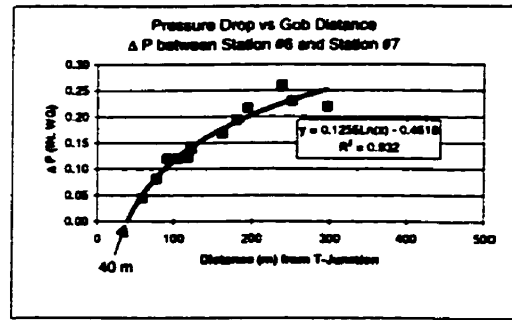
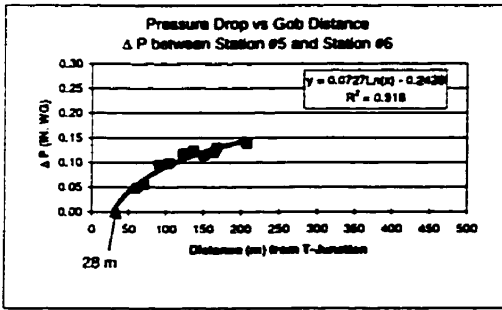


Figure 7.7 Differential air pressure measurements between stations no. (6 and 7), (7 and 8), (8 and 9), and (9 and 10)

Also, the curve fit lines indicates that full gob consolidation in the top level does not occur until about 100 m behind the face T-junction.

Figures 7.8 and 7.9 have been derived from the equations in Figures 7.6 and 7.7 and presents the neutral point as determined from the convergence of each curve to zero pressure drop and as a function of the Lower Sandstone Unit height above the coal seam and its thickness in the top level.

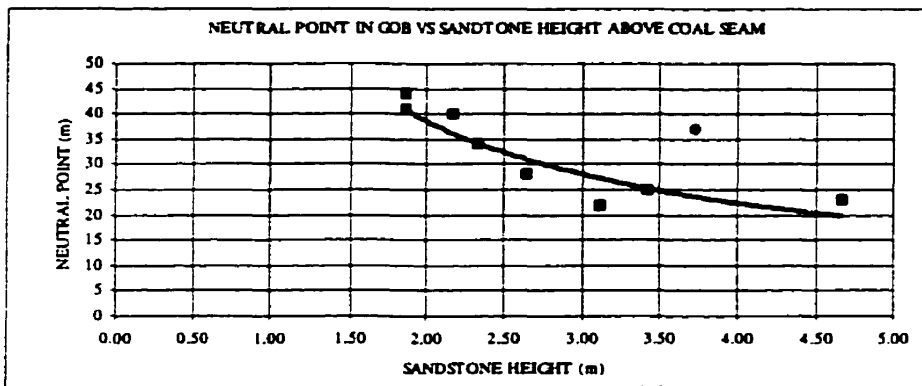


Figure 7.8 Neutral point in the gob versus sandstone height above coal seam

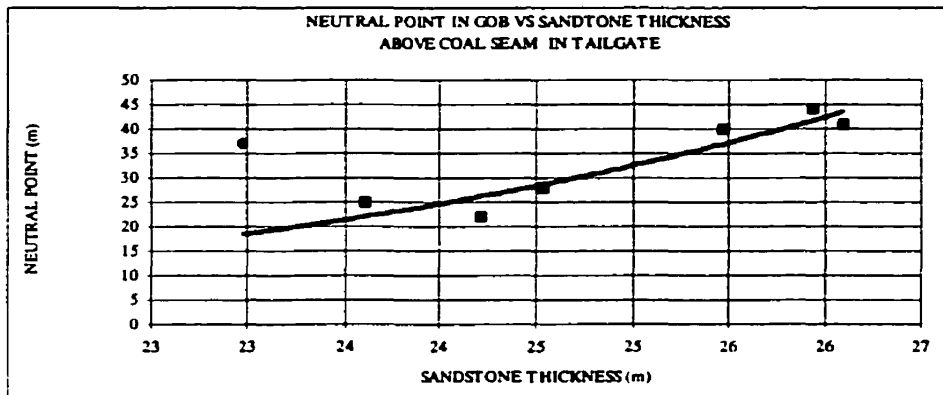


Figure 7.9 Neutral point in the gob versus sandstone thickness above coal seam

Both show a trend of decreasing neutral point distance inby the T-junction with increasing sandstone height and thickness above the coal seam, although a considerable spread in the data is evident. One point has been left out of the plots; since, it did not follow the trend and is considered an outlier.

The sum of differential pressure measurements derived as a function of distance inby the T-junction projected to the face start line indicate a pressure gradient of ~1500 Pa over the gob (Figure 7.10).

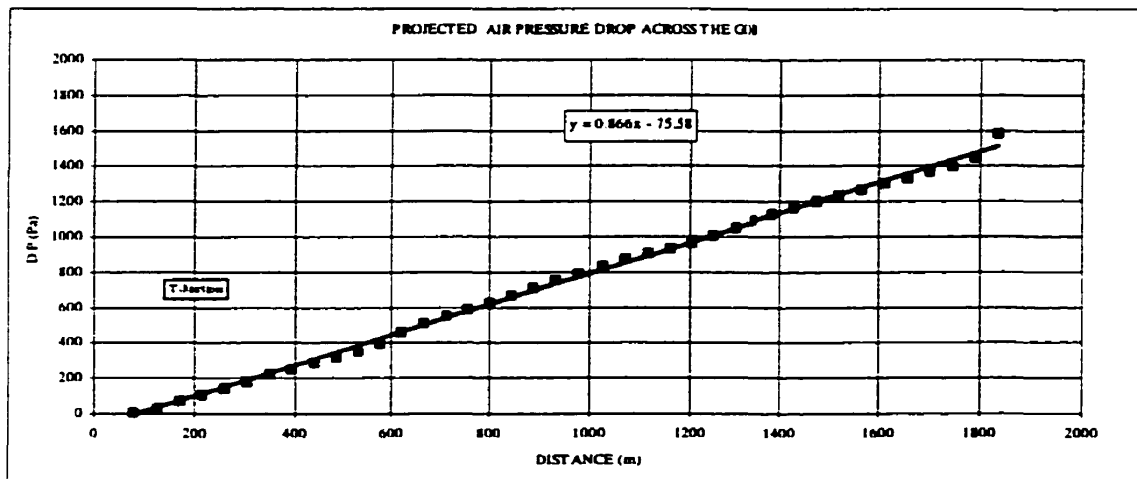


Figure 7.10 Projected air pressure drop across the gob from station no. 10 to the face start line

Although this gradient meets the criteria for a Sewergate operation, the absence of a favorable gradient ~ 20 to 30 m inby the T-junction means that an “uncontrolled zone” exists there, where methane entering this area travels back to the T- junction.

7.6.2 Tracer gas determination of neutral point of 7 East Top Level gob

Six tracer gas experiments were conducted to more precisely determine the neutral area of the collapsed 7 East Top gob. For each test described in this section, a steady state background concentration of tracer gas was found for the return airway by releasing a steady flow of tracer gas into the airway prior to injection of tracer gas into the gob. This

can be compared to the concentration of tracer gas in the return airway after its injection into the gob tubebundle station which determines if the neutral point had been reached or not and how much tracer gas was captured by the Sewergate.

On August 28, 1996 a tracer gas experiment was conducted to determine the neutral area location for 7 East Top Level gob. On this date, the un-caved gob was ~ 28 m from the T-junction and stretched ~ 20 m down behind the face supports (Figure 7.11).

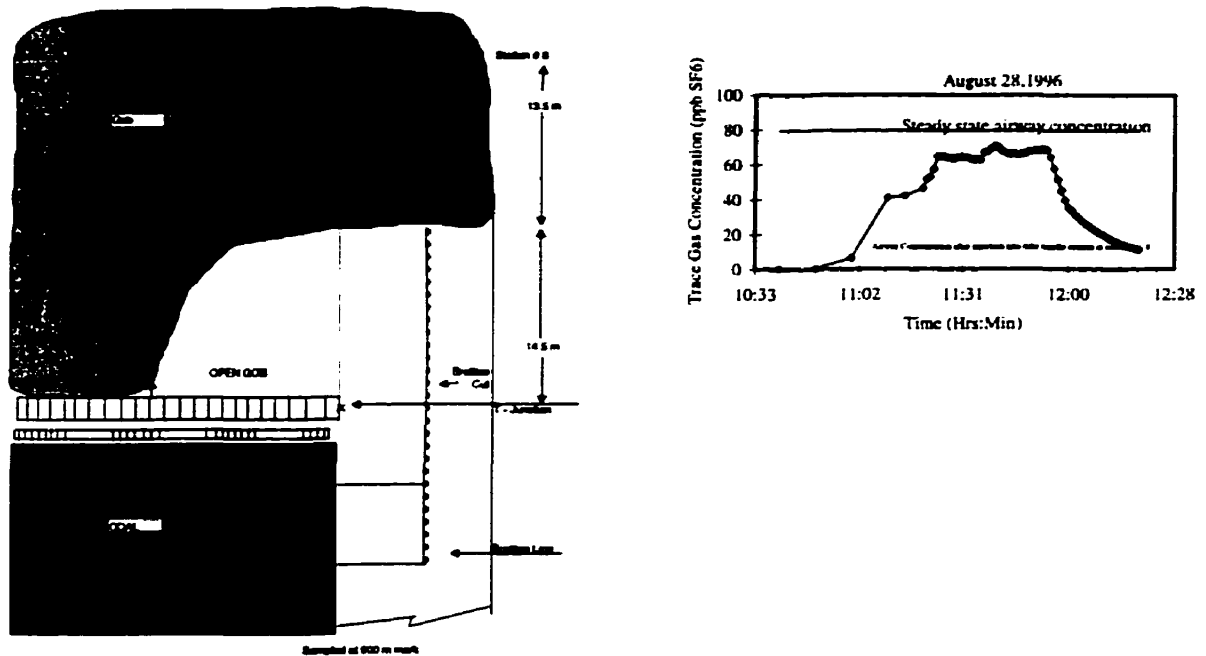


Figure 7.11 7 East Top neutral point study - 28 m inby the T-junction (August 28,1996)

The Lower Sandstone Unit had dropped to its closest point to the coal seam in the top level (< 2 m) for the first segment of the tubebundle experiment. Tracer gas was injected into station no. 8, located 28 m inby the T-junction and the majority of the tracer gas returned to the T-junction indicating the neutral point was greater than 28 m inby. Sampling at station no.1 located ~ 300 m inby station no.8 indicated the presence of tracer gas which showed that the neutral area was close to station no.8.

On August 30 1996, the same experiment was repeated, with station no.8 located 32 m inbye the T-junction. On this test over 20 % of the tracer gas traveled toward the T-junction that indicated that the neutral area had been reached (Figure 7.12).

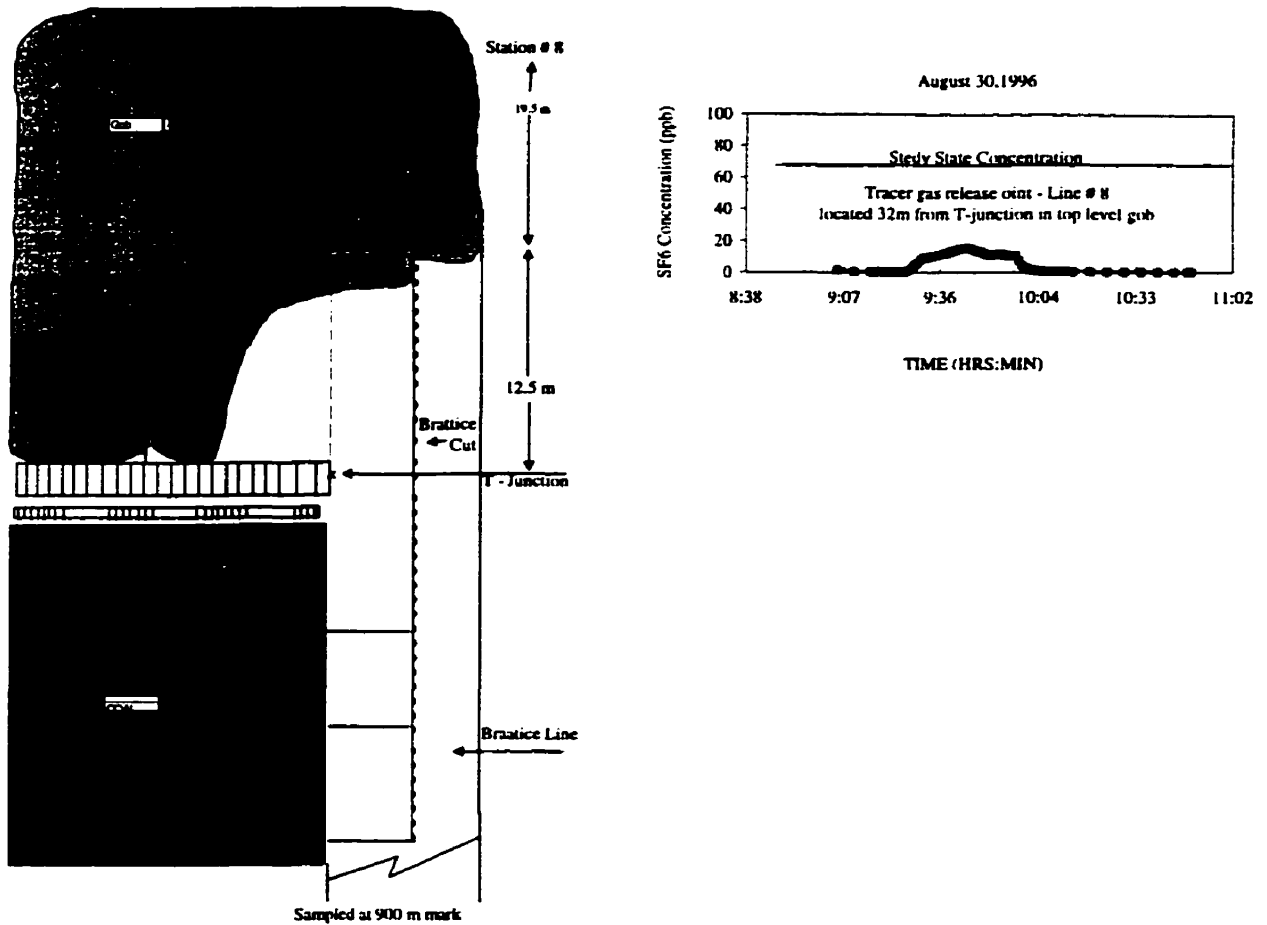


Figure 7.12 7 East Top neutral point study - 32 m inbye the T-junction (August 30,1996)

On November 5, tracer gas was injected into station no. 11, located 26 m in by the T-junction (Figure 7.13).

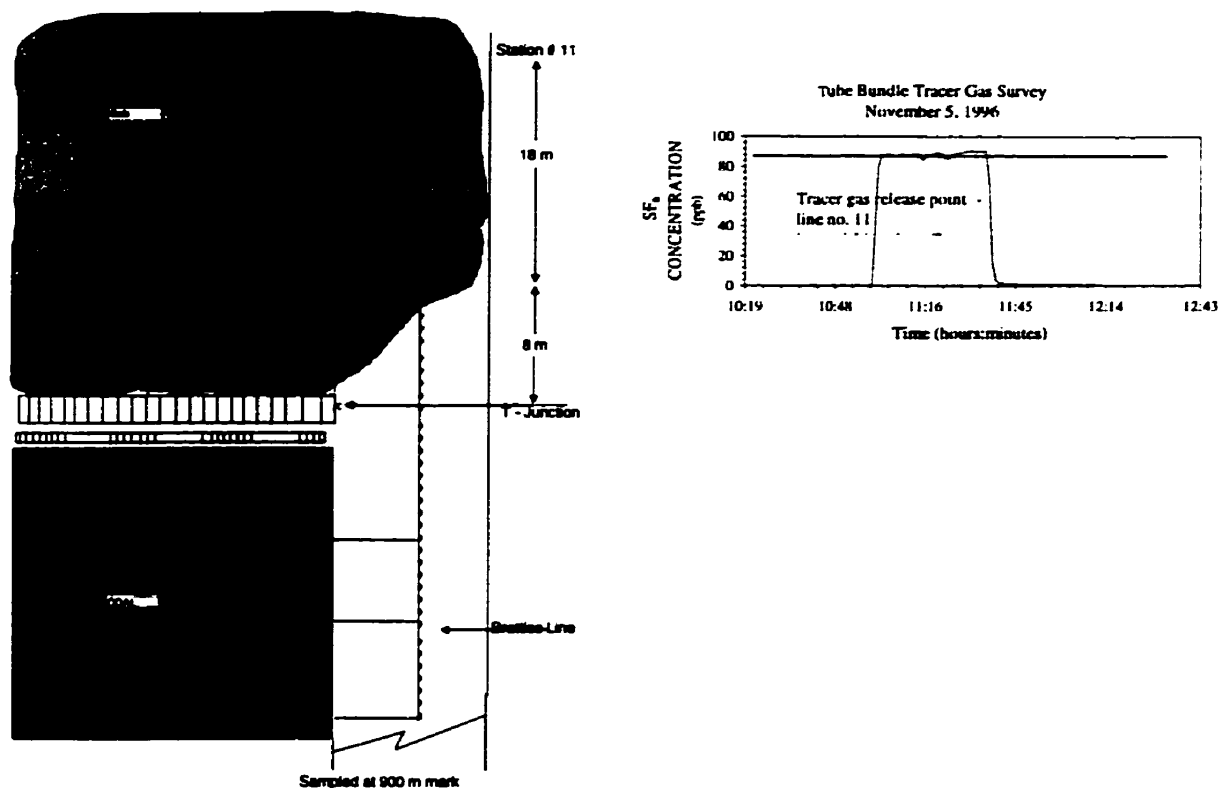


Figure 7.13 7 East Top neutral point study - 26 m in by the T-junction (November 5, 1996)

The sandstone had risen to 2.4 m above the coal seam in the top level and consolidation of the top level roadway appeared good. The majority of the tracer gas released into station no. 11 returned to the top level

Further sampling from station no.1 located ~ 424 m in the gob showed no signs of tracer gas. The difference in the steady state gas concentration curve and the station no. 11 curve is probably due to a change in air flow during the test period.

On November 7th, the same experiment was repeated under similar conditions with station no.11 28 m from the T-junction. Essentially the same results were obtained; most of the tracer gas had returned on the top level (Figure 7.14).

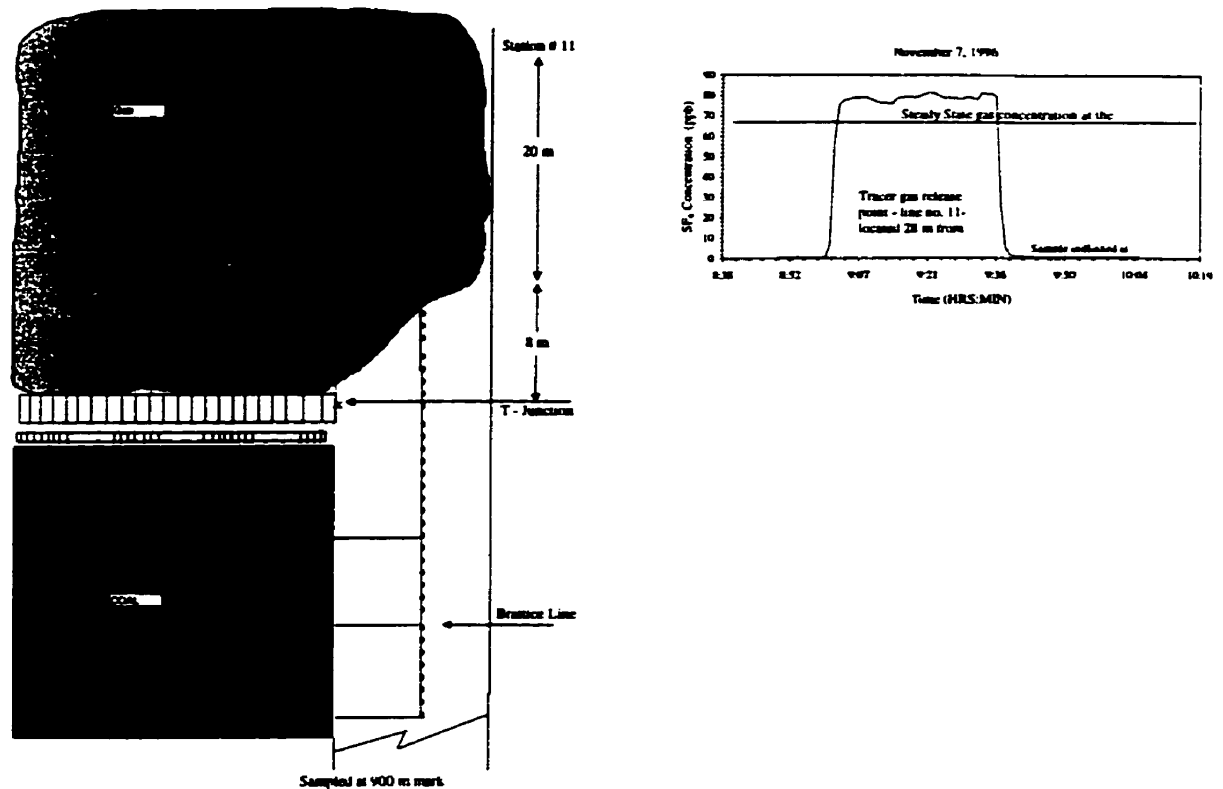


Figure 7.14 7 East Top neutral point study - 28 m in by the T-junction (November 7, 1996)

However, sampling of station no. 1, ~426 m in the gob, showed the presence of tracer gas indicating that station no. 11 was near the edge of the neutral point.

On March 3rd and 23rd two further tracer gas injections experiments were conducted as described previously. Tracer gas was injected into station no. 20 and 23 which were 12.5 and 15 m in the gob respectively from the T-junction. On these two days the gob was well consolidated and the sandstone height was 6.6 and 12.9m above the seam, with the latter being the highest point for the top level since the tubebundle experiment had begun.

Figures 7.15 and 7.16 present the tracer gas results and indicates that the majority of the tracer gas released into station no. 20 and 23 returned to the top level airway.

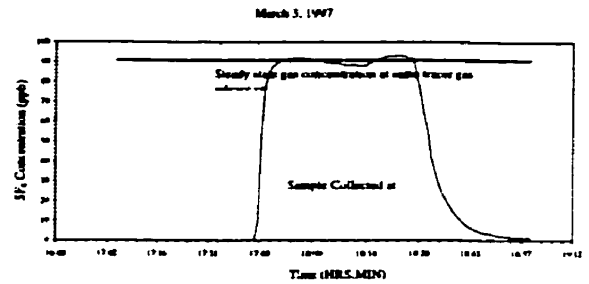
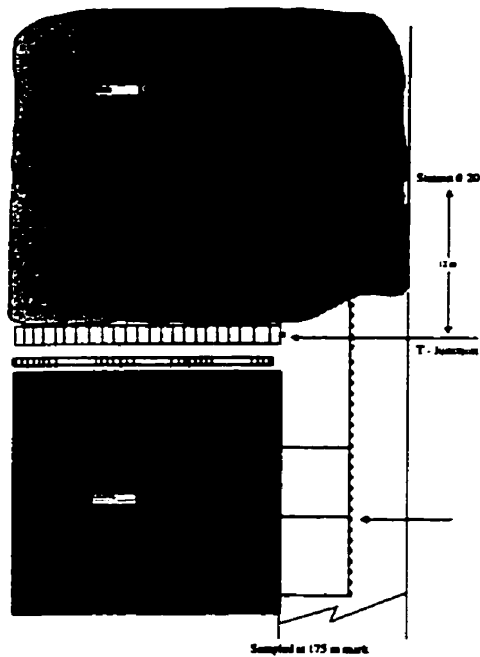


Figure 7.15 7 East Top neutral point study - 12.5 m inby the T-junction (March 3, 1997)

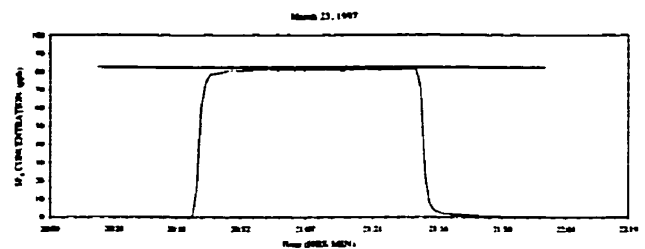
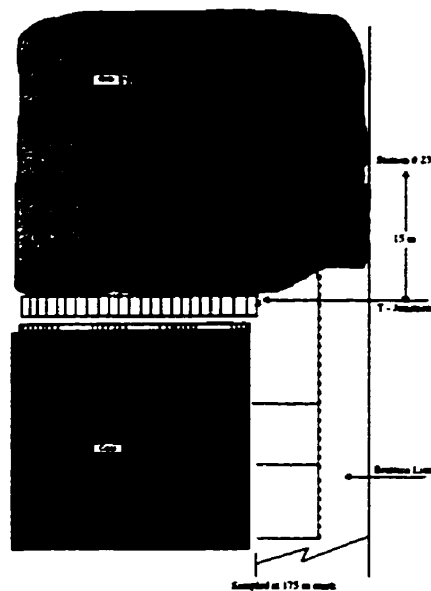


Figure 7.16 7 East Top neutral point study - 15 m inby the T-junction (March 23, 1997)

Further sampling at station 18 located ~ 90 and 200 m in the gob respectively showed signs of tracer gas which suggests the neutral point under these conditions is located ~ 20 m inbye the T- Junction.

Overall, both differential air pressure measurements and tracer gas tests results indicate that the neutral point is about 20 to 40 m inbye the T junction. The position of the neutral point appears to be a partial function of the Lower Sandstone Unit's height and thickness above the coal seam. The air pressure gradient between in 7 East Top level between the T- junction and an area 20 to 40 m inbye in the gob is toward the return airway; therefore, an uncontrolled area exists here; methane entering this area travels back to the T junction. The question to be answered at this point, is how far down behind the face supports does this uncontrolled area cover.

7.6.3 Channel flow in 7 East Top Level

A tracer gas experiment was conducted to determine the air velocity and migration paths in the 7 East Top Level gob once the neutral point was passed. Tracer gas was injected into station 14, 40 m inbye the T- junction and air samples were drawn from stations 12, 11, 10, 8, 6 and 1. The results of testing on air samples are shown in Figure 7.17.

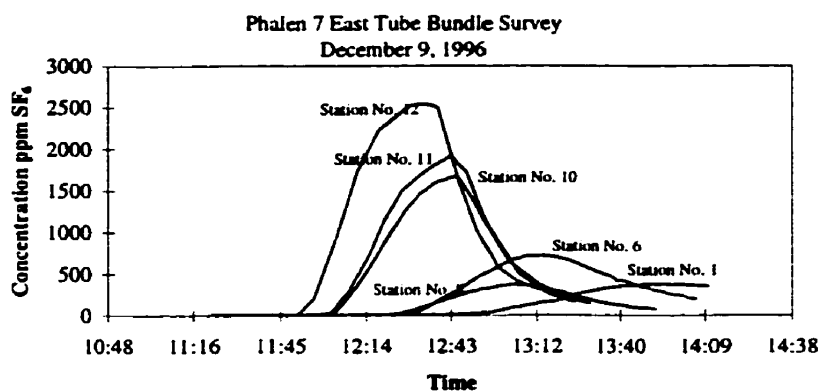


Figure 7.17 Tracer gas study of Phalen 7 East Top Level gob - Channel flow and air velocity

Tracer gas results show that the flow of air in by the neutral point is similar to that of channel flow. Essentially most of the air leakage across the face ends up in this low resistant area of the toplevel gob. The average air velocity along the 7 East Top Level gob from this experiment was estimated to be ~ 0.16 m/s. Now dividing the original cross section of the top level roadway (~ 10 m²) by tracer gas determined airflow leakage through the face (~ 1 and 2 m³/s) results in an the average air velocity in the range of ~ 0.1 to 0.2 m/s, almost equal to the previous estimate.

Both estimates imply that the majority of air leakage across the face occurs in the 7 East Top and Bottom levels at some point behind the face line. This is not the principle of operation for a Sewergate, but that of 4 and 5 East systems. This leads to a condition where high concentration of methane in the gob is simply being “picked away” around the fringes of the gob by a low bleeder road airflow.

7.7.0 45 m Tubebundle experiments - 7 East Wall Face

The flow or leakage of air through the 7 East gob is described in chapter 8. The direction and penetration of the pressure gradient across the immediate gob is a function of the pressure drop along the face. The penetration and flow of air through the gob area is a function of this pressure drop. To what extent or how deep this flow regime exists in the gob is the subject of the following experiment.

From previous tubebundle experiments in the collapsed tailgate, it was determined that a neutral point existed some 20 to 40 m in the gob. Beyond this point, the migration of gob gas and air is toward the East Back Bleeder. It is also at this point where the last influence of the wall face pressure gradient directs air flow through the collapsed tailgate toward the return airway. The flow of air through the gob along the wall face can be very complicated and for now can be imagined as a series of sub-parallel flow paths to the wall face that diminish at some point in the gob.

7.7.1 45 m Tubebundle layout

The following experiment was conducted when the wall had experienced improved strata conditions. The sandstone had risen and thinned out and weighings were less frequent. Also, the gob had compacted to the extent that the 1500 m tubebundle stations had been pinched off and survival of the remaining stations entering the gob was low. Specific emissions from the gob to the return airway had decreased substantially and production rate had nearly doubled. Methane concentration at the wall face and high side rib monitor moved closer together, all indicating improved ventilation conditions i.e. reduced gob methane.

Three 45 m tubebundles were installed at the bottom level, face end, at the 1/3 and 2/3 face line position (Figure 7.5). The bottom tubebundle was suspended from the low side rib 45 m outbye and to the T-junction. Two 4 core, 45 m tube wall face tubebundles were suspended from spools fasten to the wall face supports and were passed into the gob under these supports (Figure 7.18).

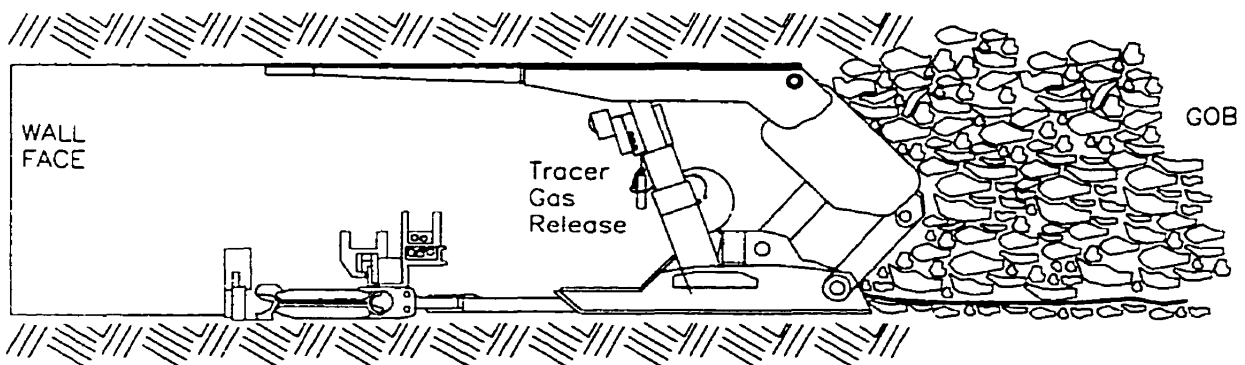


Figure 7.18 45 m tubebundle location and tracer gas release system on face support

Each tubebundle provided access to tubes for air pressure measurements and gas sample retrieval as well as tracer gas release points into the gob behind the supports.

The pressure drop along the face and from the face to some point in the gob was conducted to determine to what extent the sub-parallel flow paths exist in the gob and to what extent the gob gas and fresh air boundary exists. Because of the small pressure drops

(1 or 5 Pa) measured between the face line and some point in the gob, tracer gas injection was used to confirm these measurements validate conclusively that the sub-parallel pathways existed deep in the gob.

Figures 7.19 presents the pressure drop measured along 7 East face during the week of April 20,1997.

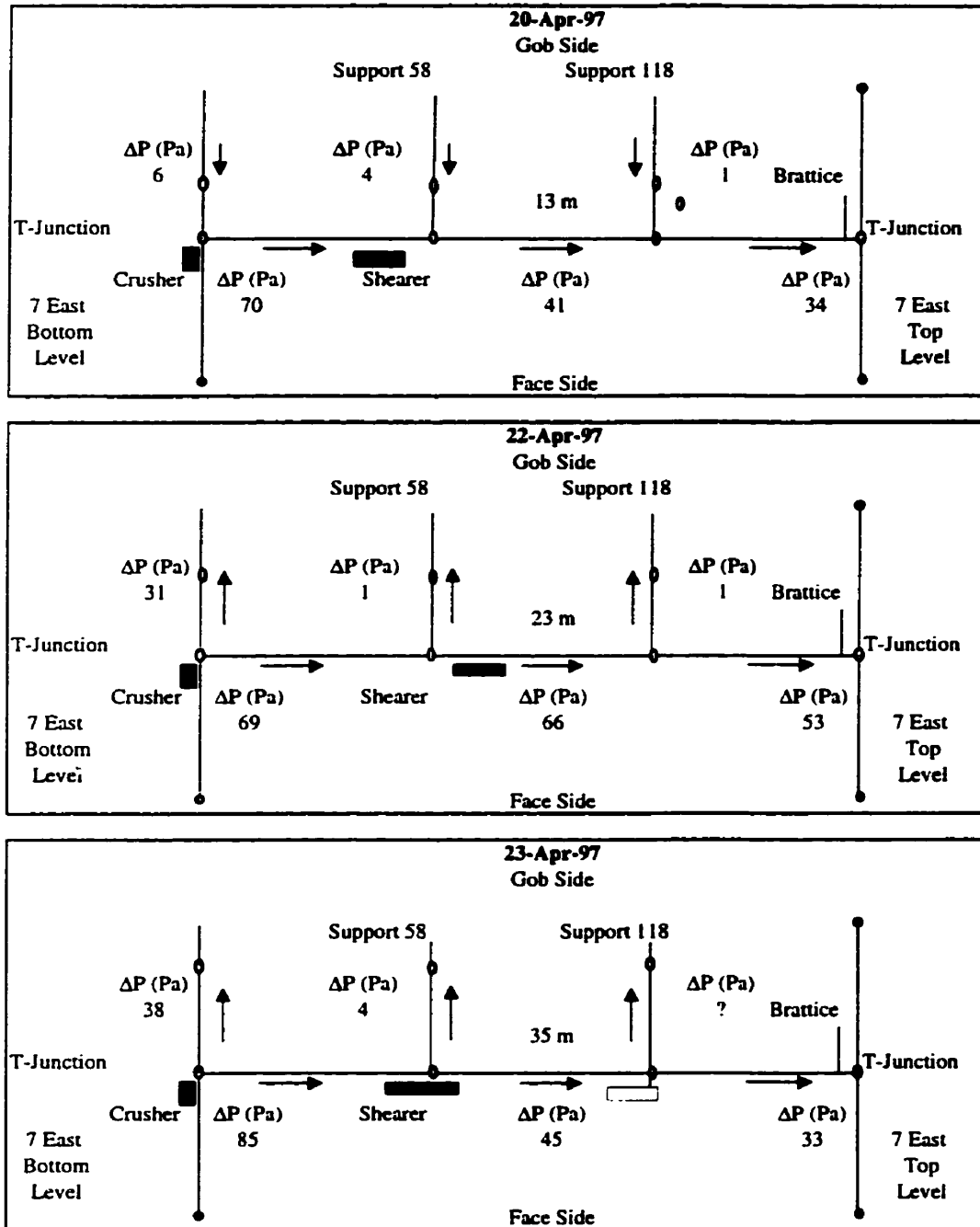


Figure 7.19 Differential pressure drops along the face and 45 m tubebundle stations

As stated it appears that during the 45 m retreat of the face, no significant pressure drop was measured from the face position to points 38 m in the gob.

Tracer gas was injected in the tubebundles in a series of four experiments. In the first two tests, tracer gas was injected at both the 1/3 and 2/3 wall face location, on separate shifts, when the tubes were 13 m in the gob. Tracer gas migrated toward the return air way as determined by air samples taken outby. Pressure drop between the face and the 13m point in the gob was near 0.

The experiment was repeated for the 1/3 point when the wall had retreated 38m and again the tracer gas migrated to the return airway. The experiment failed for the 1/3 face location because of pinching of the tubes by the gob material.

7.7.2 Final results

The experiment presented some final details in the assessment of the Sewergate system:

An uncontrolled zone of at least 40 m in the gob was effected by pressure gradient across the face. No appreciable amounts of methane was entering the gob in this 40 m zone. The boundry between where the neutral point exists was beyond the 40 m mark in the gob. This also implies that the area where high purity methane enters the gob was beyond the 40 m zone and probably closer to 100 m where other measurements indicated gob consolidation was occurring and emissions from other gas sources were occuring.

The flow of air through 7 East Top gob is both a function of the pressure gradient and resistance through the collapsed roadway. If the gradient remains the same through the collapsed roadway, and the resistance increases with the lengthening of this roadway, than airflow will reduce. If this airflow was the main controlling factor for clearing methane from behind the 7 East Top Face area, then this explains why more and more methane collected and migrated to the return level with face retreat. There was simply a lack of airflow in the 7 East Top Level gob to move methane back through the gob.

The previous sections have provided knowledge on the location of the 7 East neutral point, the pressure gradient and flow through the partially collapsed roadway. This information can be used to model air flow through partially consolidated gob material.

7.8 Observations Fabricated Back Return System

The main objective of the FBS was to eliminate gas delays at the tailgate armored face conveyor (AFC) motor which was largely achieved. The following observations were made concerning the FBS during survey and inspection periods:

- Condition of fabricated return system was maintained as well as expected.
- Difficulty was experienced maintaining a stable brattice line behind the face supports.
- The FBS acted as a mixing zone for gob emissions only and had no effect on the neutral area.
- The fabricated back return system did not fail to safety because the fringe was so close to the face.
- At times methane emissions through the brattice line, highside rib were greatest near the floor, i.e. 2% compared to the BM monitors position, i.e. 1.5%. Sometimes, floor gas emissions were suspected.

7.9 Composition of gas/air mixtures in the 7 East gob

Part of the tubebundle surveys of the 7 East Tailgate gob area included the collection of air samples from the tubebundle system for testing of methane, ethane, carbon monoxide and oxygen. The purpose of this sample collection campaign was to determine the following:

- Trend the methane/ethane concentration toward the face startline
- Profile how the gas composition changes in the gob
- Determine if other gas sources become active during gob consolidation

Samples were drawn with intrinsically safe sampling pumps into gas sampling bags. The samples were taken after differential pressure measurements were made from tubebundle stations in the gob and brought back to the laboratory for testing.

Figure 7.20 presents the sum of % methane and % ethane determined from gas samples versus both the face location at the T-junction and distance behind the T-junction to the sampling station in the gob for all samples collected.

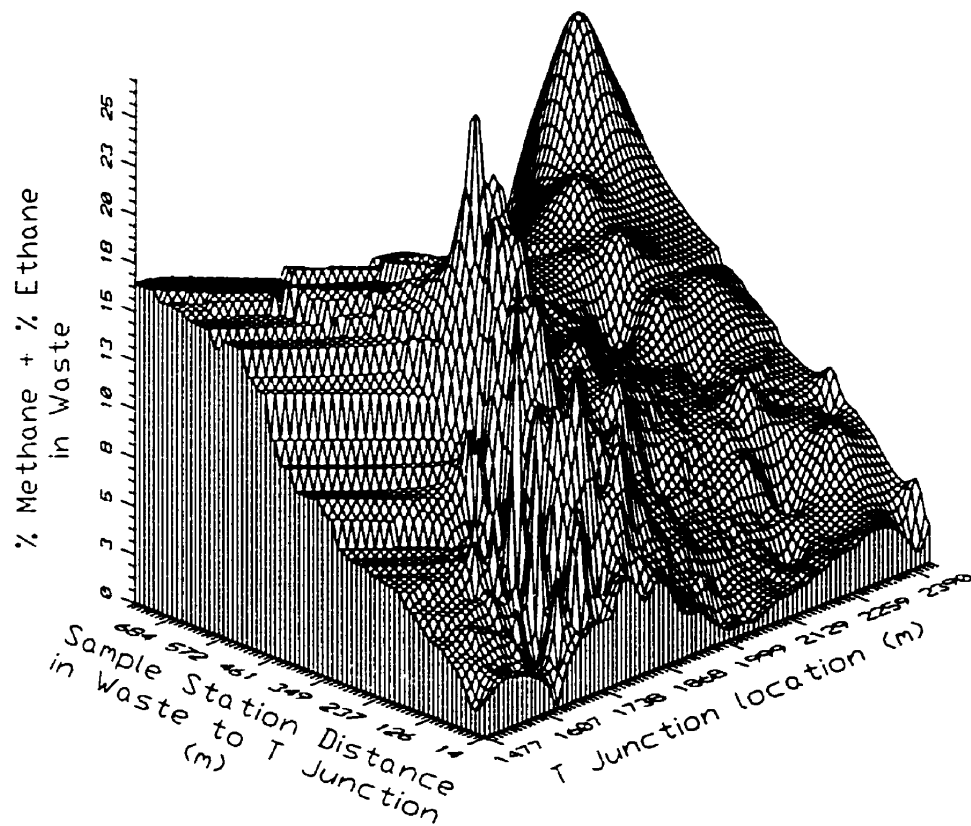


Figure 7.20 % Methane + % Ethane of samples collected behind the T-junction from tubebundle stations in the gob

Figure 7.20 indicates that the methane + ethane concentration in the gob trends toward a higher concentration with increased distance in the gob. If the trend is projected back to the face startline, it appears that the methane concentration at this point should be over 15 %, and essentially outside the explosive range. From this point in the mine, East Back Bleeder, the concentration was reduced, caused by successive air leakages flowing from previously sealed panels on the Eastside of the mine. This resulted in the occurrence of explosive gas mixtures in the East Bleeder. This air leakage could be reduced by improving the quality of the seals on the Eastside panels to reduce the air leakage.

It has been long suspected that the sandstone in the roof of 7 East panel had provided an additional gas source other than coal seams. It is a well known fact that some sandstones in Phalen and Lingan mine contained unquantified amounts of light oils and gases. However, the specific locations of these oils and gases were not always identifiable. For a large section of the retreat on 7 East, a strong 'hydrocarbon odour' was present in the return airway while the panel undercut the Lower Sandstone Unit when it was close to the top of the coal (4 m) and over 20 m thick. When the sandstone thinned and rose higher into the roof, the 'hydrocarbon odour' disappeared.

From Table 3.7 the composition of gas from a coal seam and sandstone can be compared. The interesting comparison was the methane to ethane ratio of the gas samples. The coal seam ratio was ~30:1 and the sandstone ~ 15:1. If indeed the sandstone contained a significant quantity of gas in 7 East, then this source of gas might be indicated by a changed in the proportion of methane and ethane emitted into the gob from coal seams and sandstone upon retreat.

Figure 7.21 presents a X,Y,Z contoured plot of the ratio of methane to ethane of samples collected from the tubebundle stations versus sample station distance in the gob to the T- junction and face T-junction location in the tailgate.

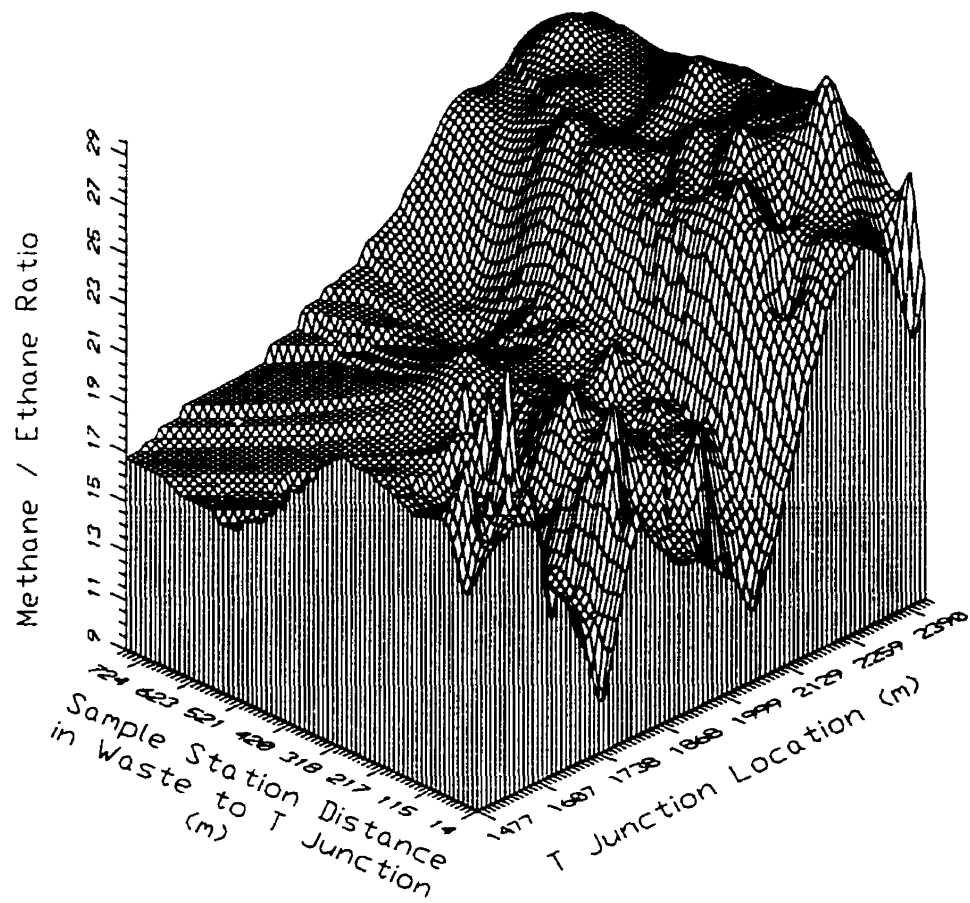


Figure 7.21 Methane / Ethane ratio of samples collected behind the T-junction from tubebundle stations in the gob

This plot clearly indicated that at about 2100 m the composition of the gases in the gob changed dramatically and this coincided with three other events.

- First, the Lower Sandstone Unit had essentially begun to rise and thin out in relation to the top of the coal seam.
- Secondly, the 'hydrocarbon smell' disappeared.
- Thirdly, the specific emissions from the gob of coal mined reduced substantially from an average of $\sim 4.5 \text{ m}^3/\text{tonne}$ while mining through the sandstone channel to $\sim 0.9 \text{ m}^3/\text{tonne}$ while not.

Although the evidence was strong that the sandstone channel had proven an addition gas source, the soon to be discovered Stony coal seam in the floor of 9 East Top Level at a

depth of 18 m complicated the gob gas composition problem. If the frequent face weightings caused by the thick Lower Sandstone Unit had caused stress related conditions in the floor and early release of floor gas (assuming the Stony seam was indeed present in 7 East floor). This could also explain why there was a reduction in the gob emissions to 7 East Top airway due partly to the infrequency of face weightings and the potential for reduced floor emissions.

Methane flow and caving processes of the longwall gob

8.0 Methane flow and caving processes of the longwall gob

In section 7, the information obtained was used to describe the operation of the Sewergate ventilation system, especially, the flow of methane and ventilation air through the gob to the return airways of Phalen 7 East. Each tracer gas experiment and ventilation pressure reading taken was analysed in order to define the flow regime through the gob and to help better define the performance of the Sewergate system.

In reality, the flow regime in the gob is a much more complex network of tortuous flow paths affected by equally complex methane release system from the roof and floor strata into the gob. In all the gob consists of two major systems of varying permeability joined together at an equally complex boundary. The permeability of the gob is affected by the composition of roof rock and the compaction pressure exerted by adjacent strata on the caved rock all which affect the porosity, therefore, its permeability. The permeability of the roof strata consists of a complex fracture system determined by the parameters of strata composition, strength and the stress induced by longwall mining.

In terms of methane flow from coal strata, a sub-fracture and permeability system exists, which is affected by the unique desorption characteristics of the coal which are directly affected by longwall mining induced stress. The combination of the non-coal and coal strata permeabilities and resulting methane gas flow interfaced with the caving gob material provides a complex flow system. To model such a system would involve some ingenious mathematical concepts, field data, supported by equally powerful computer applications such as Computation Fluid Dynamic (CFD) computer systems to process the algorithms. This is beyond the scope of this report.

However, this section has been added to present some appreciation for some basic concepts to consider when discussions on the mechanisms and parameters at play in describing and modelling the gob. It will reflect on passed research, theories and experimentation by others to discuss but a few parameters effecting the flow of methane and air into the gob. This information is not used for any other purpose in this report.

8.1 Longwall Mining

Longwall coal mining is normally done in sedimentary strata beds of variable thickness and composition. The roof strata beds are in most cases well defined and can usually be approximated as separate units, so strata stability and cavability may be analysed as a series of planar rock “plates” or “beams” (Jeremic, M.L., 1982).

As mining progresses, support for the roof is removed and a span of roof begins to sag and when it can't support its own weight it eventually collapses filling in the void below. The length of the span depends on the strength of the rock forming it and on the stress conditions around the face. The fragmented rocks that fall differentially, rotate creating void spaces so that the overall volume per unit weight increases and gradually fills the cavity until the upper beds bend and sit on top of the unconsolidated caved material (Jeremic, M.L., 1982)

8.2.0 Caved material volumetric relationships

The active zone is the cavity or boundary between the caved material and the intact strata where failure occurs. The upper limit of caving can be calculated from the volumetric equation:

$$H = \frac{T}{BF-1} \quad \text{eq 1}$$

Where: T = seam thickness

BF = the bulk ratio defined as the caved volume (V_c) divided by the intact rock volume (V_r)

H = height of the active caving limits above the seam.

$$BF = V_c/V_r \quad \text{eq 2}$$

$$V_c = V_v + V_r \quad \text{eq 3}$$

Where:

V_v = Void volume in caved material

substituting eq 3 into eq 2

$$BF = \frac{V_v + V_r}{V_r}$$

or

this becomes

$$BF = \frac{V_v + 1}{V_r} \quad \text{eq 4}$$

Free falling gobs rarely exceed the bulking factors of 1.3 (Jeremic, M.L., 1982). Strong roof beds above the seam in the active caving area, can cause periodic weightings on the face and supports due to the formation of roof cantilevers with larger than normal spans before failure. The upper limit of the upper caving zone will generally be controlled by the the rigidity and strength of the strata beds in this zone.

8.2.1 Composition of caved gob rock

Sedimentary rock is composed of two components: a detrital fraction (pebbles, mud, sand) brought together with and a chemical fraction (calcite, gypsum, and others) formed very near the site accumulation (Krumbein W.C and Sloss L.L, 1963). A clastic rock such as conglomerate, sandstone, shale is composed of mostly detrital material. Detrital rocks commonly have a fragmental texture, and have properties determined by the type of particles that formed the deposit. The particle properties are (1) size (2) shape (sphericity) (3) roundness (4) surface texture (5) orientation (6) mineralogic composition. For large particles the volume may be used as an expression of size, converted to its nominal diameter by computing the diameter of a sphere having the same volume as the particle. The operation sphericity of a particle is defined by the width of the intermediate to the

maximum intercept and the shortest to the intermediate intercept, and with these formulats can be classified according to shape (Figure 8.1.) (Krumbein W.C and Sloss L.L, 1963).

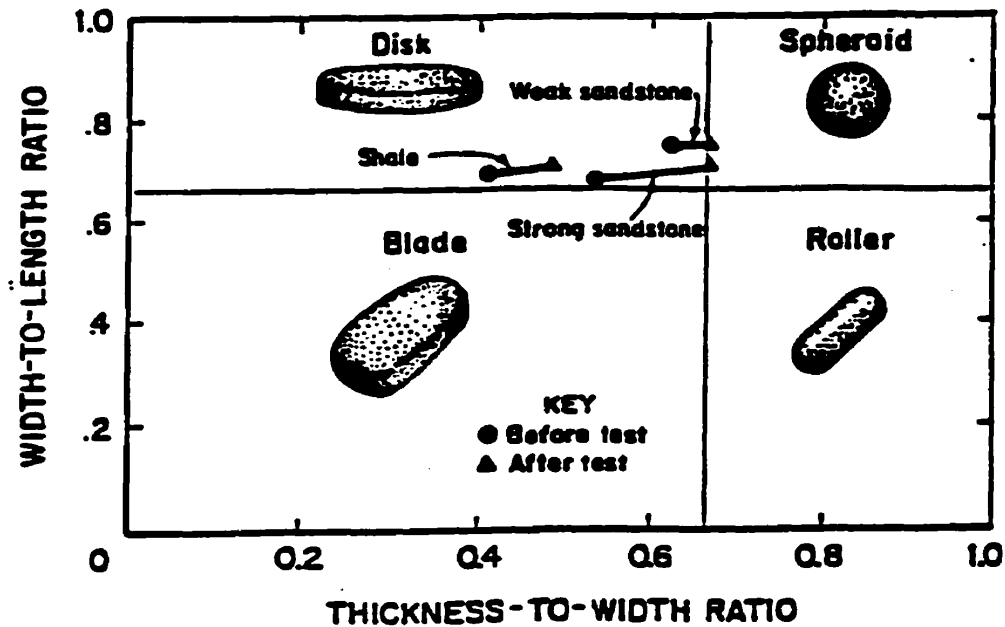


Figure 8.1 Zingg's diagram showing classification of different shapes associated parameters (after Krumbein and Sloss, 1963)

This Figure is a Zingg's classification of pebble shapes and shows that particles of varying sizes according to the eye may have the same value of sphericity. In its original form sphericity compared the surface area of particle to its corresponding sphere. The point of this discussion is to state that the shape of the rock depends on the particles composing it, and this does not change much with degradation, but the type of strain that can be induced in the particle depends on its shape. Therefore gob caved rock shape and size depends on the rock type.

8.3 Porosity of caved material

Porosity is defined as the ratio of free voidage in the gob material to volume of broken rock:

$$\frac{V_v}{V_r} = \phi \quad \text{eq 5}$$

This is the same factor in equation eq 4

Substituting eq 5 into eq 4: $BF = \phi + 1$ eq 6

or

$$\phi = BF - 1$$

8.4 Bulking factor as a function of compressive stress and caved rock shape

In a series of experiments on strong sandstones, weak sandstones and shales, (Pappas and Mark, 1993) determined that the bulking factor is proportional to the rocks strength and its thickness to width ratio. The research determined indicates that the rock strength and thickness to width ratio increase the bulking factor. The thinner and disk-shape rocks have a lower bulking factor; this infers a weaker rock that can be broken into smaller pieces and therefore decrease voidage. The impact overall is that strong sandstones have a higher bulking factor and build more porous gobs capable of flowing a greater volume of air and gas than a weaker rock type. In these experiments (Pappas and Mark, 1993) determined a series of equations presenting bulking factors as a function of particle size and rock strength (uni-axial compressive strength = X_1) and (thickness to width ratio of the particle = X_2) at a constant stress level (σ_1) for strong and weak sandstones and shales. The equations derived from experimentation are as follows:

$$\sigma_1 = 400 \text{ psi} \quad BF = 0.0000184 * X_1 + 0.267 * X_2 + 1.16 \quad \text{eq 12} \quad R^2 = 0.828$$

$$\sigma_1 = 600 \text{ psi} \quad BF = 0.0000203 * X_1 + 0.274 * X_2 + 1.06 \quad \text{eq 13} \quad R^2 = 0.875$$

$\sigma_1 = 800$ psi	$BF = 0.0000187 * X_1 + 0.262 * X_2 + 1.04$	eq 14	$R^2 = 0.873$
$\sigma_1 = 1000$ psi	$BF = 0.0000185 * X_1 + 0.269 * X_2 + 0.992$	eq 15	$R^2 = 0.892$
$\sigma_1 = 1500$ psi	$BF = 0.0000160 * X_1 + 0.209 * X_2 + 1.00$	eq 16	$R^2 = 0.901$
$\sigma_1 = 2000$ psi	$BF = 0.0000150 * X_1 + 0.221 * X_2 + 0.963$	eq 17	$R^2 = 0.908$
$\sigma_1 = 2500$ psi	$BF = 0.0000136 * X_1 + 0.247 * X_2 + 0.931$	eq 18	$R^2 = 0.894$

Another important finding of this experiment was the determination of a particle degradation curve made from image analysis of photographs of caved gob rock from several Virginian mines. It was determined that the particle distribution within the photographs adjusted for hidden rock mass matched the experimental degradation curves of rock particles as determined from sieve analysis. This confirms that caved rock shape and size depends on the rock type and that the stress - strain was not effected by the maximum particle size, but changing the gradation appeared to influence the stress strain behavior.

8.5 Phalen gob compaction

One of the keys to gob compaction at Phalen mine Eastside walls mining west is that the horizontal stress measured at 30 Mpa (4350 psia) for Phalen mine coming across at about 27-30 degrees North of East off the levels creates voids in the gob because of the following reasons (Payne. D.A and DeMarco, M., 1994).

(1) A horizontal stress reduction in the top level causing excellent roof and floor conditions in the top level. (eg. the horizontal stress field travels around the roof and floor in order to go above or below the gob).

(2) A stress concentration in the bottom level at the corner of the wall as the stress concentrates here to avoid the gob causing increased floor heave and roof lowering in the bottom level. In this case the floor is shot and mucked out so that loading equipment can be moved through this area. In the top end the roof in the gob is supported by the coal face, supports and the coal pillar. The material is very strong in this area in terms of sandstones

plus it is bolted from the original drivage. The stress in the top level has actually reduced; therefore, the roof must cave under its own weight. In this case the roof can hang a long way and has been observed to be intact as far as 30 m in the level and down the faceline. In the bottom level stress is double the normal before the wall arrives. This may drive the roof to fall in the bottom more than the top but this still depends on the strength of the roof rock. Vertical stress is greatest at the center of the wall where there is no support system for the strata other than its own weight and gob material. However weightings on the face are a normal occurrence and cavage in some respects depends on stress relief associated with the breaking of the cantilever creating the stress. The overall effect of these strong roof rocks and the prevailing horizontal stress conditions in 7 East wall has led to low gob compaction, especially, in the in the top end. As mentioned previously, this is detrimental to the Sewergate operation.

To conclude, a strip of high gas permeability exists in the 7 East Top and Bottom collapsed levels. These are connected together by another strip of permeability that exists in back of the face supports. These areas of permeabilities are the main conducting pathways for air leakage across the face toward the gob.

8.6.0 Methane flow into the gob

The distribution of methane flow in the gob occurs in two ways. On a line perpendicular to the face, the methane flow increases from 0 to to a maximum value located a certain distance from the longwall and then decreases to 0 again as the longwall departs.

On a second line parrallel to the face, flow is higher near edges of the panel than near its centre. This is due to the existence of cracks, over and under these particular zones, resulting from the movement of strata which occurs there after caving-in and relaxation. These cracks are ideal paths for firedamp flowing out from distant beds toward the working (Christian.,Tauziede, Moulleau, Yvon, & Boutet Remy, 1996).

8.6.1 Models for airflow in porous mediums

Spacially periodic structures are the simplest structures that can be seen in nature; for this reason, they were first to be studied in terms of fluid flow in porous mediums (Pierre M. A, 1992). A spacially periodic medium can be constructed in the following way (Figure 8.1). Consider a parallel piped whose sides can be referred to by three vectors I_1, I_2, I_3 .

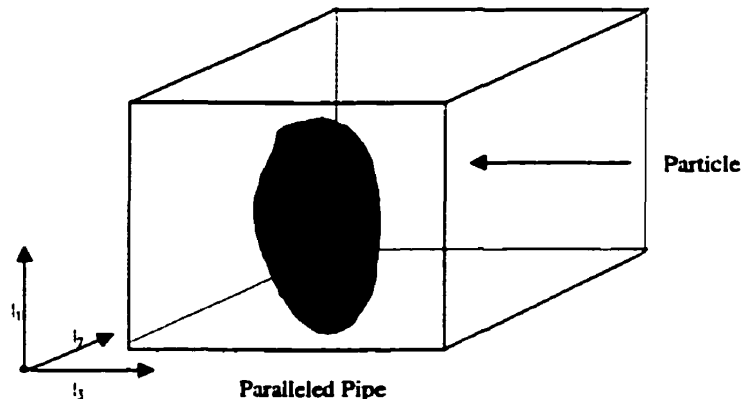


Figure 8.2 Spacially periodic structures and particle for modelling porous medium

The content of the this parallel pipe is for the moment arbitrary; it can be composed of particles of any number. The three vectors must form a three dimensional space or volume (V_v). The caved gob consists of a complicated arrangement of broken rock arranged in a random manner. The flow of air and gas through this arrangement of broken rocks depends on the porosity, the size of the particles, and the diameter of the pores. The three vectors can be considered a simplified version of the direction of airflow through the space V_v . If we consider a plane denoted by the vectors I_1 and I_2 and assume that flow is two directions only, then it is possible to construct a network of flow paths where the magnitude of the vector is a function of the medium in that plane. The medium therefore is considered homogenous and the plane represents an average of the original space. It also restricts the flow of air through the medium to two orthogonal directions denoted as X_1 and Y_1 (Figure 8.3) (Banik, J., 1994).

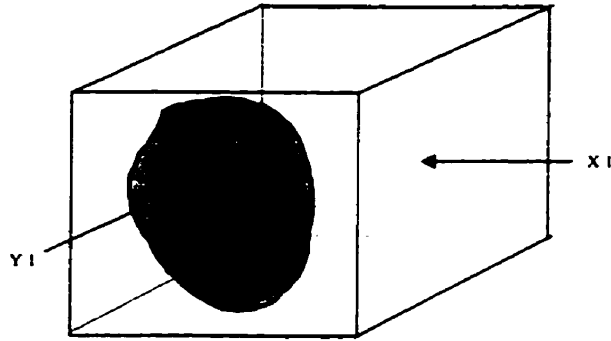


Figure 8.3 Airflow pathways in two orthogonal directions for constructing a grid pattern for mine airflow analysis

Arranging the structure in this way makes the analysis of airflow using a Proprietary ventilation network analysis software program “V-net” by constructing a series of connecting two dimensional parralled pipes connected in a grid pattern (Figure 8.4).

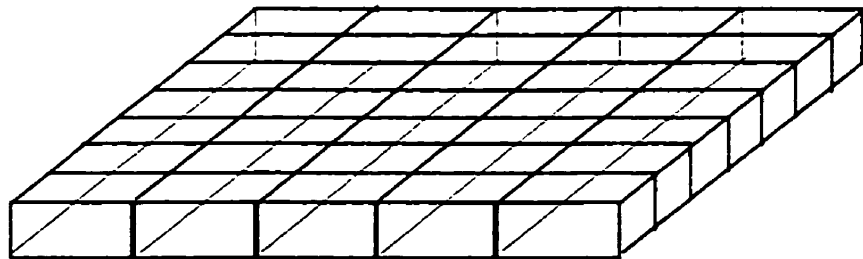


Figure 8.4 Grid pattern for airflow in two orthogonal directions representing the gob

8.6.2 Fluid flow through porous mediums

The magnitude of fluid flow through a porous medium has been extensively studied and some empirical relationships have been defined.

The coeficient of permeability or the measure of the conductivity of air and gas through porous medium or in this case the caved material in the gob can be determine from these

three parameters expressed in the empirical Kozeny- Carman equation (Christian.,T., Moulleau, Y., & Boutet R., 1996)

$$K_p = \frac{\phi^3}{(1-\phi^2)*k*S_o^2} \quad \text{for } \phi < 0.8 \quad \text{eq 7}$$

Where: K_p = Coefficient of permeability of the medium

S_o = specific surface of the particles in the medium

k is the Kozeny - Carman constant between 5 and 6

The specific surface of a particle can be related to an equivalent sphere of equal volume where the ratio of the surface area of a sphere to its volume is defined as its specific surface. The volume of a sphere V_s is given by the following:

$$V_s = \frac{\pi}{6} * D^3 \quad \text{eq 8}$$

Where D = diameter of the sphere or particle

The area A_s of the sphere is given by the following:

$$A_s = \pi * D^2 \quad \text{eq 9}$$

Therefore the specific area = $\frac{A_s}{V_s}$ eq 10

Substituting eq 10 into eq 7 gives the following:

$$K_p = \frac{D^2 \phi^3}{(1 - \phi^2) * k * 36} \quad \text{eq 11}$$

The porosity of the medium is defined as the ratio of the voidage within the medium to the volume of material. This parameter is defined in eq 6 for which is expressed in terms of bulking factor. Substitution of eq 6 into eq 11 gives an equation relating bulking factor and the coefficient of permeability of the caved gob rock.

$$K_p = \frac{D^2 (BF-1)^3}{(1 - (BF-1)^2) * k * 36} \quad \text{eq 12}$$

This defines the permeability of caved material in terms of particle diameter and bulking factor.

8.6.3 Laminar and turbulent resistances in porous mediums

The flow of air-gas mixture through caved material is laminar in nature and the resistance to flow is given by the following equation:

$$R = \frac{\mu * L}{K_p * A} \quad \text{eq 13}$$

Where:

- R = flowpath resistance (Ns/m⁵)
- μ = dynamic viscosity (Ns/m²)
- L = length of the flow path (m)
- K_p = coefficient of permeability (m²)
- A = area of cross section of flow (m²)

(Banik, 1994) has set a criteria for converting laminar resistance to turbulence resistance for use in V-net a mine ventilation software program designed for simulating mine

airflow. He assumes that air flow through caved material or porous medium is mixed in nature. Reynolds number is considered the decisive parameter in determining whether flow is turbulent or laminar in nature: Reynolds number for flow in porous medium is given by the following equation:

$$Re = \frac{\rho * V * d}{\mu} \quad \text{eq 14}$$

Where: R = Reynolds number

ρ = density of the fluid (kg/m³)

V = fluid velocity around a particle (m/s)

d = diameter of the particle or block (m)

μ = dynamic viscosity (Ns/m²)

When $Re < 1$ ~ flow is laminar

$Re > 1$ ~ flow is turbulent

The fluid flow through the medium is defined by the following equation:

$$P = (R * Q^n)$$

Where: P = Frictional pressure drop within the medium (Pa)

Q = fluid flow through the medium (m³/s)

R = Laminar or turbulent flow resistance determined by Reynolds number criteria (Ns/m⁵, Ns/m⁸)

n = is a function of mix flow nature throughout the medium.

V-Net Model

9.0 V-Net Model-Phalen Sewergate

V- NETPC for Windows program is a Windows based application that is designed to aid mine environmental engineers in the planning of subsurface ventilation layouts and is used by Phalen mine engineering staff to conduct mine airflow analysis (Mine Ventilation Services, Inc, 1996). Figure 9.1 shows a typical network for Phalen Ventilation analysis.

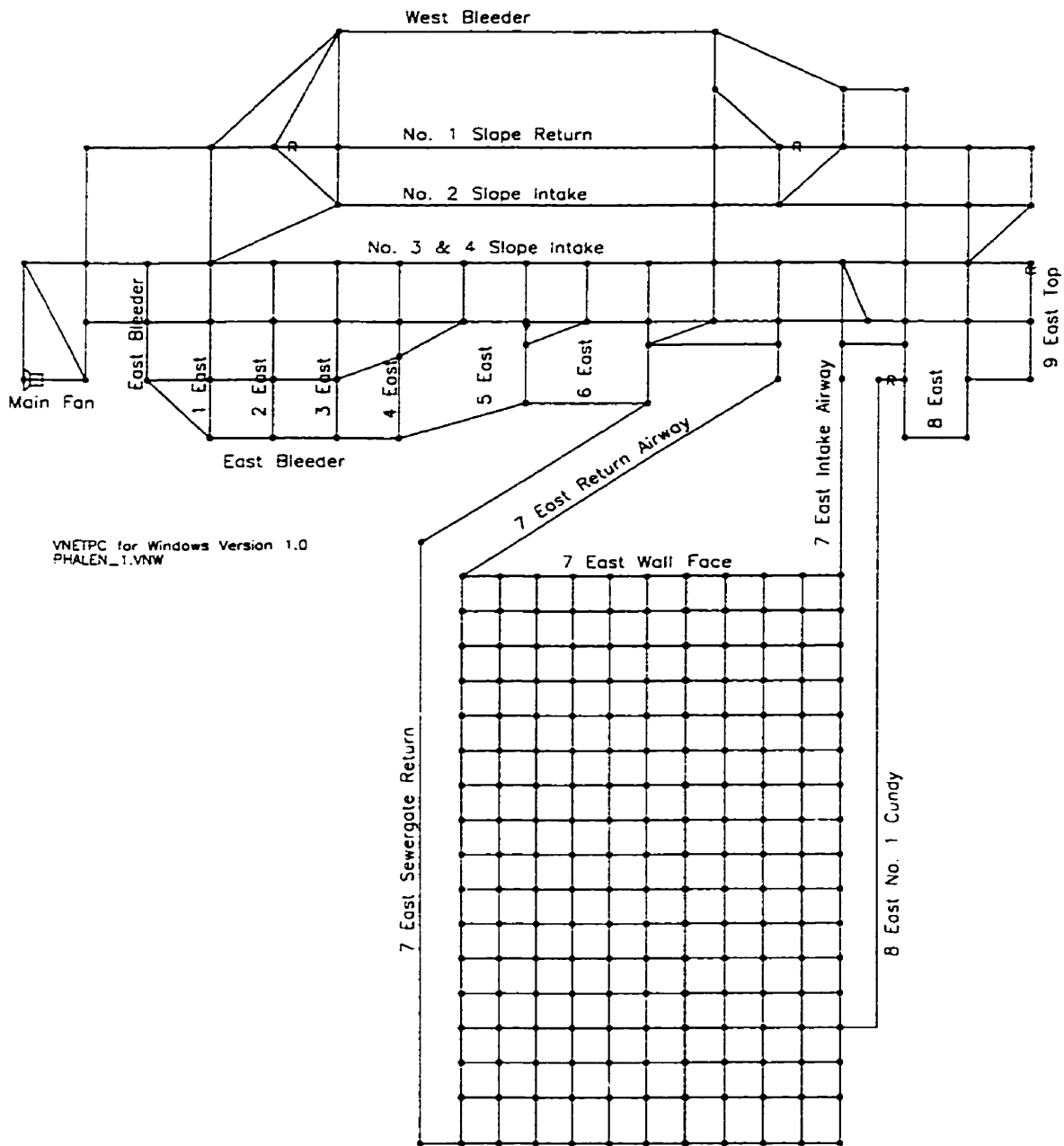


Figure 9.1 V-Net - Model of Phalen mine ventilation system

Figure 9.1 the V-net model of Phalen mine includes an additional 16 by 10 grid constructed for Phalen 7 East district. See Figure 9.2.

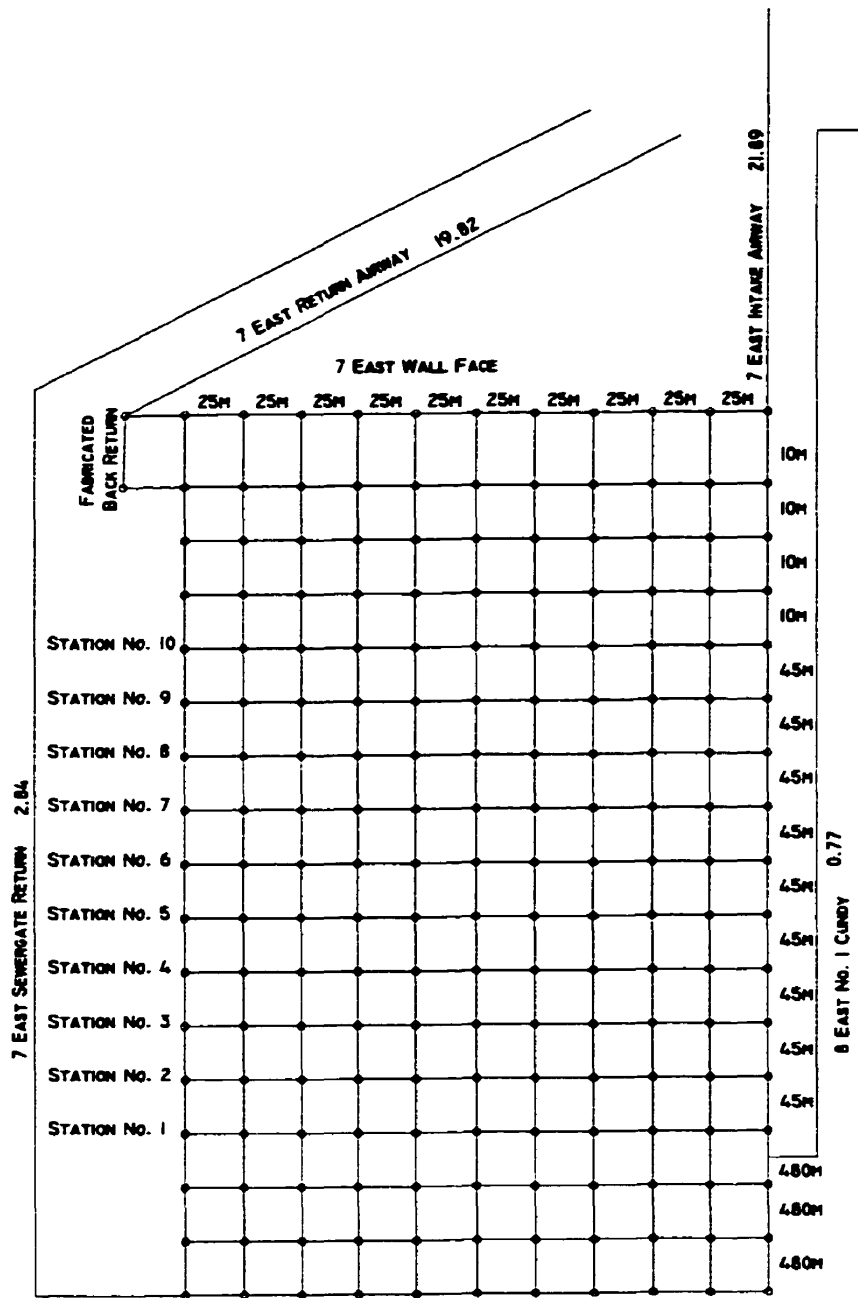


Figure 9.2 V-net gob model of Phalen 7 East gob including the face

Because an uncontrolled zone and neutral point were discovered to exist behind the supports of 7 East face, a more detailed grid was designed for the immediate face and gob

area. The whole gob consists of three parts. The first part is a grid 10 block wide (25 m per block) representing the face and a 4 block deep (10 m per block) representing an area from the face line toward the gob. The second part is a grid 10 block wide (25 m block) by 9 block deep (45 m per block) covering tubebundle stations no.1 to no.10. This part of the network was constructed for resistance values calculated from differential air pressure measurements made between stations no. 1 and no.10 in the collapsed top level. The third part of the network represents the remaining gob and consists of a 10 block wide (25 m per block) by 3 block deep (480 m per block). This part of the network incorporates crosscut no. 2 from 8 East Top Level and contains a stopping.

The return air from the face contains a fabricated return system. The leakage resistance across the brattice system has been set at 125 resistance units. The airway resistance along the brattice and highside rib has been set to 0.1 units.

Air flow (Q) leakage across 7 East face has been determined to be ~ 1 m³/s and 2 m³/s at a projected frictional air pressure drop (P) of 1500 Pa. Airflow through the gob is considered laminar in nature; however, most airflow occurs through the unconsolidated gates; therefore, resistance can be expressed in terms of turbulent resistance:

$$R = P/Q^n$$

If it is assumed that airflow is approaching unity for both gates, both can be expressed in either turbulent or laminar low resistances. Each gate would have an equivalent resistance of (1500 /1²) or (1500/1) either Ns/m⁸ or Ns/m⁵ resistance units ; furthermore, if we consider the two resistances in parallel then the equivalent resistance would equal 750 units. This is close to the reported estimates of gob resistances. This projection was later confirmed when CBDC drilled a small pilot hole to the 7 East face startline from 8 East Bottom through the coal pillar. Ventilation measurements confirmed that the pressure drop across the gob was ~ 1250 to 1350 Pa. In order to get even close to this projected pressure drops in the gob using V-net, resistance units as high as 8000 to 10000 units are required in the model to create values of pressure drop similar to projected ones.

Some initial modelling of 7 East has led to two interesting findings. If resistances of 2000 units are used for the major portion of the gob, small air leakage is produced from the gob to the return airway at the T-junction (Figure 9.3).

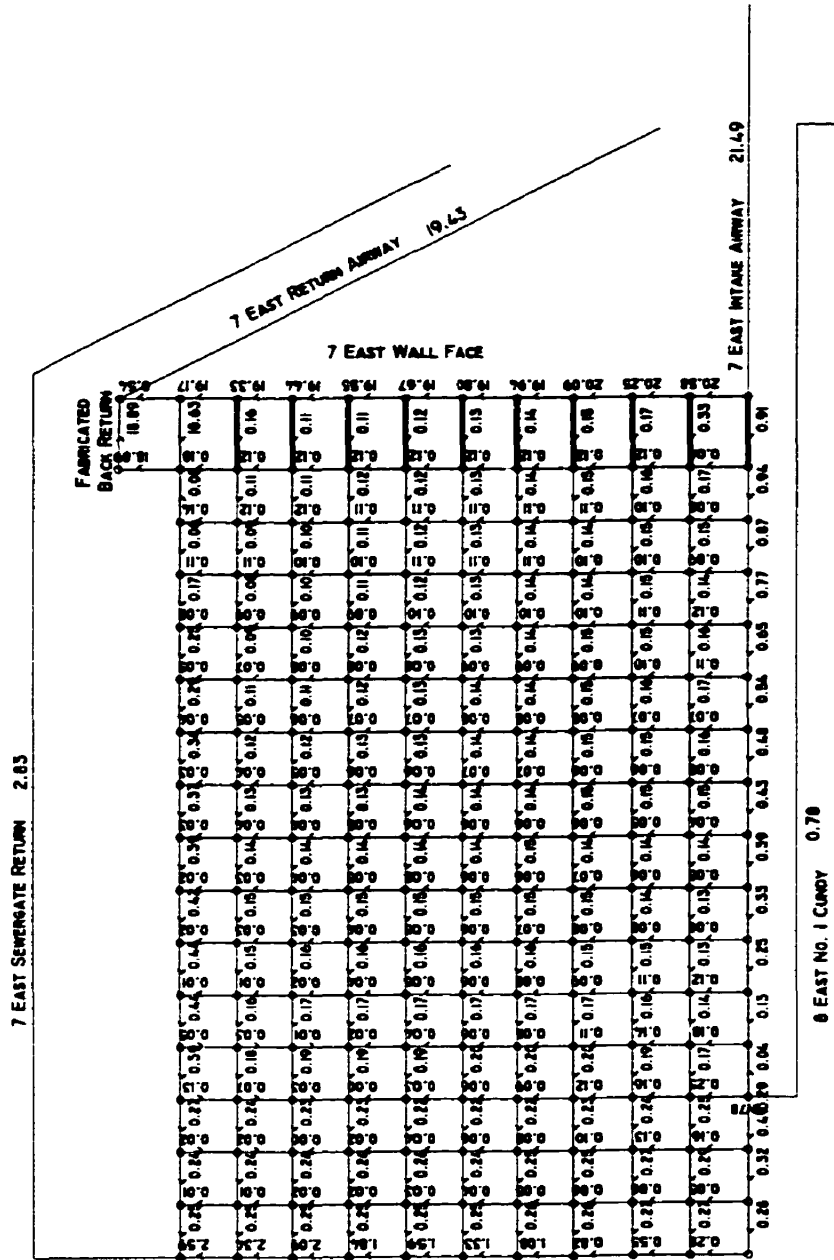


Figure 9.3 V-net model of Phalen 7 East - high resistance gob

If the gob resistance is reduced in a series of steps to 50 units from the midpoint on the face to an area inby the T₂ junction, air leakage from the highside rib increases (Figure 9.4, 9.5, and 9.6; bold lines indicate 50 resistance unit branches).

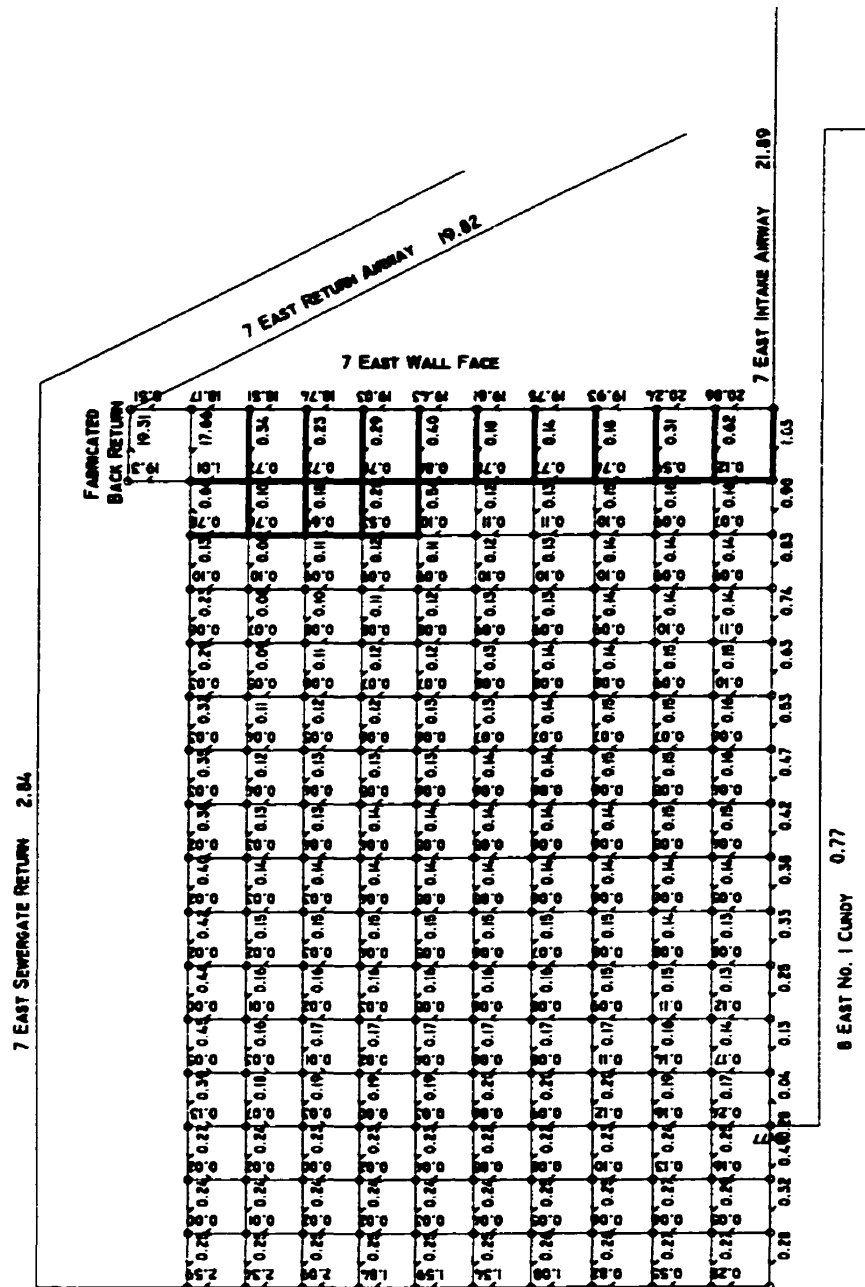


Figure 9.4 V-net model of Phalen 7 East - 1st stage of reduced upper gob resistance

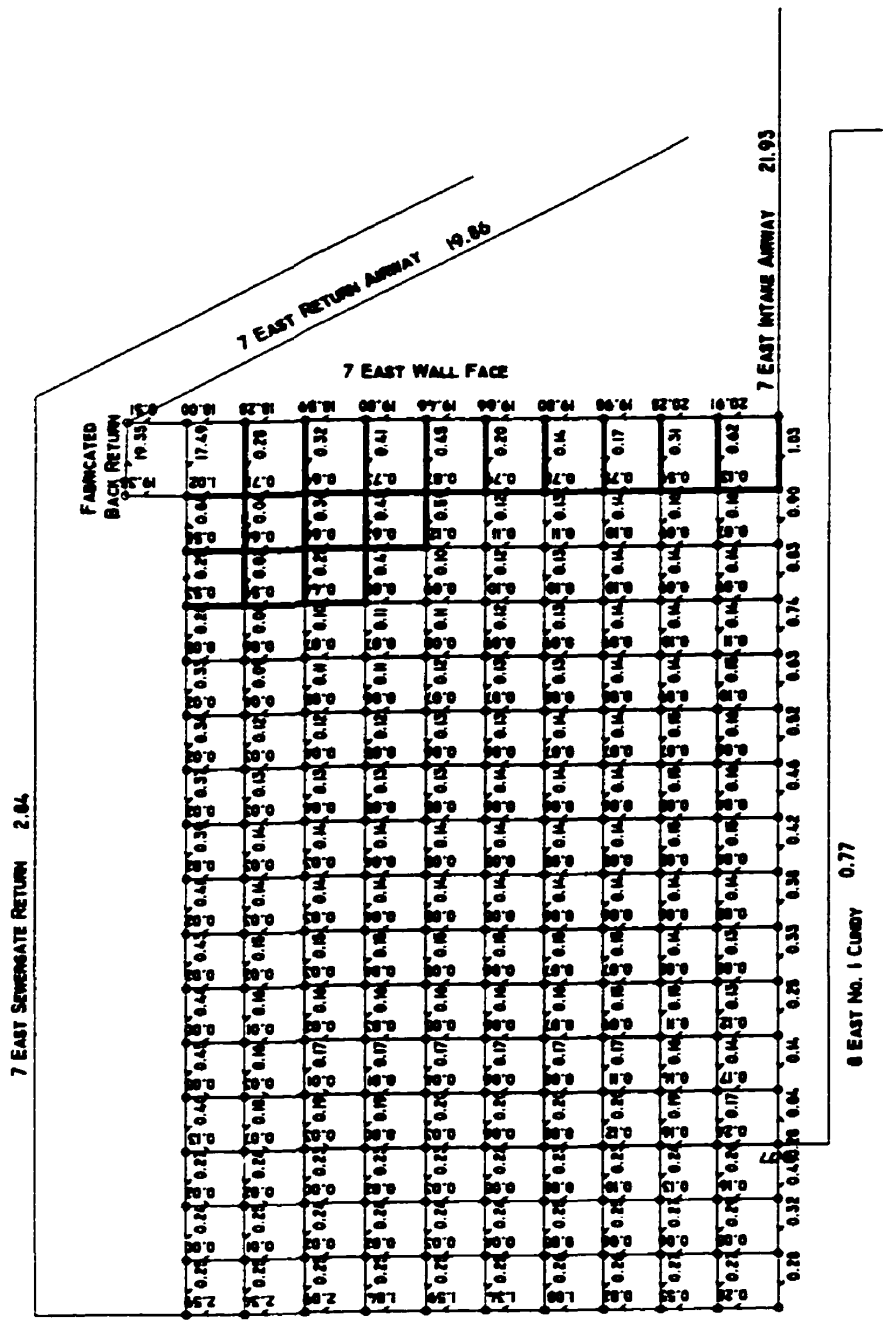


Figure 9.5 V-net model of Phalen 7 East - 2nd stage of reduced upper gob resistance

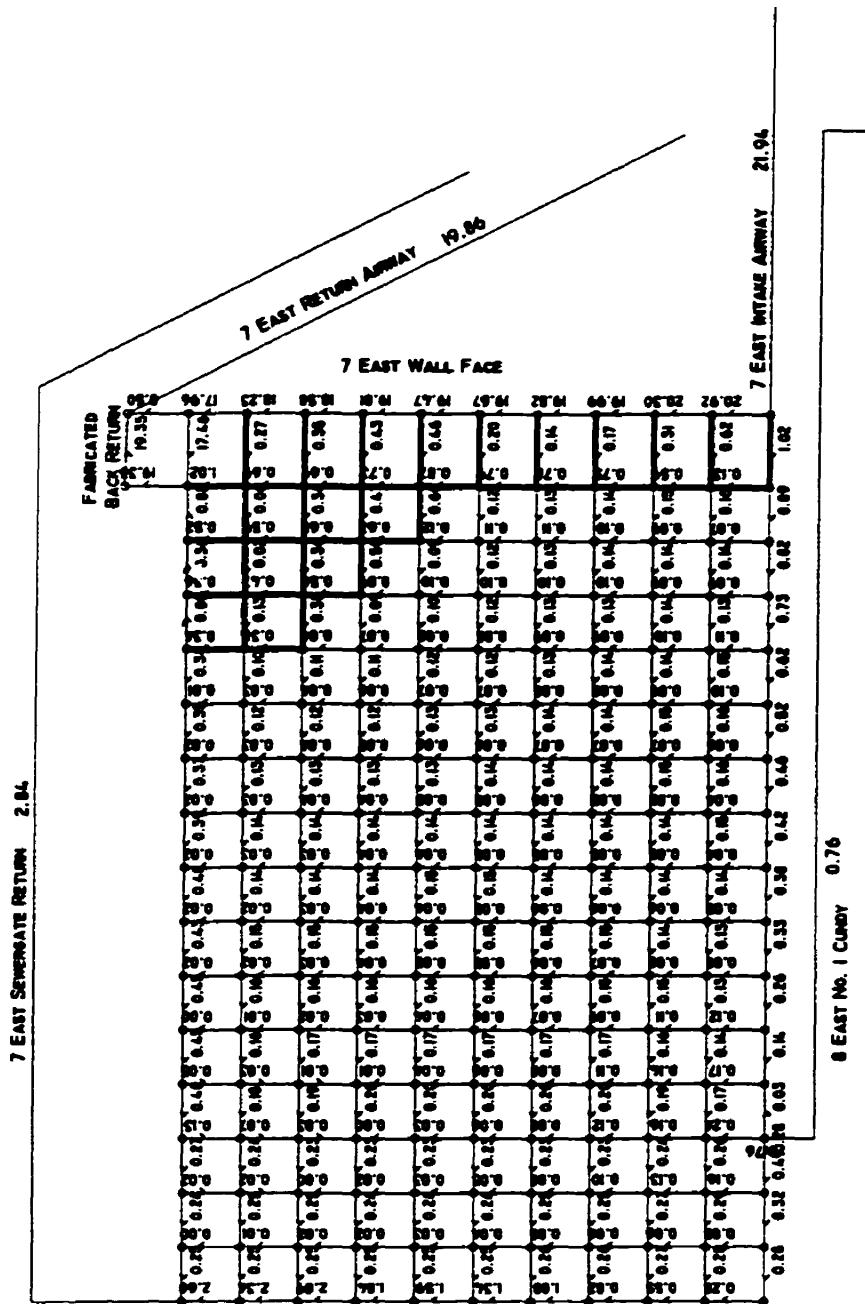


Figure 9.6 V-net model of Phalen 7 East - 3rd stage of reduced upper gob resistance

Using 50 units is a dramatic decrease in resistance; however, it is carried in these models to demonstrate that a low resistant gob behind the top face supports can cause a significant airflow back to the T-junction where the air has penetrated along the face. Any methane entering this zone will be brought back to the return airway.

To conclude, the models demonstrate how a low resistance of 7 East upper gob can further damaged the ability to control methane emissions from the gob. Airflow paths can penetrate deeper into the gob and capture a greater percentage of the gob produced gas.

Even with what appears to be good consolidation in the gob, methane leakage still occurs along the highside rib. In some respects, the Sewergate is operating as a U ventilated wall within the uncontrolled zone.

Conclusions and Recommendations

10.0 Conclusions and Recommendations

10.1 Conclusions – Measured and predicted methane emissions from Phalen mine

The difference in predicted versus actual methane flow is close to those reported in other reports using the Airey method (Technical Coal Research, 1986). The average difference indicates that the method gives a reasonable estimate of the methane flow from coal seams adjacent to the working seam of Phalen mine.

The predicted estimates are based on specific emissions from coal seams and on regular coal producing periods. It does not predict methane flow for non coal producing periods. Therefore, methane flows for vacation, down times or low production weeks cannot be predicted with the abridged Airey method. This is a weakness in the abridged program and is probably better solved in the more complete computer programs of the MRDE model.

The method does not consider non coal strata and as a result emissions from other gas sources such as sandstone beds cannot be assessed. But the method has been validated for use at Phalen 4 and 5 East, probably to an accuracy of +/- 20%.

The accuracy of predicting methane emissions from mining is only as good as the data available for the model and whether the model meets the criteria of scientific evaluation. Moreover, the Lower Sandstone Unit was suspected as a source of gas or at least affecting the release of gas from other coal seams. This remains probably the biggest unanswered question and further research in this area is required to confirm or deny whether sandstone was and is a significant contributor to the methane emissions into Phalen mine.

This report can be used hopefully to aid mine planners in the selection of mine ventilation systems and a basis to further study the methane emissions associated with ventilation systems used at Phalen mine.

In this evaluation, the data is the best available; however, predicted emissions are sensitive to the assumptions made in estimating such critical parameters such as in-situ gas content and pressure. The assumptions made can only be further validated by the extraction of coal cores from virgin in-seam conditions and the testing of these cores for gas content. More testing is required to measure the in-seam gas pressure associated with the Phalen coal seam to validate assumptions made in this report. Further methane isotherm testing is required to derive better and more relevant temperature and pressure corrections for the Phalen seam coal.

The methane prediction model gives in a global sense, reasonable estimates of methane emissions from coal seams adjacent to the working seam of Phalen mine. However, other factors such as whether emissions from floor gas sources, which could represent ~ 40 % of the total emissions, were based on general estimates of Emery seam thickness and proximity to the Phalen worked seam. Until more accurate borehole information becomes available this gas source might not be as predicted.

10.2 Conclusion – Sewergate Performance – Phalen 7 East

Methane flow as measured in the Phalen 7 East Top Level (outside end) compared to 4, 5 and 6 east East had increased significantly. This increase can be attributed in part to increased coal front emissions with mining depth, the effect of the Lower Sandstone Unit and to gob emissions associated with the change in ventilation method from Bleeder Deep U-ventilation to Sewergate.

In order to assess the Sewergate performance, tubebundle experiments were devised to acquire differential air pressure measurements from the gob and to collect gob gas samples for composition and to conduct tracer gas experiments. These measurements were

modelled and used to determine that an uncontrolled point existed 50-100m in the gob behind the face line.

More specifically, 7 East Top tubebundle experiment showed that the neutral point of 7 East Top Level gob was 20 to 40 m in by the T-junction and appeared to be a function of the height and thickness of the Lower Sandstone Unit above the coal seam which effects gob consolidation, possibly creating a low resistance gob. This reduced the effect of Sewergate pressure gradient which in theory depends primarily on gob resistance.

Furthermore, 7 East Wall Face tubebundle tracer gas experiments showed that a neutral zone existed in 7 East gob. This zone appeared to exist between a distance of 50-100 m behind the face line supports.

Some very basic V-net modelling of tubebundle measurements was used to demonstrate the flow of air in the gob. Even with the limited modelling conducted in this project, air flows were in the range of those measured for 7 East.

The present "V-net" model of 7 East was contrived to make air flow into the gob through the face line and then have air flow leakage occur along the highside rib in a direction toward the T-junction; however, predicted air pressure drops across the entire gob were lower than expected. This was due to the fact that "V-net" is normally used to calculate turbulent airflow, not laminar, as was the case for airflow in 7 east gob. Laminar flow could not be simulated in the modelling exercises.

Future Computation Fluid Dynamic (CFD) modelling will help improve the present model to better understand airflow in the gob. To model such a system would involve some advanced mathematical concepts and field data, supported by powerful computer applications and systems to process the algorithms. This is beyond the scope of this report.

10.3 Summary Conclusions

- Methane monitoring indicates there has been a large increase in methane emissions to Phalen East return airways (4 to 7 East).
- Sewergate ventilation of 7 East worked beyond the 50 - 100 m uncontrolled zone in the gob. Sewergate captured 40 to 80% of the gob gas (based on predicted methane flow).
- The methane flow into the uncontrolled zone increases with both Lower Sandstone Unit thickness and proximity to the Phalen seam. It reduced greatly when < 20 m thick and > 4 m above the seam. The following observations were made in regards to a major transition in the Lower Sandstone Unit at 2100m on 7 East:
 1. Firstly, the Lower Sandstone Unit had essentially begun to rise and thin out in relation to the top of the coal seam.
 2. Secondly, the 'hydrocarbon smell' disappeared.
 3. Thirdly, the specific emissions from the gob per tonne coal mined reduced substantially from an average of ~ 4.5 m³/tonne while mining through the Lower Sandstone Unit to ~ 0.9 m³/tonne while not.
 4. Fourthly, the Lower Sandstone Unit might be the source of gas that entered the 7 East uncontrolled zone by evidence of a distinct change in the proportion of methane and ethane emitted into the gob when the LSU had begun rise and thin above the Phalen seam upon retreat.
- %Methane + %Ethane concentration in the gob trends toward a higher concentration with increased distance in the gob. If the trend is projected back to the face startline, it appears that the methane concentration at this point would be over 15 %, and essentially outside the explosive range.
- With the recent discovery of the Stony coal seam there is further concern that floor emissions related to sandstone weightings may have resulted in early gas in 7 East's uncontrolled zone.

10.4 Recommendations for Phalen 8 East

- **Determination of the presence of the Stony seam in the floor of 8 East.**
- **Connection to and inspection of 7 East wall face startline.**
- **A more effective ventilation system for methane control is a U.K. style triple entry with Sewergate connection.**
- **Reseal Eastside Walls, 100 L/s maximum air leakage per seal to attempt to maintain the methane content in the bleeder above the high explosive limit.**
- **If Sewergate is selected by CBDC for 8 East wall, a coal and/or wood snicket back return would be preferred over a Fabricated Back Return.**
- **Installation of tubebundles to test performance of 8 East Sewergate.**
- **CBDC to support CFD modeling of 7 East Sewergate for planning purposes.**

References

REFERENCES

- Airey, E.M., 1968. "Gas emission From Broken Coal, An Experimental and Theoretical Investigation ", *International Journal of rock Mech., Min. Sci.*, Volume. 5, pp 475-494.
- Airey, E.M., 1971. "International Conference of Safety in Miines Research, Donezk, USSR.,report no.21.
- Airey, E.M.,1979. "A theory of gas Emission in Coal Mining Operations, Part 2: Gas Emission from Seam Adjacent to Worked Seams",Mining Research and Development Establishment, report No. 21,1979.
- AMCL, 1991. "Methane Drainage at Phalen Colliery", Amcl Calgary, pp. 28.
- Banik, J., 1994., "Preventing Spontaneous Combustion in gob of Retreating Longwall Panels by Ventilating without Bleeders", Doctor of Philosphy, Dissertation submitted to the Virginia Polytechnic Institute, pp 89.
- Cain, P., Stokes, A., and Genter D., 1984, "Preliminary Report On Studies Into gob Leakage In The Sydney Coalfield", Energy Research Program, Coal Research Laboratories, ERP/CRL 84-43 (OP), pp 2, 3.
- Castellan G.W., *Physical Chemistry*,Third Edition, ISBM, ISBN 0-201-10386-9.
- Cecala, A.b., Konda, B.W., and Klinoski, G.W., "A Comparison of Methane Flow Patterns on Advancing and Retreating Longwalls", *Proceedings 4th. US Mine Ventilation Symposium*", Chapter 59, pp 484 - 489.
- Christian., Tauziede, Moulleau, Yvon, & Boutet Remy, 1996" *Modelling of Gas Flows in the goaf of retreating faces*", Ineris, Verneuil en Halatte, France, pp 45.
- Clayton J.L. 1993, "Composition of crude oils generated from coals and coaly organic matter in shales", AAPG, 1993, "Hydrocarbons from Coal, AAPG studies in Geology#38, pp 206.
- Coal in Nova Scotia, Nova Scotia Department of Mines and Energy, Canadian Cataloguing in Publication Data, ISBN 0-88871-072-0.
- Creedy, D.P. 1981. "Evaluating the gas content of disturbed and virgin coal seams",XIX Conference of Safety in Mines rsearch, Katowice,1981 pp 9.
- Creedy,D.P., 1992, "Reducing Gas emission Constaints on High-Production Retreat Coalfaces", *Mining Engineer*, June 1992, pp 335.
- Curl S.J., 1978. "Methane prediction in coal mines", Report Number ICTIS/TR 04, December 1978, London, IEA Caol Research.

Creedy, D.P. and Kershaw, S.1988. Firedamp Prediction - "A Pocket Calculator Solution", Mining Engineer, February 1988, pp 377-379.

Farrell and Associates,1995, "Development of a Conceptual Design for Methane Control at Phalen Mine", Canadian Department of Supplies and Services Contract no. 02SQ.23440-4-1160, appendix A 2, pp 10.

Feng K.K., Cheng K.C, and Augsten R., 1983 "A Preliminary Study on Methane Desorption of Sydney Coal from Devco Mines", Energy Research Program, Mining Research Laboratories, Division Report ERP /MRL 83-113(TR), pp 8.

Feng K.K., Cheng K.C, and Augsten R., 1981, "Test Procedure for the the methane desorption from coal by direct method", Division report, ERP/MRL 81-63 (TR), Energy, Mines, Resources, Mining Research Laboratories, Canadian Explosives Laboratory.

Forgeron S.,1996. Personal Communications, Head Geologist, Cape Breton Development Corporation, September 1996.

Hacquebard, P.A., 1964. Environments of Coal Deposition Symposium, Coal Geology Society of America,Annual meeting, Miami, Florida,1964. Pg 1.

Hacquebard, P.A., 1976a. "Distribution and Amounts of Thermal and Metallurgical Coal Resources in the Sydney Coal Field of Nova Scotia" Department of Energy Mines and Resources Geological Survey of Canada Atlantic Geoscience Centre, Bedford Institute of Oceanography", technical report No. 11-k/G-76-1, pp 13-23.

Hacquebard, P.A., 1976b. " Coal Rank Changes in the Sydney and Pictou coalfields of Nova Scotia; cause and economic significance" CIM, Bulletin, May 1984, pp. 55.

Harpalani, S. and McPherson, M.J.1988, "An Experimental Investigation to Evaluate Gas Flow Characteristics of Coal, fourth International Mine Ventilation Congress, Queensland,July 1988 pp 175.

ICCP, 1971,"International Committee for coal petrology 1971", International handbook of Coal petrography, First supplement to Second Edition, CNRS, Paris France. Pp. 186

International Coalbed Methane Symposium; High pressure microbalance sorption studies. May 17-21,1993, pp 251.

Jeremic, M.L., 1982, "Strata Mechanics in Coal Mining", Laurentian University, Sudbury, Ontario.

Jones Jones, J.M.,Davis, A.,Cook A.C.,Murchison,D.G., and Scott,E., 1984, "Provincialism and correlations between some properties of vitrinite", International journal of Coal Geology, v.3, pp.315-331.

Konda, B.W., and Kochuhar, j., 1985, "Methane Emission and Control at Lingan Colliery.", 16th Annual Institute on Coal Mining Health, Safety, and Research, Blacksburg, Virginia.

Krumbein W.C and Sloss L.L, 1963 "Stratigraphy and Sedimentation", Freedman, second Edition. pp 93 108.

LaFosse MacLeod, H., 1992, "Geological Services" Canadian Department of Supplies and Services Contract no. 039SQ.23440-0-9189, pp 3.

Law.B.E. and Rice D.D.,AAPG, 1993a, "Hydrocarbons from Coal, AAPG studies in Geology#38", pp 59.

Law.B.E. and Rice D.D.,AAPG, 1993b, "Hydrocarbons from Coal, AAPG studies in Geology#38", pp 209.

Law.B.E. and Rice D.D.,AAPG, 1993c, "Hydrocarbons from Coal, AAPG studies in Geology#38", pp 120.

Liney, A., 1997, "Continuation of Research of Methane Control in the Sydney Coalfield", Interim Report 1 April to 31 August, CANMET Professional Services Contract.

Levine (1991a) "New methods for assessing Gas Resources in thin bedded,high ash coal, Paper 9125 9126", Proceedings of the 1991 Coalbed methane symposium,tuscaloosa, Alabama, November 16-19 pp 115 -125.

Littke.R., and Leythaeuser, D., 1993 "Migration of Oil and Gas in Coals", Chapter 10,. Hydrocarbons from Coal, AAPG studies in Geology#38, pp 59.

Lobbe Technologies Ltd., 1987. "Modelling Methane flow into Underground Longwall Coal Mines", Canadian Department of Supplies and Services DSS Contract, 2344-7-9141/01-sq.

Macdonald R.J., D.A.Payne,1992, "Changing Mining Methods at CBDC", Cape Breton Development Corporation, pp 8.

McPherson,M.J., 1993. "Subsurface Ventilation and Environmental Engineering", Chapman and Hall, pp 426.

McPherson,M.J., 1975. "The Occurrence of Methane in Mine workings", Journal of the Mine ventilation Society of South Africa, Vol.28,no.8, August 1975.

MRDE, 1978. "Prediction of Firedamp",Final Report on ECSC Research Project 7220-AC/801. Pg 39.

National Coal Board.,1976-1978, "Prediction of Firedamp Emission", Commision of the European Communities, Directorate general, Final Report on ECSC Research Project 7220-AC-/801., pp 39.

Norwest Resource Consultants Ltd.1985. "A detailed Review and evaluation of methane prediction techniques and their applicability to Canadian coal mines", Canadian Department of Supplies and Services DSS Contract, Serial Number: 23440-5-9008/85-00024SQ, Pp (3-9) - (3-13).

Payne. D.A. and DeMarco, M.1994. "Vertical Stress Redistribution Around a Retreating Longwall Faces end" ,14 th Ground Controll Conference in Mining).

Pappas, D.M, and Mark,M.,1993, "Behavior of Simulated Longwall gob Material", RI 9458, United states Bureua of Mines, pp 23.

Patching, T. 1981. "Gas Desorption and Emissions Studies on Canadian Coals", Department of Mineral Engineering, University of Alberta, 1981 pp.95

Patchings T. and Mikhail M.,1981. "Studies of Gas Sorption and Emission on Canadian Coals", Professor Emeritus, Dept.of Mining Engineering, University of Alberta, and Head Coal Preparation Research Unit, Coal Research, Laboratory, Canmet, Edmonton.

Pierre M. A, 1992, "Porous Media, Geometry and Transport", Butterworth-Heinemann, 1992, pp. 30.

Scott, A.R., 1993. "Composition and Origin of Coalbed Gases from Selected Basins in the United States", Proceedings of the 1993 International Coalbed methane Symposium", University of Alabama, Tuscaloosa, May 17-21, 1993. pp. 207.

Technical Coal Research, 1986. "Investigation of Firedamp and its Emission in coal seams", Report EUR 11477 EN.,Commission of the European Communities. Pp 3.

Ulery,J.P., 1988. "Geological factors effecting the gas content In southwestern Pennsylvania", RI9195, Us Bureau of Mines, "Hydrocarbons from Coal, AAPG studies in Geology#38, pp 206.

Walker, S., 1993. "Major Coalfields of the world", IEACR/51, January 1993,IEA Coal Research, London.

Resource Enterprises, 1992. "Assessment of the Coalbed Methane Potential of the Donkin Mine Site, Cape Breton, Nova Scotia, Canada.", Prepared for Nova Scotia Department of Natural Resources, Halifax, Nova Scotia,. pp 29.

Young D.A. and Chipman,D.G., 1996. "A Procedure to Determine the Methane Isotherm of Coal", MMSL 96-109(TR), Mineral and Mining Sciences Laboratories, Natural Resources Canada.

Young D.A., 1996. "Methane of Coal Samples A and B", MMSL 96-108(CF), Mineral and Mining Sciences Laboratories, Natural Resources Canada.

Young D.A., 1989. "A Procedure for the determination of the total gas content of coal", Division Report Coal Research 89-51(TR), Energy Mines & Resources, Mining Research Laboratories, Canadian Explosives Laboratory.